THESIS

STUDY ON k~0 BIEXCITONS IN CuCl BY NONLINEAR SPECTROSCOPY

非線形分光法による塩化第一銅の波数ゼロ近傍の励起子分子の研究

Masahiro Hasuo

蓮尾 昌裕

THESIS

STUDY ON k~0 BIEXCITONS IN CuCl BY NONLINEAR SPECTROSCOPY

非線形分光法による塩化第一銅の波数ゼロ近傍の励起子分子の研究

Masahiro Hasuo

蓮 尾 昌 裕

Submitted to

Department of Physics, School of Science

The University of Tokyo

January, 1995

Contents

Preface

CuCl, which is one of direct gap semiconductors, is very famous due to the simple structure of the lowest exciton band reflecting the simple band structure and the variety of the nonlinear optical phenomena associated with the two-photon resonance of biexcitons. The exciton system in CuCl has been investigated deeply as one of the model systems for the study of the optical properties associated with excitons and biexcitons. Therefore, many physical parameters of the exciton system in CuCl have been evaluated very precisely. Nowadays, device oriented researches on this exciton system and tests of fundamental physics by using this exciton system have been carried out on the bases of these precise knowledges.

Among such researches, following two subjects were carried out in this thesis by using the nonlinear spectroscopy methods:

(1) Measurement of the two-photon resonance of k~0 biexcitons in CuCl and relevent $\chi^{(3)}$ precisely by developing a high resolution spectroscopy system.

(2) Development of a new method to investigate the k=0 biexciton state and the coherency inherent in the Bose-Einstein condensation for the study of the possibility of the Bose-Einstein codensation of biexcitons in CuCl.

According to (1), the discovery of systems with high efficiency nonlinear optical properties has been one of the incentive subjest in device oriented researches because such systems will lead to develop the fundamental aspects of physics, such as in the generation of the squeezed state light and the number state light, as well as the optically controlled data processing devices, such as the fast-respondent optical swiching. For these purposes, a large optical nonlinearity, i.e., $\chi^{(3)}$, in a transparent region of the medium is necessary. The two-photon resonance of k~0 biexcitons in CuCl is one of the most hopeful candidates (k is the wave number of biexcitons) because of the

following advantages:

- The optical nonlinearity associated with the two-photon resonance of k~0 biexcitons is very large due to the giant oscillator strength effect and the resonance effect of the intermediate state of this resonance.
- Such a nonlinearity exists in the transparent energy region of the crystal reflecting the large binding energy of a biexciton.
- The polarization selection rule of this resonance is very simple due to the simple symmetry of the biexciton state.

Details of these advantages will be explained in Chapter 1.

To examine the possibility of this system for the applications for such devices, quantitative estimation of $\chi^{(3)}$ is necessary. However, there have been two serious problems that make the evaluation of $\chi^{(3)}$ associated with the two-photon resonance of biexcitons in CuCl difficult. One is the saturation effect that is observed even under the very low excitation intensity. The other is the large spectral width of the laser light from a conventional pulse dye laser system, which has been used to measure the two-photon resonance of biexcitons in CuCl, compared with the very narrow level width of the k~0 biexciton state. Therefore, a new light system to measure the two-photon resonance of biexcitons at k~0 and to evaluate $\chi^{(3)}$ precisely are demanded for further progress.

According to (2), the Bose-Einstein condensation in exciton systems is another incentive subject that has been gathering much notice. Usually, excitons have been regarded as polarizations when the optical responses of the exciton system are considered. On the other hand, an exciton can be regarded as a particle (quasi-particle) that has mass and can move freely in the crystal. An exciton or a biexciton, which is composed of even number of Fermi particles, is regarded as a Bose particle. Therefore, it has been expected that the phase transition to the Bose-Einstein condensation occurs when a high density of excitons or biexcitons is created at a low temperature. Biexciton system in CuCl is one of the candidates to realize and examine the Bose-Einstein condensation because of the following advantages:

- Biexciton state is very stable due to the large binding energy of a biexciton.
- Precise knowledge about the dispersion of biexcitons, i.e., the effective mass of biexcitons, has been obtained.
- Various optical nonlinear phenomena associated with the giant two-photon resonance of biexcitons are observed.

Details of these advantages will be also explained in Chapter 1.

Conventionally, method to study the distribution of biexcitons in momentum space has been due to the analysis of their emission spectra. However, by this method, it is not so easy to obtain informations about the k=0 biexcitons, i.e., biexcitons of zero momentum, and the coherency inherent in the Bose-Einstein condensation which are very important in the study of the Bose-Einstein condensation. Therefore, a new method is demanded to overcome these difficulties.

The structure of this thesis is as follows:

In chapter 1, fundamental concepts which relate to this work are given briefly. Excitons and biexcitons in CuCl are explained firstly in details. Secondly, the origin of the giant two-photon resonance of biexcitons is explained. Lastly, the Bose-Einstein condensation in exciton system is explained.

In chapter 2, an explanation about the preparation of samples is given. The method to evaluate the sample quality is also explained because it was found that the sample quality affected the results of the experiment very much.

In chapter 3, the experimental study on k~0 biexciton state by high resolution polarization spectroscopy is explained.

In chapter 4, the experimental study on the k~0 biexcitons by phase conjugation spectroscopy for the Bose-Einstein condensation of biexcitons is explained.

In chapter 5, conclusions of this work and the future prospects are given.

In Appendices, theoretical backgrounds and other experimental studies which relate to this work

are explained briefly.

1. Generalities

1-1. Exciton system in CuCl

1-1-1. Excitons in CuCl

CuCl is an ionic semiconductor composed of Cu^+ and Cl^- crystallized in the zincblende lattice that is shown in Fig.1-1. Its symmetry is T_d^2 ($F\bar{4}3m$) in space group. Because CuCl is a direct gap semiconductor, i.e., the top of the valence band and the bottom of the conduction band are located at Γ point, the symmetry of CuCl can be treated as T_d ($\bar{4}3m$) in point group when the optical transitions are considered.

The band structure of CuCl is shown in Fig.1-2, schematically. The conduction band is mainly composed by 4s-orbitral of Cu^+ and its symmetry is Γ_6. The valence band is a hybrid of 3d-orbital of Cu^+ and 3p-orbital of Cl^- and its symmetry is $\Gamma_7+\Gamma_8$. The valence band splits into Γ_7-band and Γ_8-band by the spin-orbit interaction. The energy relation between these Γ_7-band and Γ_8-band is determined by the ratio between d-orbital and p-orbital. In CuCl, non-degenerated Γ_7-band is located at higher energy position than that of Γ_8-band[1].

The lowest energy exciton band in CuCl originates from the coupling of an electron in Γ_6-conduction band and a hole in Γ_7-valence band. It is well known that this exciton band is very simple reflecting the non-degenerate character of the valence band. This exciton band is called the Z_3-exciton band. On the other hand, the exciton band that originates from the coupling of an electron in Γ_6-conduction band and a hole in Γ_8-valence band is called the $Z_{1,2}$-exciton band. The reflection spectrum and the transmission spectrum of CuCl are shown in Fig.1-3 and Fig.1-4, respectively[2]. The structures appeared around 3868 Å (3.204eV), 3786 Å (3.275eV) and 3683 Å

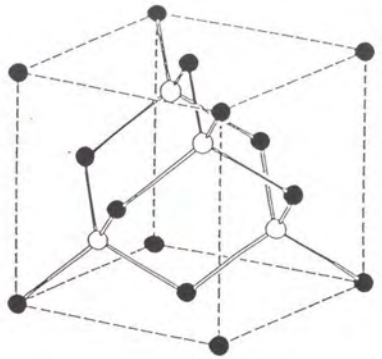

Fig.1-1 Structure of zincblende lattice

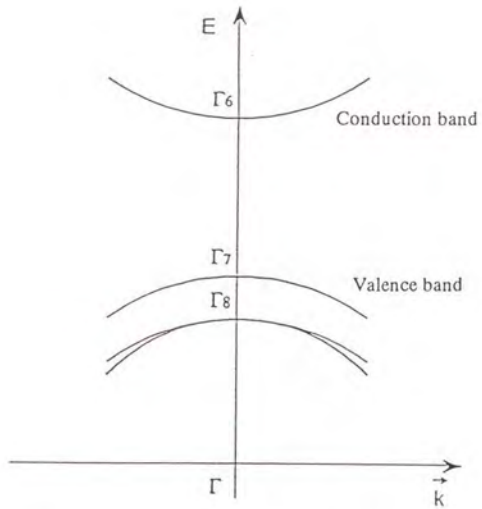

Fig.1-2 Band structure near Γ point in CuCl
Valence band splits into two bands. The non-degenerate Γ_7-band locates at higher energy position than that of the degenerate Γ_8-band contrary to other copper halide crystals.

(3.366eV) are due to the Z_3-1s exciton, the $Z_{1,2}$-1s exciton and the Z_3-2s exciton, respectively.

In this work, we will be interested mainly in the Z_3-1s exciton. Because the envelope function of this exciton is s-orbital function, the symmetry of this exciton is given as follows:

$$\Gamma_6 \otimes \Gamma_7 \otimes \Gamma_1 = \Gamma_2 \oplus \Gamma_5 \qquad (1\text{-}1).$$

The Γ_5-exciton is a mixed state of spin singlet and spin triplet states and splits into a non-degenerate longitudinal exciton state and a twofold degenerate transverse exciton state by the dipole-dipole interaction. It is well-known that the transverse exciton in CuCl couples with a photon strongly and produces a polariton. On the other hand, the Γ_2-exciton is pure spin triplet state, then optically forbidden. This exciton state becomes optically allowed in the presence of a magnetic field or an axial stress[3]. The splittings of the Z_3-exciton band are summarized in Fig1-5. Hereafter, the Γ_5-transverse exciton, the Γ_5-longitudinal exciton and the Γ_2-exciton are expressed in this thesis as T-exciton, L-exciton and t-exciton, respectively.

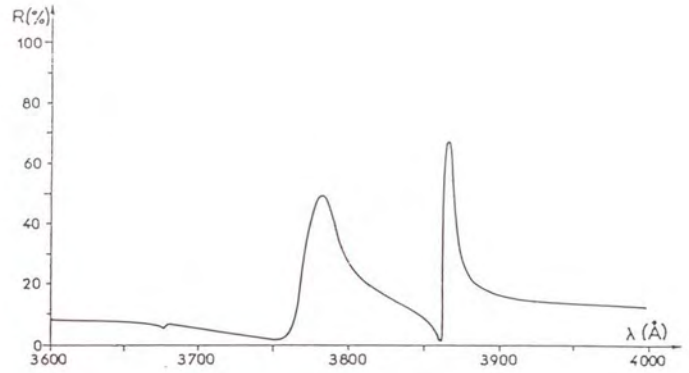

Fig.1-3 Reflection spectrum of CuCl at 4.2K [2]

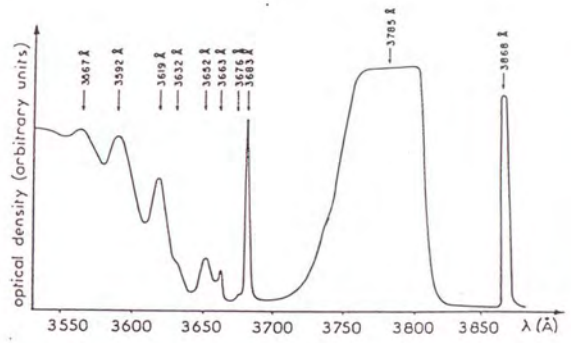

Fig.1-4 Absorption spectrum of CuCl thin film at 4.2K [2]

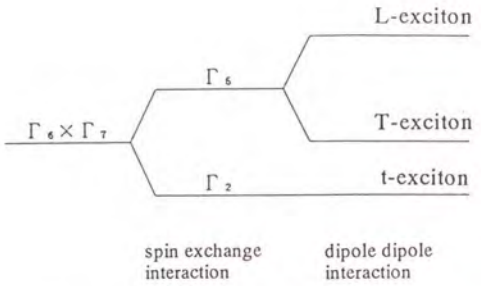

Fig. 1-5 Splittings of the Z_3-1s exciton band at Γ point
L-exciton, T-exciton and t-exciton represent the Γ_5-longitudinal, the Γ_5-transverse and the Γ_2-exciton states, respectively.

1-1-2. Biexcitons in CuCl

Two excitons with mutually opposite spins of their electrons and holes attract each other resulting in a bound state of two excitons similar to a hydrogen molecule or a positronium molecule. This bound state is called a biexciton or an excitonic molecule. According to the theory[4], biexciton is stable for any values of the electron-hole masses ratio, $\sigma=m_e/m_h$. The energy levels of biexcitons and excitons and optically allowed transitions are shown in Fig. 1-6[5][6]. In CuCl, only Γ_1-biexciton has been found sofar. Hereafter, "biexciton in CuCl" in this thesis means the Γ_1-biexciton.

Figure 1-7 shows the dispersion curves of the biexciton and the L-exciton and the T-exciton polariton in a wide range of wave number about one-fifth of the Brillouin zone obtained by Mita et al., experimentally[7]. It is clear that the effective mass approximation is valid for this system. This is the definite evidence of the presence of biexcitons and excitons and strong support for the validity of the particle picture of biexctions and excitons. From this measurement, the effective masses of the biexciton, the L-exciton and the T-exciton are obtained to be $m_M=5.29m_0$, $m_L=3.14m_0$ and $m_T=2.3m_0$, respectively, where m_0 is the free electron mass.

When a high density of excitons is generated in a crystal, biexcitons are generated through bimolecular collisions of excitons[8][9]. A biexciton emits a photon leaving an exciton behind as shown in Fig. 1-6. This emission is called M-emission. Fig. 1-8 shows the emission spectrum around the Z_3-exciton band at several excitation intensities. The emissions that appear under a weak excitation show linear dependence on the excitation intensity. The emissions denoted by Ex-2LO and I_1 in the figure (a) are the 2LO-phonon side band emission of the T-exciton polariton and the emission of an exciton bound to a neutral acceptor, respectively. As the excitation intensity increases, the structures denoted by M_T and M_L appear and increase remarkably as shown in the figure (b) and (c). These emissions are the M-emission mentioned above. The emission of a biexciton leaving a T-exciton behind is called the M_T-emission. In turn, the emission of a biexciton

leaving an L-exciton behind is called the M_L-emission.

Due to the difference between the effective masses of excitons and biexcitons, the shape of the M-emission reflects the distribution of biexcitons in momentum space as will be shown in Chapter 4.

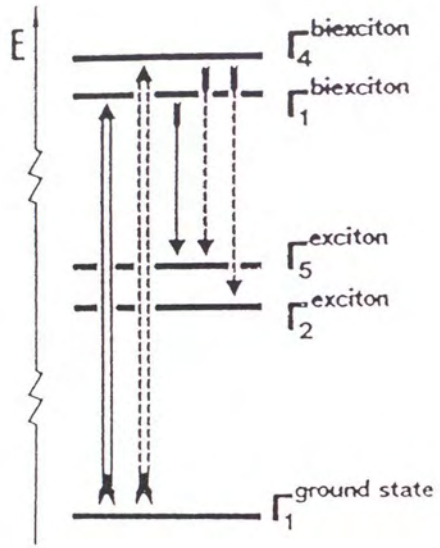

Fig.1-6 Schematic energy diagram of exciton and biexciton states in CuCl [6]
The solid (broken) arrows incidate strongly (weakly) allowed transitions. Double (single) arrows indicate two-photon (one-photon) processes.

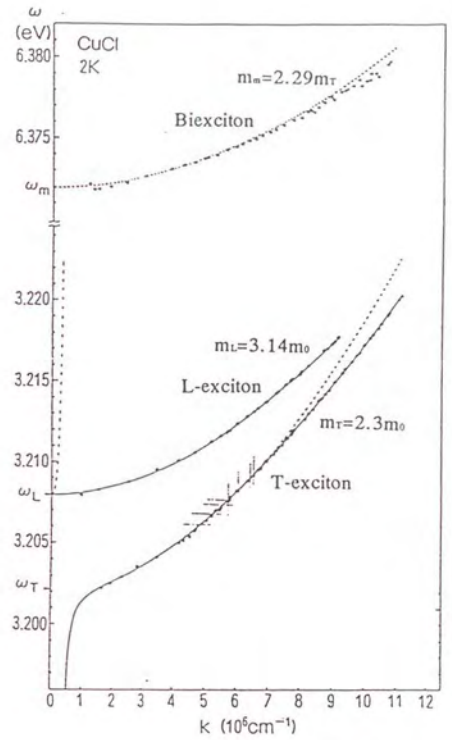

Fig.1-7 Dispersion curves of the biexciton, the L-exciton and the T-exciton polariton in CuCl at 2K [7]

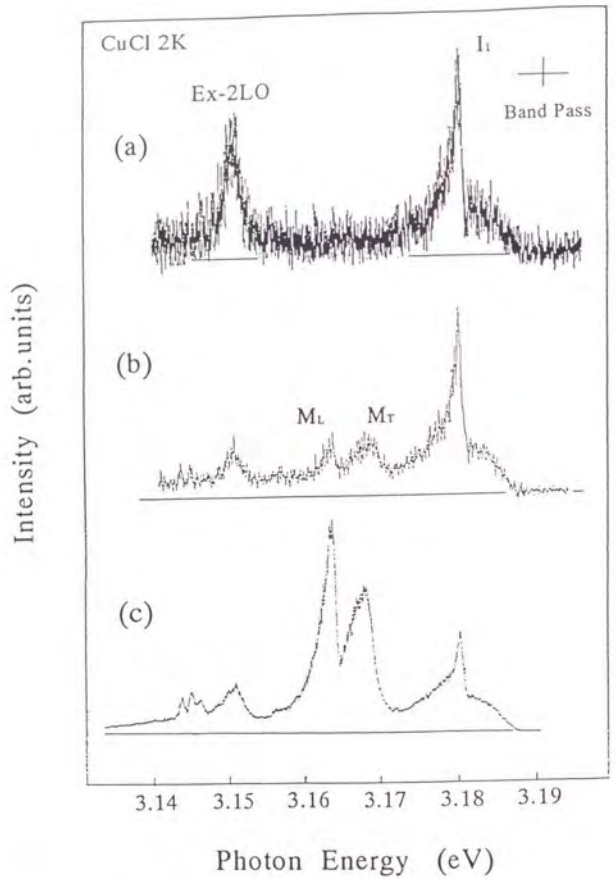

Fig.1-8 Band edge emissions of a CuCl single crystal at several excitation intensities at 2K
The emissions denoted by Ex-2LO and I_1 are the 2LO-phonon side band emission of the T-exciton polariton and the emission of an exciton bound, respectively. The emissions denoted by M_T and M_L are biexciton emissions.
Excitation intensity increases from (a) to (c).

1-2. Giant two-photon absorption (GTA) of biexcitons

It is well-known that the biexcitons in CuCl can be created by the two-photon transition from crystal ground state directly. This transition is called the giant two-photon absorption (GTA) because its efficiency is very large both due to the giant oscillator strength effects and due to the resonant effect of the intermediate state of this transition[10][11][12][13]. An example of the transmission spectra around the GTA band is shown in Fig.1-9. In this case, a single laser beam was used. A large absorption that is comparable to the exciton absorption appears at the two-photon resonant energy of biexcitons as shown in Fig.1-9(b). Following the large $\chi^{(3)}$ associated with this two-photon resonance, the third order nonlinear optical phenomena such as the resonant two-photon Raman scattering, the four wave mixing and the nonlinear polarization rotation occur at GTA remarkably. The dispersion curves of the biexciton and the L-exciton and the T-exciton polariton shown in Fig.1-7 were obtained by using the two-photon Raman scattering[7].

Besides the very large $\chi^{(3)}$, there are following characteristics in this transition:

1) The polarization selection rule for this two-photon transition is very simple. The efficiency of the two-photon transition to Γ_1-biexcitons is proportional to the scalar products of the polarization vectors of the related two photons[5][6]. This is the reason why the two-photon absorption of biexcitons did not appear when a circular polarized single laser light beam was used for the excitation as shown in Fig.1-9(a). This characteristic is very imporant when one is interested in the photon statistics or the photon correlation between two photons contributing to this transition.

2) One can choose the wave number of excited biexctions by adjusting the combination of the photon energies and directions of relevant two photons that contribute the two-photon excitation of biexcitons as shown in Fig.1-10.

In this work, k~0 biexcitons are examined. There are following additional advantages in the two-photon resonance of k~0 biexctions:

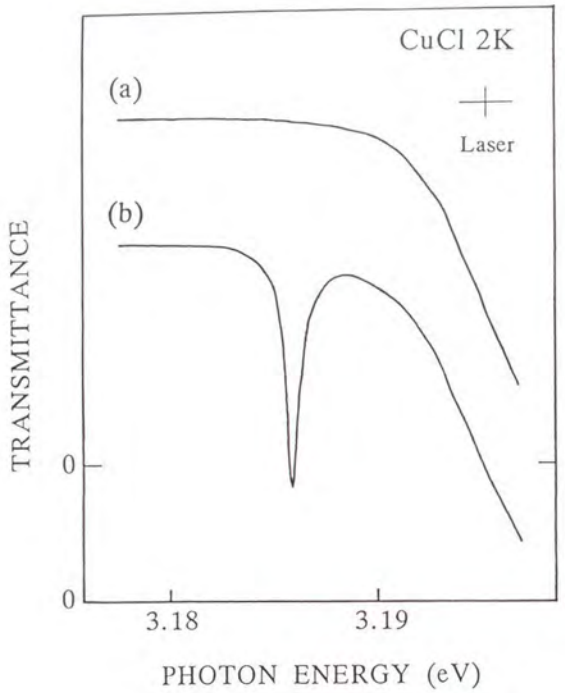

Fig.1-9 Transmission spectra around the GTA band of CuCl obtained with a circular polarized single laser beam (a) and a linear polarized single laser beam (b) at 2K
The intensity of the excitation light was 4MW/cm^2.

1) As the result of the large binding energy of a biexciton in CuCl which is about 32meV, the two-photon absorption of k~0 biexctions locates in a transparent energy region of the crystal. For the degenerate two-photon absorption, the corresponding photon energy is 16meV below the exciton resonance. This is the case shown in Fig.1-9(b). This characteristic, which means that this transition is almost free from linear absorption, is very important for the applications such as a generator of the squeezed light.

2) As can be seen in Fig.1-10, the two-photon transition to the k~0 biexciton state does not accompany the real excitation of excitons contraty to the transition to biexcitons of a large k. In this case, the transient time of the intermediate T-exciton responce is expected to be very fast. H.Akiyama et. al measured the time response of the nonlinear polarizaion rotation signal associated with the two-photon resonance of biexcitons in CuCl from the view of the application of ultra fast optical switching[14]. They found that the time response is of the order of 1ps.

On the other hand, M.Kuwata et al. measured the wave number dependence of the biexciton linewidth by the two-photon polarization spectroscopy[15]. The results is shown in Fig.1-11. The linewidth increases as k increases. They analized this broadening with the increase of the biexciton relaxation with an acoustic phonon emission. The result is shown by the solid curve in the figure. On the other hand, biexcitons of small k are free from single acoustic phonon scattering. Therefore, the relaxation of k~0 biexcitons is thought to be determined by the radiative processes. This means that the quantum yield of the k~0 biexciton emission is very large. This will be very important for the application of this system to quantum optics.

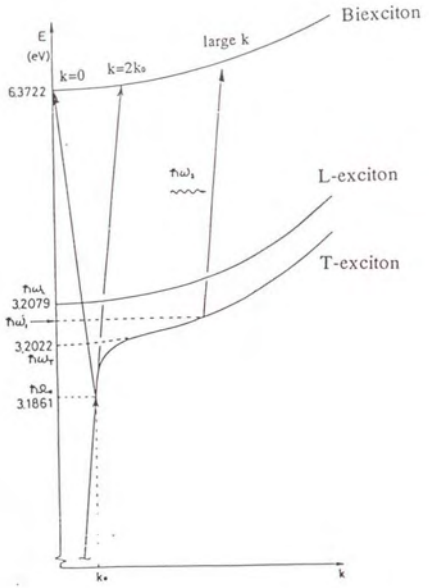

Fig.1-10 Schematic illustration of the two-photon excitation of biexciton state of a small wave number (k=0, $2k_0$) and a large wave number (after ref.(7))
Biexcitons of a lerge wave number are excited via the T-exciton state.

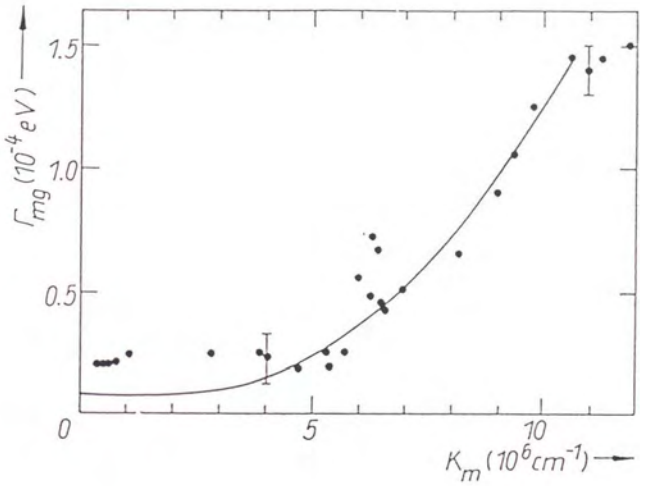

Fig.1-11 Wave number dependence of biexciton linewidth of CuCl at 1.6K measured by the two-photon polarization spectroscopy [15]
Solid curve represents the best fit results theoretically obtained.

1-4. Bose-Einstein condensation (BEC) in the exciton system

An exciton or a biexciton, which is composed of even number of Fermi particles, can be regarded as a Bose particle in the low density limit. Since the first theoretical work predicting the BEC of excitons by S.A.Moskalenko[16] and I.M.Blatt et al.[17], it has been expected that the phase transition to the BEC occurs when a high density of excitonic particles such as excitons and biexcitons is created at a low temperature.

There are several features in the exciton system in connection with BEC phenomenon:

1) The first feature is due to the light effective mass of excitons. Typical effective masses of excitonic particles are of the order of the free electron mass. As shown in Appendix A, the ideal Bose gas model predicts a critical density n^c for the BEC as

$$n^c = 2.612 \left(\frac{2\pi m k_B T}{h^2}\right)^{\frac{3}{2}} \qquad (1\text{-}2),$$

where m, k_B and T are the mass of the particle, Boltzmann constant and the temperature of the system, respectively. Therefore, one can expect the critical density is rather low in comparison with other system such as liquid ^{4}He.

2) The second feature stems from the fact that the density of excitonic particles can be easily controlled by changing the intensity of the excitation light.

3) The third feature relates to a finite lifetime of an excitonic particle. An exciton has a probability to recombine with a photon emission. This emission gives the information about the distribution of excitonic particles in momemtum space.

However at the same time, the finite lifetime of the excitonic particles causes a difficulty to the BEC phenomenon. In order to define such thermodynamical concepts as temperature and chemical potential of the system, it is necessary for the system to achieve quasi-thermal equilibrium within their lifetime. However, this feature puts forward a new fundamental theoretical problem of the very first stage of the quasi-equilibrium BEC dynamics.

Usually, since the interaction between excitons with mutually opposite spin structure is

attractive, two excitons compose a biexciton[4]. A biexciton is the stablest electron-hole complex up to the relatively high density of biexcitons satisfying the condition of $n_m a_m^3 < 1$, where n_m and a_m are the density and the radius of a biexciton. Therefore, the biexciton system is the first candidate for possible quasi-equibibrium BEC. The only exception is the excitons system in Cu_2O. In this system, 1s-exciton is thought to be the stablest electron-hole complex in the high density limit because of the repulsive exction-exciton potential due to the strong electron-hole exchange interaction and nearly equal electron and hole effective masses. The BEC of excitons in Cu_2O has been studied by several groups[18][19][20].

Moreover, the biexciton system in CuCl is a suitable system to examine the BEC because the binding energy of biexciton is very large , i.e., the biexciton state is stable even in high density regime. The effective mass has been already precisely evaluated and the validity of the effective mass approximation of biexcitons at the vicinity of k=0 is verified in next chapter. Furthermore, as explained in the foregoing sections, the exciton system in CuCl has been studied in details as a model system to examine optical properties associated with the excitons and biexcitons. Therefore, many physical parameters of CuCl have been evaluated precisely as shown in Table 1. This allows a direct numerical modeling of the experimental results.

Table 1 Parameters in CuCl (2K)

Crystal structure	Zincblende
Symmetry	T_d^2
Lattice constant	0.5409 nm [21]
Sound velocity (LA phonon)	$u = 3.6 \times 10^5$ cm/s [22]
LO phonon energy	$E_{LO} = 25.9$ meV [23]
TO phonon energy	$E_{TO} = 20.2$ meV [23]
Static dielecric constant	$\varepsilon_0 = 7.5$ [24]
High frequency dielectric constant	$\varepsilon = 3.7$ [24]
Band gap energy	$E_{gap} = 3.399$ eV [25]
Z_3-1s exciton	
t-exciton energy	$E_t = 3.1997$ eV [26]
T-exciton energy	$E_T = 3.2022$ eV [7]
L-exciton energy	$E_L = 3.2079$ eV [7]
Effective mass of T-exciton	$m_T = 2.3\ m_0$ [7]
Effective mass of L-exciton	$m_L = 3.14 m_0$ [7]
LT splitting energy	$\Delta_{LT} = 5.7$ meV [7]
Binding energy	$G_{ex} = 190$ meV [25]
Bohr radius	$a_{ex} = 0.703$ nm [27]
Deformation potential energy	$E_{ex}^d = -0.4$ eV [28]
Background dielectric constant	$\varepsilon_B = 5.59$ [7]
Biexciton	
Biexciton energy	$E_m = 6.3722$ eV [7]
Effective mass of biexcitons	$m_m = 5.29\ m_0$ [7]
Binding energy	$G_m = 32$ meV [12]
Deformation potential energy	$E_m^d = 0.72$ eV [29]

2. Sample preparation and its characterization

Usually, sample quality is crucial for the experimental results. In this chaper, the preparation of samples and the characterization of the sample quality are described in details.

2-1. Purification and crystallization

High quality powder of CuCl (Wako chemical co.) was purified several times by the vacuum sublimation method. Then, purification was done by the zone-melting method in hydrogen atmosphere. After this procedure, materials were kept in a vacuum desiccator because they suffer considerably much damage by the humidity in open air.

A few grams of the material were put in a quartz tube, which had been previously washed by king water and baked. Hereafter, we call this tube a sample tube. The sample tube was sealed with high quality Ar buffer gas with a pressure of about 360mmHg. Then, the temperature of the tube around the material was kept about 415 ° C by a furnace. Single crystal platelets were grown in the vapor phase during 4~5 days. Several platelet crystals of the thickness about 10 μm and the diameter about 1~5mm were obtained.

Special attention was given to avoid the mechanical damages of the crystals. Between the experiments, samples were kept in the vacuum desiccator.

Usually, the qualities of the samples are not same even if they were prepared in almost the same conditions. The differences of the sample qualities are observable for the samples grown in the different sample tubes. Sometimes, the differences of the qualities are observed even if they were grown in the same sample tube.

Recently, T.Ikehara et al. measured the lifetime of the T-exciton polariton and compared it with the band edge emissions of CuCl crystals[30]. The emission spectra of three samples of different qualities under the photo-excitation of the $Z_{1,2}$-exciton band are shown in Fig.2-1. In the first sample where the lifetime of the T-exciton polariton is long (the quality of this sample is thought to be good here), the shapes of the resonance emission of the T-exciton polaritons, which is denoted by Ex in the figure, and its 2LO-phonon side band emission are sharp. The corresponding luminescence intensities are strong. Here, the T-exciton polaritons can relax to the bottle neck of the dispersion by the scattering on the acoustic phonons. It happens because the lifetime of the T-exciton polaritons is longer than the charactaristic scattering time. On the other hand, the shapes of the resonance emission of the T-exciton polaritons and its 2LO-phonon side band emission are deformed and their intensities are weak in the sample of low quality. These phenomena are thought to be due to the relative increase of the number of excitons that are destroyed before reaching the bottle neck.

Because the results of this experiment depend on the sample quality very much as will be mentioned in Chapter 4, the sample quality was checked by comparison with the results obtained by T.Ikehara et al. before starting the experiments.

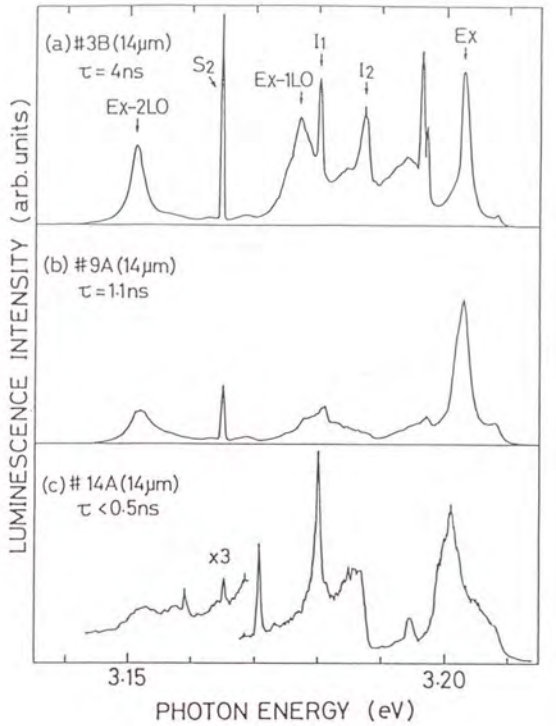

Fig.2-1 Emission spectra in three different samples with the same thickness under the excitation of the $Z_{1,2}$-exciton of CuCl at 2K [30]
The emissions denoted by Ex, Ex-2LO and I_1 in the figure (a) are the resonance emission of the T-exciton polariton, its 1LO-phonon side band emission and its 2LO-phonon side band emission, respectively. The emissions denoted by S2, I1 and I2 are extrinsic bound exciton emission.
The lifetime, τ, for the total number of the T-exciton polariton in each sample is shown on the left-hand side of each curve, which is evaluated from the decay time of the spectrally integrated intensity of the Ex-2LO emission.

3. High resolution two-photon polarization spectroscopy on the k~0 biexciton state

3-1. Introduction

As mentioned in Chapter 1, an extremely large optical nonlinearity of the two-photon resonance of biexcitons takes place for the photon energy in a transparent spectral region of the crystal. The quantitative evaluations of this nonlinearity, i.e., the magnitude of $\chi^{(3)}$, associated with the two-photon resonance of k~0 biexcitons had been carried out by the several methods such as two-photon absorption, optical phase conjugation and nonlinear polarization rotation. The reported peak values of $|\chi^{(3)}|$ ranging between 10^{-9} and 10^{-5} esu in dependence on the type of samples and the detection methods. N.Nagasawa et al. attempted to remove these inconsistencies and to determine a reliable value of $|\chi^{(3)}|$ in an international cooperative project in the framework of the CNRS-JSPS Sientific Program[31]. They found that the two-photon polarization spectroscopy is the most precise method. They obtained the peak value of $|\chi^{(3)}|$ in thin CuCl films evaporated on fused silica substrates to be 5×10^{-7} esu. The peak value of $|\chi^{(3)}|$ for single crystals has been measured to be 5.4×10^{-5} esu as a lower limit.

There are two serious problems that make it difficult to evaluate $|\chi^{(3)}|$ for single crystals precisely: One is the saturation effect of the relevant optical nonlinearity. Typical examples of the signal intensity and the width of the two-photon resonance as a function of the excitation intensity are shown in Fig.3-1 and Fig.3-2, respectively[31][32]. As seen in the figures, the saturation of the peak value of $|\chi^{(3)}|$ together with the intensity-dependent broadening of the spectral width of the resonance are observed even under the very low excitation intensity. Therefore, one has to analize the signal within the lowest order approximation. The other problem is the large spectral width of the laser light from a conventional pulse dye laser system compared with the true width of the biexciton state. Usually, the spectral width of the signal which resonate with the k~0 biexciton state

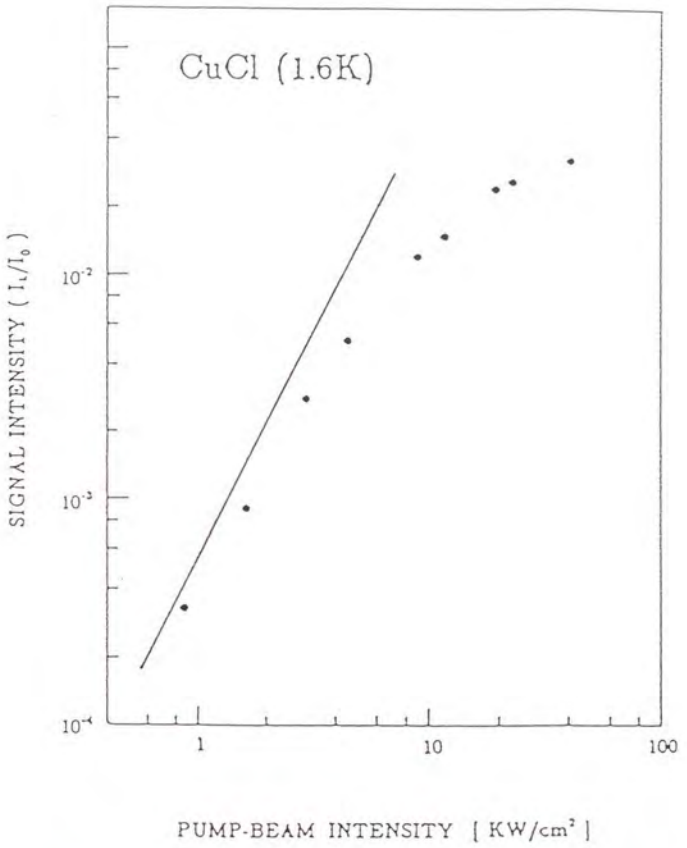

Fig.3-1 Dependence of the nonlinear polarization rotation signal measured at the resonance peak on the exciation laser intensity [31]
Solid line represents a quadratic law.

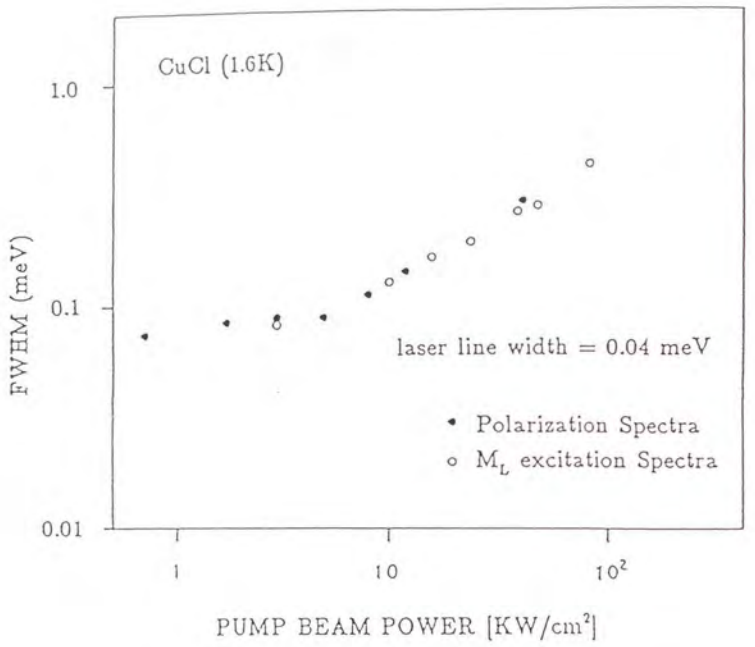

Fig.3-2 Dependence of the linewidth of biexciton resonance on the excitation laser intensity [32]

at the lowest excitation level corresponds to the laser spectral limit as can be seen in Fig.3-2. The level width of the k~0 biexciton state is thought to be very narrow of the order of ~10μeV. Therefore, one has to deconvolute the signal spectum to obtain the correct value of $|\chi^{(3)}|$. However, it is not easy to apply the deconvolution technique to the nonlinear spectroscopy.

On the other hand, when the distribution of biexcitons in momentum space is considered, the effective mass approximation of biexcitons is usually assumed. The effective mass approximation of biexcitons in CuCl was verified in a wide range of Brillouin zone experimentally by Mita et al. as mentioned in Chapter 1. However, the validity of this approximation in the vicinity of the k=0 state has not been confirmed clearly as can be seen in Fig.1-7. S.Shimano et al. measured the optical Stark effects on the $k=2k_l$ biexcion state, where k_l is the wave number of the excitation light whose photon energy is $E_M/2$[33]. They obtained in their experiment that the k=0 state located at lower energy position than that of the $k=2k_l$ state. On the other hand, A.L.Ivanow et al. recently discussed an anomal change of the dispersion curve of biexcitons in CuCl in the close vicinity of k =0 theoretically using the biexciton wave function that includes the polariton effects[34]. They showed that the k=0 state located at slightly higher energy position than that of the $k=2k_l$ state. In this case, biexcitons do not accumulate into k=0 state when the BEC can occur because the k=0 state is not the lowest energy state any more. Therefore, it is necessary to measure the dispersion of biexcitons in the vicinity of the k=0 state in order to check the validity of the effective mass approximation. Unfortunately, it is also difficult by using a conventional pulse dye laser system because the energy defference between the k=0 state and the $k=2k_l$ state estimated from the effective mass approximation is very small, about 57μeV.

In order to clarify these points clear experimentally, a new laser system with a very narrow spectral width of the order of 1μeV and a high enough intensity to observe the two-photon resonance of biexcitons has been developed. By using this laser system, the two-photon resonance of k~0 biexcitons has been examined adopting the two-photon polarization spectroscopy.

3-2. Principle of the two-photon polarization spectroscopy

A schematic illustration of the experimental configuration of the two-photon polarization rotation spectroscopy is shown in Fig.3-3[35]. The pump light beam is circular polarized (σ^+). The probe light beam is linear polarized. These two light beams propagate through a sample.

The linear polarized probe beam can be expressed by the coherent superposition of σ^+ and σ^- components with the same amplitudes. Because the two-photon resonance of biexcitons occurs only in the combination of the pump beam and the σ^- component of the probe beam due to the polarization selection rule mentioned in Chapter 1, the phase and amplitude of only the σ^- component of the probe beam change after passing through the sample. As a result, the polarization of the probe beam becomes elliptical. The intensity of the probe light that is transmitted through the analyzer ,whose polarized axis is completely perpendicular to the polarization of the incident probe beam, is given by

$$I_{sig} = I_0 \times \left| \frac{e^{\Delta n k_0 d} - 1}{2} \right|^2 \qquad (3\text{-}1).$$

where Δn is the nonlinear change of the complex refractive index between the σ^+ and σ^- components of the probe light[35]. k_0 is the wave number of the probe light out side the sample. d is the sample thickness. I_0 is the intensity of the probe beam. Here, the reflection and the linear absorption of the light beams at the sample are neglected in order to make the discussion simple.

When the following condition is satisfied

$$\Delta n k_0 d << 1 \qquad (3\text{-}2),$$

the signal intensity is simply given as

$$I_{sig} = I_0 \times \left| \frac{\Delta n k_0 d}{2} \right|^2 \qquad (3\text{-}3).$$

Because the relation between Δn and $\chi^{(3)}$ is given as

$$\Delta n = \frac{2\pi}{n_0} (\chi^{(3)} |E_{pump}|^2) \qquad (3\text{-}4),$$

one can evaluate the $|\chi^{(3)}|$ from the analysis of the polarization rotation spectrum. Here, n_0 is the linear refractive index of the crystal for the probe light. E_{pump} is the amplitude of the electric field of the pump light.

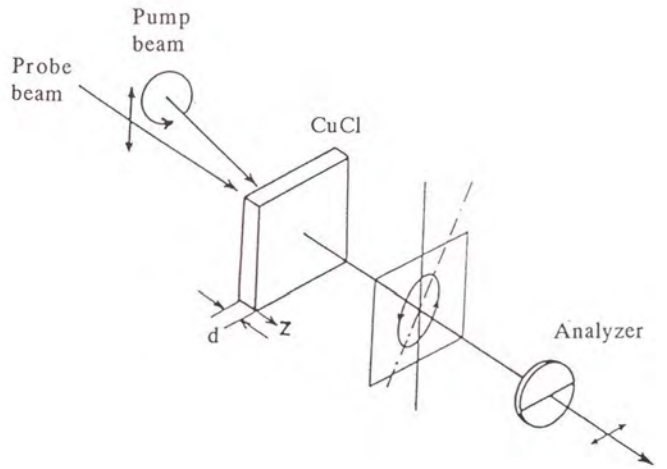

Fig.3-3 Schematic illustration of the principle of the two-photon polarization rotation spectroscopy [35]

3-3. Experiment

3-3-1. New laser system[36]

The set-up of the new laser system is shown in Fig.3-4(A), schematically.

A Ti-sapphire ring laser (Coherent 899-02) was pumped by an Ar^+ laser (NEC GLG3203) of 2W (multi-mode). The output power and the spectral width of the continuous wave (CW) IR light were about 150mW and less than 10MHz, respectively. The stabilities of the intensity and the frequency of IR light were monitored by a photo-diode and a spectral analyzer (Nihon Kagaku Engineering SA40C), respectively. The IR light was amplified by passing through an organic dye medium (Oxazine750 in DMSO) that was pumped by a XeCl laser (Lambda Physik 53 EMC). The power and the repetition rate of the excimer laser were ~2mJ/pulse and 10Hz, respectively. To eliminate the amplified spontaneous emission from the dye cell, a polarizer and a diaphragm were used. The intensity of the amplified IR light as a function of the intensity of the incident CW IR light is shown in Fig.3-5. The linear extrapolation shown by the solid line is quite good within the measured intensity region.

The amplified IR light was converted to UV light by a $LiIO_3$ frequency doubler. After forming the output UV beam into a parallel beam by a cylindrical lens, the monochromatic UV beam was selected by a prism and a slit. The intensity of the UV light as a function of the intensity of the amplified IR light is shown in Fig.3-6. This graph was obtained by changing the intensity of the amplified IR light. The quadratic dependence shown by the solid line extrapolates very well within the measured intensity region. On the other hand, Fig.3-7 shows the intensity of the UV light as a function of the intensity of the CW IR light obtained by changing the intensity of the CW IR light. From Fig.3-5 and Fig.3-6, one can expect that the quadratic dependence will approximate the experimental results. Such a dependence indeed talkes place as shown by the solid line qualitatively.

The pulse duration of the UV light, Δt, was about 10ns. According to our measurements by a pressure scanning air space Fabry-Perot interferometer (Burleigh VS-25) as shown in Fig.3-4(B), the spectral width of the UV light, ΔE, was measured to be less than 1μeV. This value almost corresponds to the transform limit, $\Delta E \sim h/\Delta t \sim 0.4\mu eV$.

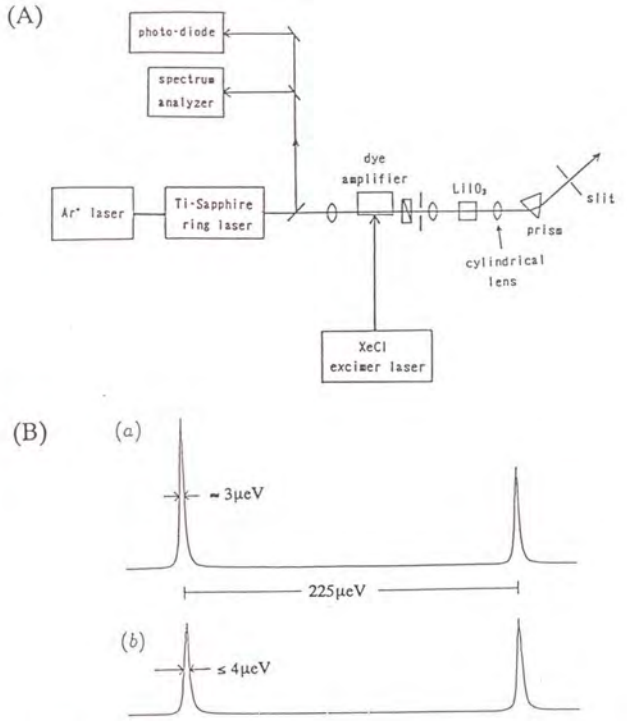

Fig.3-4 (A) Schematic diagram of the new laser system
(B) (a) Resolution and FSR of the Fabry-Perot interferometer used to measure the spectral width of the UV light from the new laser system, (b) Transmitted intensity of the UV light from the new laser system through the interferometer
The difference between the linewidths in (a) and (b) corresponds to the spectral width of the UV light from the new laser system.

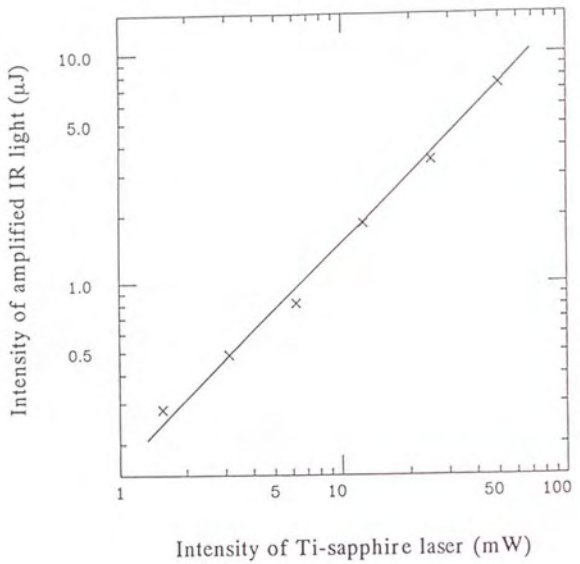

Fig.3-5 Dependence of the intensity of the amplified IR light on the intensity of the incident CW light (Ti-sapphire laser light)
Solid line shows the linear relation.

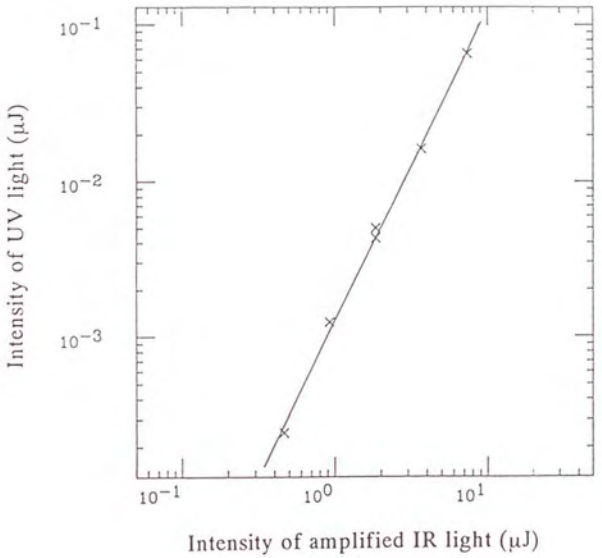

Fig.3-6 Dependence of the intensity of the UV light converted by a SHG crystal on the intensity of the amplified IR light
Solid line shows the quadratic relation.

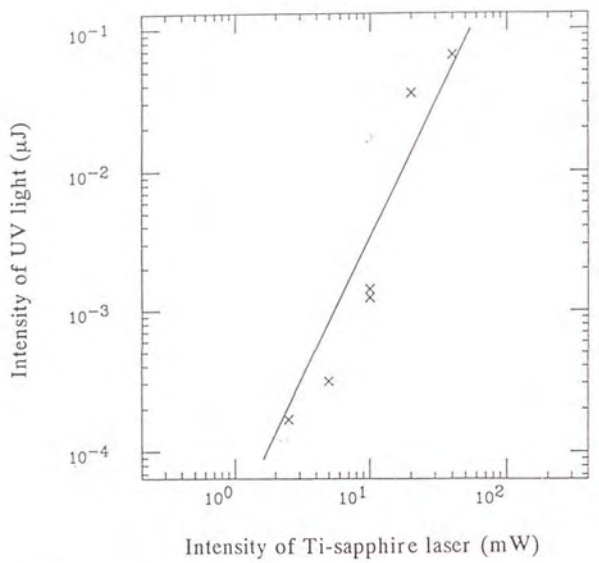

Fig.3-7 Dependence of the intensity of the UV light on the intensity of the incident CW light (Ti-sapphire laser light)
Solid line shows the quadratic relation.

3-3-2. Experimental set-up

Figure 3-8 is a schematic diagram of the experimental set-up for the high resolution polarization rotation spectroscopy[37].

The part enclosed by a dashed line is the newly developed laser system explained in last subsection. The light from this laser system was made circularly polarized and used as the pump light.

Another UV light of broad spectral width (~170μeV) was obtained from a conventional dye laser pumped by the same excimer laser. After passing this UV light through an air space Fabry-Perot interferometer (FSR=225μeV, Finesse=75), UV light of spectral width 3μeV was obtained. This UV light was made linearly polarized and used as the probe light. The intensity of the probe light on the sample surface was about 0.18kW/cm^2. The photon energy of the probe light can be tuned by controlling the air pressure in the interferometer. The intensity of the probe light transmitted through the sample and a crossed polarizer (analyzer) was measured by a photomultiplier (Hamamatsu R654).

Single crystal platelets of CuCl, typically 10μm thick, were held in an immersion-type cryostat at 2K.

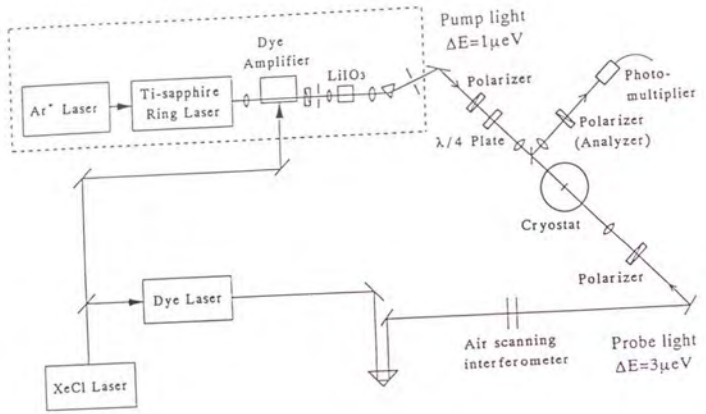

Fig.3-8 Schematic diagram of the experimental set-up for the polarization spectroscopy [37]

The experiment was carried out with two samples of similar quality. The polarization spectra due to the two-photon resonance of the biexciton as a function of the sum of the photon energy of the probe and pump light at several excitation intensity of the pump light are shown in Fig.3-9. The photon energy of the pump light was 3.18622eV. The polarization spectra shown in Fig.3-9(A) were obtained from the sample whose emission spectrum under the weak excitaiton of UV light is shown in Fig.3-10. The thickness of this sample was 9.8μm. This sample is called the sample #1 hereafter. On the other hand, the polarization spectra shown in Fig.3-9(B) were obtained from the sample #2. The corresponding emission spectrum under the weak excitaiton of UV light is shown in Fig.3-11. The thickness of the sample #2 was 22.8μm. The quality of the sample #2 is thought to be a little worse than that of the sample #1 because the shape of the EX-2LO emission has a sharp edge on the low energy side. In this sample, T-exciton polaritons can not relax to the bottle neck completely during their lifetime.

In order to analyze the polarization spectrum obtained in this experiment, the following procedure was used.

The solid line in Fig.3-12 is an example of the polarization spectrum which is the same spectrum shown in Fig.3-9(A)(b). Here, the signal intensity, $J(\omega_{probe})$, is defined by the intensity of the signal light, $I_{sig}(\omega_{probe})$, normalized by the intensity of the probe light, $I_0(\omega_{probe})$, at the frequency of the probe light, ω_{probe}. Two peaks marked by arrows in Fig.3-12 are due to the two-photon resonances of biexcitons. In the present excitation geometry shown in Fig.3-13, the direct coupling between the counter-propagating pump and probe lights occurs. Therefore, the main peak is due to the resonance of $k=K \equiv k_{pump}-k_{probe}=3\times10^3 cm^{-1}$ biexcitons, where k_{pump} and k_{probe} are the wave numbers of the respective light inside the sample. A small peak is due to the coupling between the probe and the pump light that was reflected back at the rear surface of the sample[33]. In this case, the wave

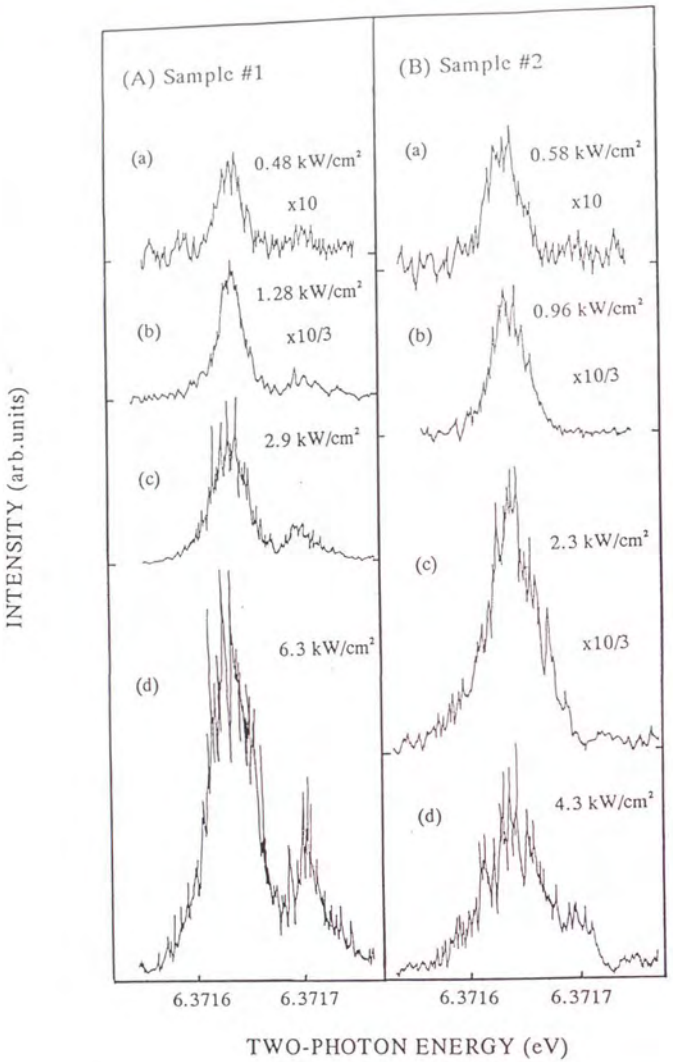

Fig. 3-9 Polarization spectra due to the two-photon resonance of the biexcitons of the sample #1(A) and the sample #2(B) as a function of the sum of the photon energies of the probe and the pump light at several excitation intensities of the pump light
The photon energy of the pump light was 3.18622eV. The intensity of the probe light was about 0.18kW/cm². The intensity of the pump light is shown in the right side of each spectrum.

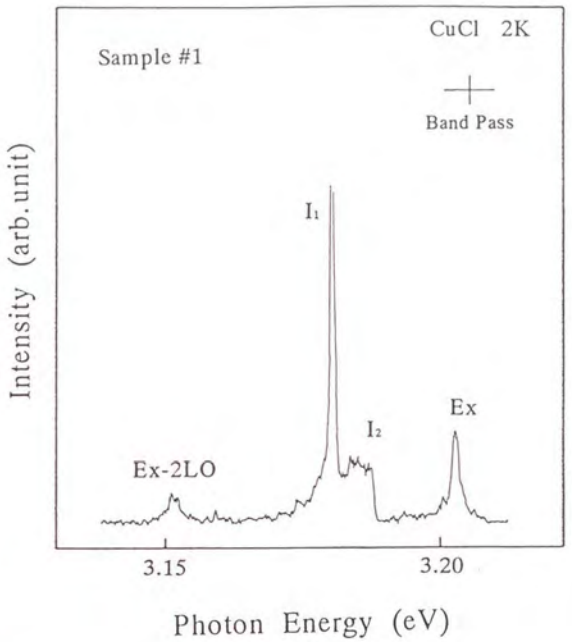

Fig.3-10 Emission spectrum of the sample #1 obtained with a weak excitation of UV light at 2K

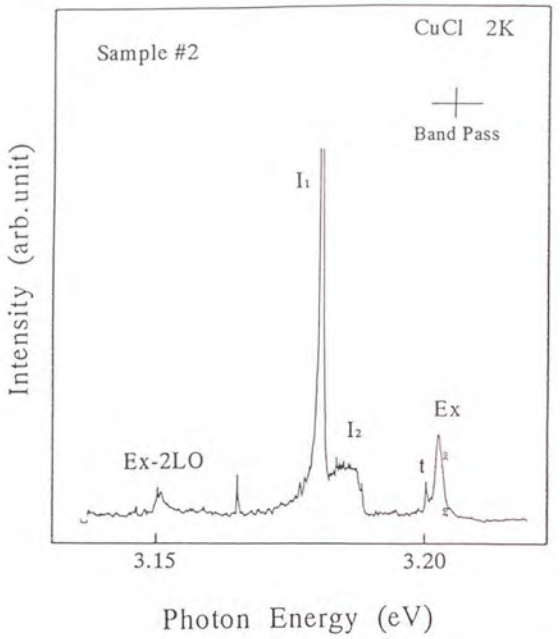

Fig.3-11 Emission spectrum of the sample #2 obtained with a weak excitation of UV light at 2K

number of the excited biexcitons is $k=K' \equiv k_{pump}+k_{probe}=8.85\times10^5 cm^{-1}$.

From eq.(3-3), the signal intensity is given by

$$J(\omega_{probe}) = \frac{I_{sig}(\omega_{probe})}{I_0(\omega_{probe})} = \left|\frac{\Delta n k_0 d}{2}\right|^2 \qquad (3\text{-}5).$$

Δn is expressed by taking account of the reflection of the pump light at the sample surface as

$$\Delta n = \frac{2\pi}{n_0(\omega_{probe})}\left(\chi^{(3)}_K |E_{in}|^2 + \chi^{(3)}_{K'} |E_{ref}|^2\right) \qquad (3\text{-}6),$$

where E_{in} and E_{ref} are the amplitudes of the electric fields of the incident pump light and the pump light reflected back at the sample surface as shown in Fig.3-13, respectively. They are approximately given by taking account of the reflection and absorption at the sample as

$$|E_{in}|^2 \sim \left|\frac{2}{n_0(\omega_{pump})+1}\right|^2 |E_{out}|^2 \frac{1-\exp(-\alpha d)}{\alpha d} \qquad (3\text{-}7)$$

$$|E_{ref}|^2 \sim \left|\frac{2}{n_0(\omega_{pump})+1}\right|^2 \left|\frac{n_0(\omega_{pump})-1}{n_0(\omega_{pump})+1}\right|^2 |E_{out}|^2 \frac{\exp(-\alpha d)-\exp(-2\alpha d)}{\alpha d} \qquad (3\text{-}8),$$

respectively. Here, E_{out} is the amplitude of the electric field of the pump light on the sample surface. $\alpha=50cm^{-1}$ is the linear absorption coefficient of the crystal at the photon energy of the pump light, $\hbar\omega_{pump}=3.18622eV$.

$\chi^{(3)}$ is assumed here to be given by a single Lorentzian as

$$\chi^{(3)}_{K,K'} \cong \frac{C_{K,K'}}{E_{K,K'} - (\hbar\omega_{pump}+\hbar\omega_{probe}) + i\frac{\gamma_{K,K'}}{2}} \qquad (3\text{-}9),$$

where E_k and γ_k are the resonant energies of biexciton states of the wave number $k=K,K'$ obtained from the effective mass approximation of biexcitons and their phenomenological damping constants, respectively. The dashed curve in Fig.3-12 is the result of a theoretical fit assuming $C_K = C_{K'}$. The experimental result is reproduced very well. From this analysis, we confirmed that the $k\sim0$ biexciton state stays lower energy than the $k\sim2k_l$ state and the the effecive mass approximation of biexcitons is valid even in the vicinity of k=0.

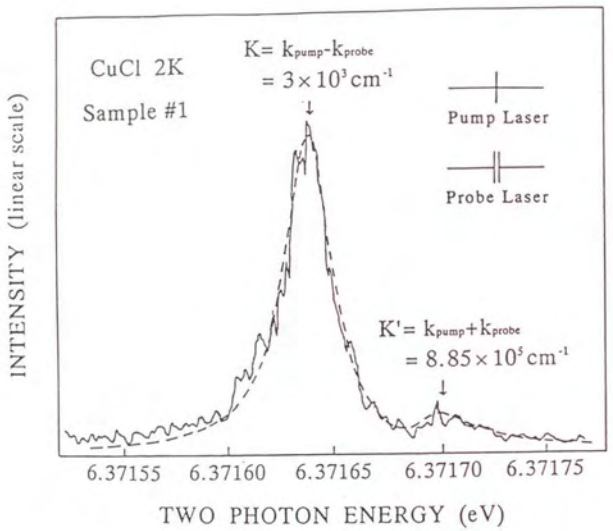

Fig.3-12 An example of the polarization rotation spectra (solid curve) [37]
The photon energy of the pump light was 3.18622eV. The intensity of the probe light was about 0.18kW/cm².
Dashed curve shows the result of the theoretical fit.

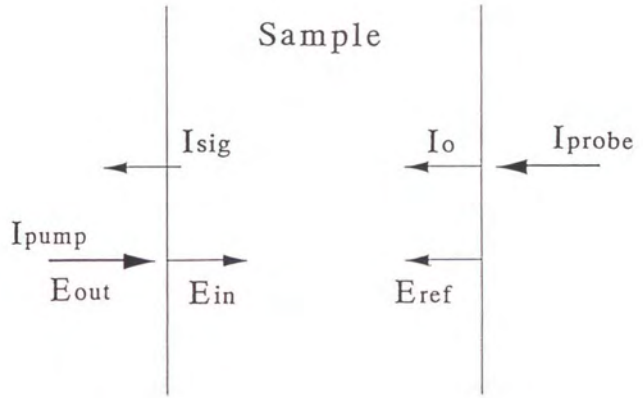

Fig.3-13 Schematic illustration showing the electric fields and the intensities of pump, probe and signal light at the sample

Figure 3-14(a) shows the phenomenological damping constant of the $k=K=3\times10^3 cm^{-1}$ biexciton state of the sample #1 as a function of the pump light intensity, I_{pump}. As usually observed, the damping constant increases with increasing I_{pump}. However, it becomes approximately a constant at the intensity level less than about $1kW/cm^2$. From this analysis, we conclude that the damping constant, $24\pm2\mu eV$, at the low intensity level corresponds to the true width of the biexciton level without saturation effects. Fig.3-14 (b) shows the similar result of the sample #2. In this sample, the true width of the biexciton level without saturation effects is obtained to be $36\pm3\mu eV$. Probably, some relaxation processes of the biexciton state that depend on the sample quality are present.

The signal intensities at the resonant peak of $k=3\times10^3 cm^{-1}$ biexciton state of the sample #1 and #2 are shown in Fig.3-15 (a) and (b) as a function of I_{pump}, respectively. According to eqs.(3-5) ~ (3-9), the signal intensity should be proportional to the square of I_{pump} where the damping constant is independent of I_{pump}. At the intensity level less than $1kW/cm^2$, this quadratic law is valid as shown by a solid line in Fig.3-15. Therefore, the signal in this intensity level is due to the third-order nonlinearity associated with the biexciton resonance without saturarion effects. The values of $|\chi^{(3)}|$ at the resonant peak of the $k=3\times10^3 cm^{-1}$ biexcitons for each sample are obtained to be $(3.0\pm0.9)\times10^{-4}$ esu and $(1.7\pm0.6)\times10^{-4}$ esu, respectively.

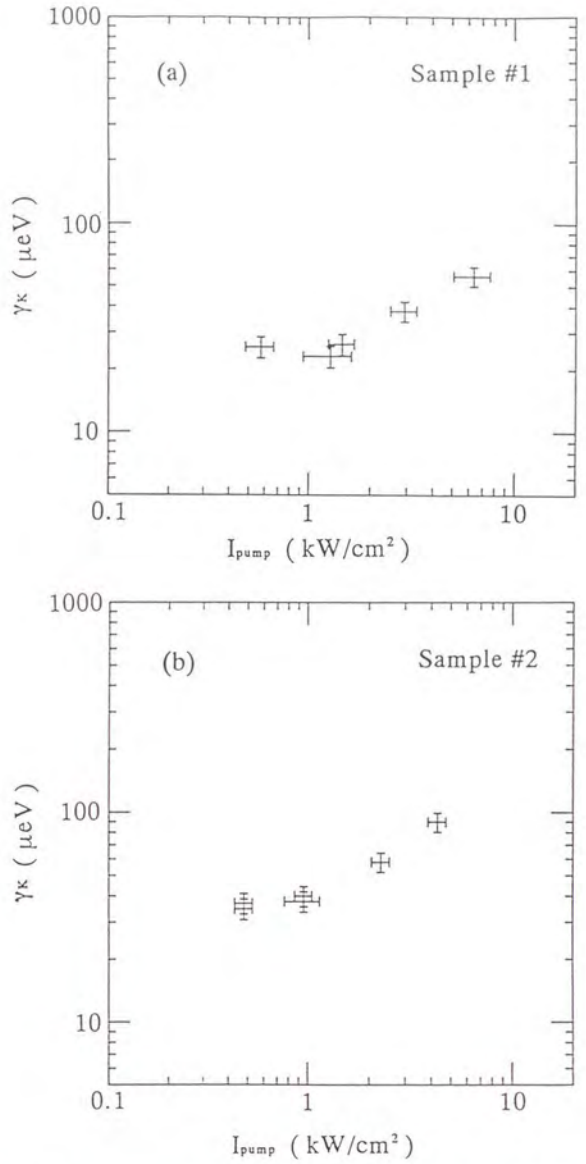

Fig.3-14 Phenomenological damping constants of the $k=3\times10^3 cm^{-1}$ biexciton state in the sample #1 (a) and in the sample #2 (b) as a function of the intensity of the pump light

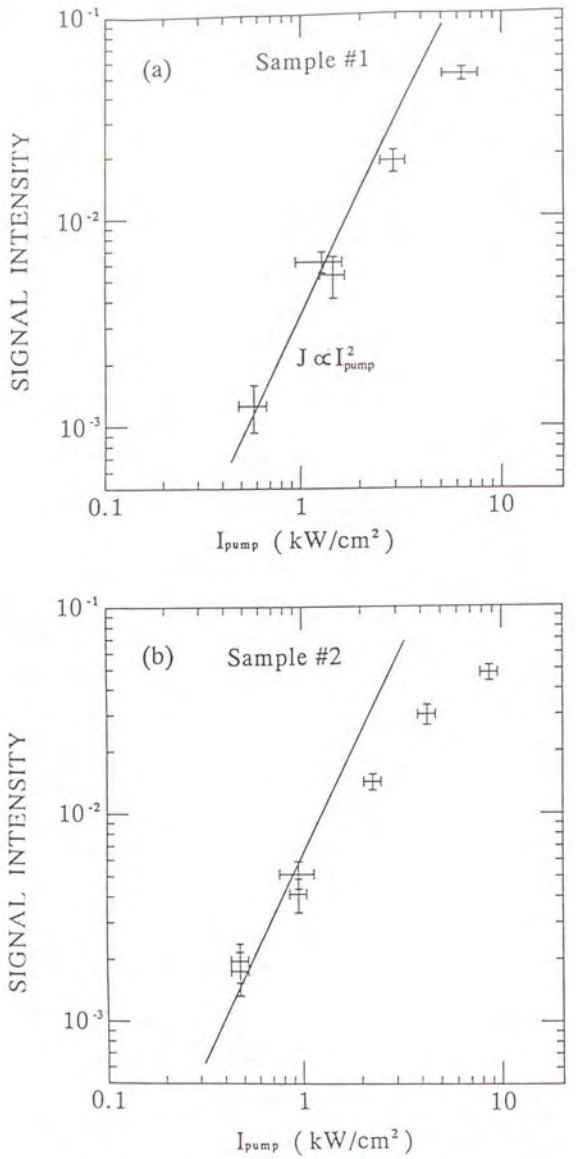

Fig.3-15 Signal intensity at the resonance peak of the k=3x10^3 cm^{-1} biexciton state in the sample #1 (a) and in the sample #2 (b) as a function of the intensity of pump light
Solid line in each figure shows the quadratic law for the eye guide.

A new laser system whose light has a very narrow spectral width of 1μeV and an enough intensity to observe the two-photon resonance of biexcitons was developed using a Ti-sapphire ring laser, a dye amplifier and a $LiIO_3$ frequency doubler. By using this laser system, the two-photon resonance of k~0 biexcitons was measured precisely using the two-photon polarization spectroscopy. The polarization rotation signal associated with the two-photon resonance of k~0 biexcitons obtained in this experiment was analized by a simple model reflecting the experimental conditions.

As the results,

1) The validity of the effective mass approximation of biexcitons in the vicinity of the k=0 state was confirmed.
2) The spectral widths of the two-photon resonance of the k=3x10^3cm^{-1} biexcitons under the weak excitation limit showed sample dependence. They were obtained to be 24±2μeV for the sample #1 and 36± 3μeV for the sample #2, respectively. These widths correspond to the phase relaxation times of 52ps and 35ps, respectively.
3) The values of $|\chi^{(3)}|$ at the resonant peak of the k=3x10^3cm^{-1} biexcitons also showed sample dependence. They were obtained to be $(3.0\pm0.9)\times10^{-4}$ esu for the sample #1 and $(1.7\pm0.6)\times10^{-4}$ esu for the sample #2, respectively.
4) The saturation of $|\chi^{(3)}|$ and the broadening of the spectral width of the biexciton resonance were found to occur beyond the excitation intensity of 1kW/cm^2. The origin of these saturation effects are not clear now.

The very large optical nonlinearity other than the two-photon resonance of biexcitons in CuCl has not been observed in a transparent region of the medium sofar. The two-photon resonance of

biexcitons will be a promising candidate to generate the squeezed light efficiently.

In the experiment, the signal at the excitation intensity less than 0.5kW/cm^2 was in the noise limit. Thus, in order to evaluate $|\chi^{(3)}|$ more quantitatively in the low-excitation regime, one has to improve the signal to noise ratio. In future, this difficulty will be overcomed by using a CW UV light converted directly from CW IR laser light by the frequency doubling. Reflecting large $\chi^{(3)}$ associated with the two-photon resonance of biexcitons, the signal can be observed at a weak excitation intensity of ~1kW/cm^2. This intensity corresponds to the intensity of the light of 10mW focused in the spot of the 10μm diameter. Such a CW UV light can be generated by the frequency doubling of a single frequency Ti-sapphire ring laser with an external cavity[38]. By using such a CW light source, the spectral resolution will be extremely enhanced to be ~0.01μeV. In this case, the duty ratio will be also considerably improved, i.e., in 10^7 times in comparison with the present experimental condition in which the duty ratio was 10^{-4}sec$\times$ 10Hz=10^{-7}. Another advantage of the CW light is that one can measure the signal in the photon counting mode very easily. The measurement of the two-photon(polariton) pair correlation associated with the two-photon (polariton) decay of k=0 biexcitons will be very easy because the polarization selection rule of the transition is very simple as mentioned in Chapter 1. It seems that further progress in the experiments on the two-photon state will be due to this new system.

4. Investigation of the BEC of biexcitons by the phase-conjugation spectroscopy (PCS)

4-1. Introduction

As mentioned in Chapter 1, the biexciton system in CuCl is one of the suitable candidates to realize and to examine the BEC phenomenon. The possible BEC of the biexcitons in CuCl has been examined extensively both experimentally and theoretically.

Conventionally, a distribution of the biexcitons in momentum space is studied by observing a shape of the M-emission band. The typical spectrum of the M-emission observed under a strong optical excitation is shown in Fig.4-1. In this case, the biexcitons have been created through the collisions of the excitons previously excited by the laser light. The shape of the M-emission band can be approximated by Maxwellean (see the dashed curve in the Fig.4-1[39]). The corresponding Maxwell distribution of biexcitons is shown schematically in the right side of Fig.4-2.

On the other hand, the momentum-selective (**k**-selective) excitation of biexcitons can be done by the GTA as mentioned in Chapter 1. By this excitation method, one can prepare the initial distribution of biexcitons in the very narrow area of momentum space. In this case, one can make the temperature of biexciton system very cold. N.Nagasawa et al. found the very sharp structure in high energy edge of the M-emission band that is shown in Fig.4-3, when the biexcitons were created in CuCl single crystals by the two-photon excitation[39]. They interpreted that this emission was a manifestation of the BEC of the biexcitons. After that, however it was found that for the same experimental conditions the two-photon Raman scattering can arise at the similar energy positions.

Later, N.Peyghambarian et al. also examined the M-emission observed at the two-photon excitation of the biexcitons in evaporated films of CuCl[40]. They found that the shape of the M-emission obeyed the Bose-Einstein distribution. They also found that the sharp structure similar to the structure observed by N.Nagasawa appeared when the excitation intensity exceeded some

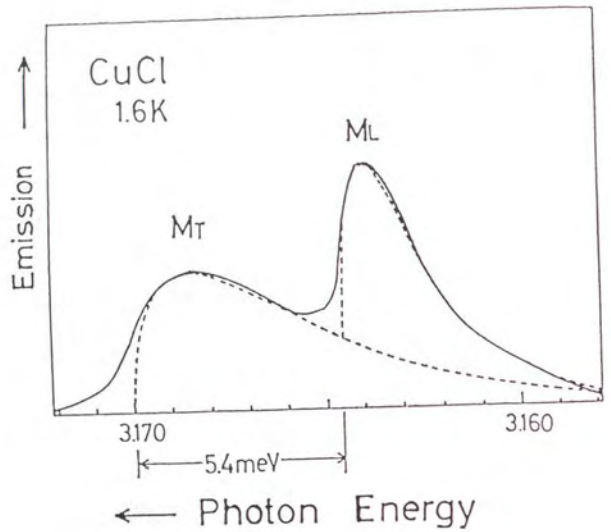

Fig.4-1 Spectrum of M-emissions observed by the N_2-laser excitation (solid curve) [39]
Dashed curve shows the Maxwell distribution.

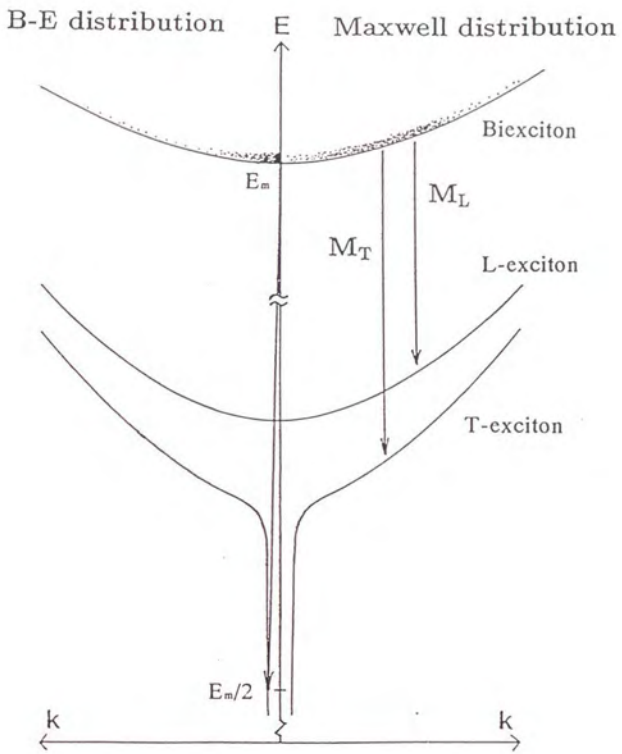

Fig.4-2 Radiative processes of biexcitons
The density of dots on the biexciton dispersion curve on right side shows the Maxwell distribution of biexcitons. The density of dots on the biexciton dispersion curve on left side shows the Bose-Einstein distribution of biexcitons.

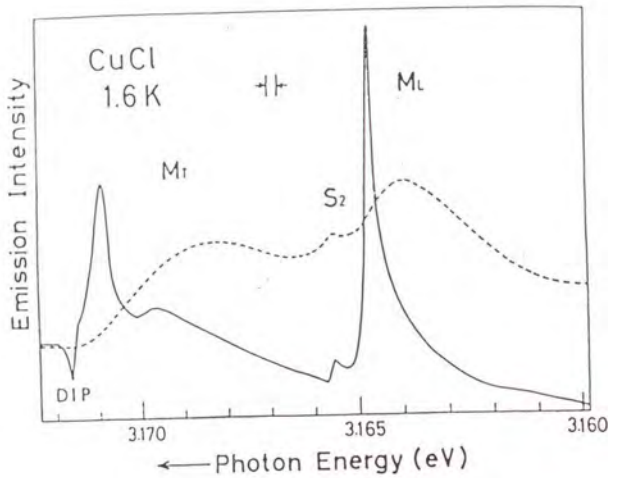

Fig.4-3 Emission spectrum observed at the two-photon excitation of biexcitons (solid curve) [39]
Dotted curve shows the emission spectrum observed at a photo-excitation of the Z_3-exciton band.

threshold. In this excitation configuration, the wave number of the excited biexctions is $2\mathbf{k}_P$ as shown in Fig.4-4, where $\mathbf{k}_P$ is the wave vector of the excitation light in the crystal. They ascribed this structure to the biexcitons condensed in $\mathbf{k}=2\mathbf{k}_P$. This pump induced transient condensation is due to the strong initial excitation of the $2\mathbf{k}_P$ biexcitons. Under these conditions, a small number of k=0 biexctions marked by an open circle in Fig.4-4 was added by another weak laser light. Then, they found that the shape of the emission from the added k=0 biexctions strongly depended on the presence or the absence of strong excitation of the $2\mathbf{k}_P$ biexcitons. The result is shown in Fig.4-5. In the presence of the $2\mathbf{k}_P$ biexctions, the shape of the M-emission band was similar to the sharp structure. They interpreted this phenomenon as attraction of the excess biexcitons beyond the critical density to the condensed biexciton state at $\mathbf{k}=2\mathbf{k}_P$.

For quasi-equilibrium BEC, the biexcitons will condense into the lowest energy state. Since the effective mass approximation of biexcitons in CuCl has been verified even in the vicinity of k=0, one can expect that excess biexcitons will be accumulated in the k=0 state when the biexciton density exceeds the critical density for the BEC. This is shown in the left side of Fig.4-2. However, contrary to the possible pump induced condensation in $\mathbf{k}=2\mathbf{k}_P$, the observation of the natural quasi-equilibrium condensation at k=0 is very difficult due to the following reasons:

1) The polarization selection rule and the momentum conservation law are not satisfied at the same time in the M_L-emission process for the k=0 biexcitons. Therefore, the M_L-emission process of the k=0 biexcitons is forbidden.

2) M_T-emission process of the k=0 biexcitons is difficult to be observed due to the polariton effects of the T-exciton.

Therefore, a new method to examine the k=0 biexciton state should be developed. Furthermore, the important informations about the coherence are usually missed in the measurement of luminescence. The new methods to detect the coherence inherent in the BEC are highly desirable.

In the international cooperative project in the framework of the CNRS-JSPS Sientific Program, A.Mysyrowicz proposed the new method to study the k=0 biexcitons. His idea was as follows.

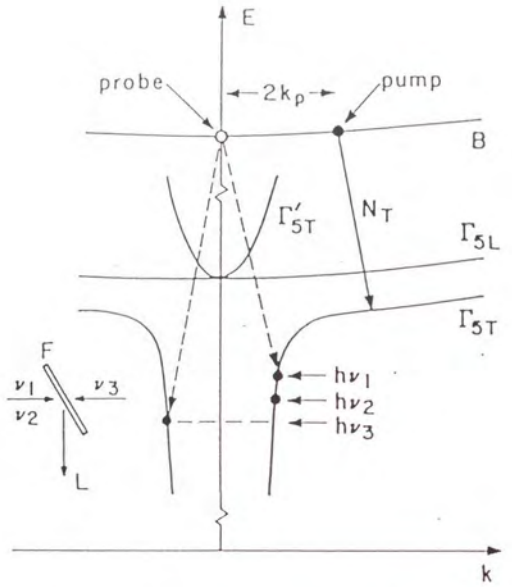

Fig.4-4 Schematic explanation of the experiment done by N.Peyghambarian et al. [40]

Schematic exciton and biexciton dispersion curves show the biexciton excitation and the radiative decay processes near k=0. B, Γ_{5L} and Γ_{5T} indicate the biexciton, the L-exciton and the T-exciton, respectively. Geometry for the pump and probe experiment is shown in the inset at lower left; ν_1 and ν_3 are the frequencies of the counter-propagating probe laser beams, ν_2 is the frequencies of the intense resonant pump laser beam, L is the detected luminescence in the nearly backward direction relative to the pump beam.

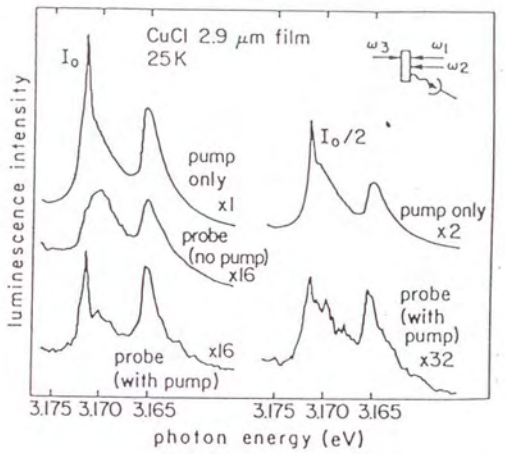

Fig.4-5 Biexciton luminescence at 25K for the excitation and detection conditions described in Fig.1-19 [40]

If the BEC of biexcitons occurs, macroscopic coherence will appear at the k=0 state. Thus, one can treat the possible biexciton condensate as a macroscopic nonlinear polarization. This point of view was noticed by G.Lasher in exciton system[41]. This polarizaton corresponds to the macroscopic nonlinear polarization generated by the two-photon excitation of the k=0 biexcitons. Thus, this nonlinear biexciton polarization can generate the phase-conjugation (PC) light.

Usually, the PC light is generated using the three coherent laser beams in the geometry shown in Fig.4-6. Details of the PC light generation and its realization in the polarization picture are explained in Appendix B. Here, the time sequence of the photon events responsible for the generation of the PC light is explained in order to see why the PC can give an evidence of the BEC of biexcitons.

The PC signal at the biexciton resonance is predominantly due to the two-photon resonance term. This term can be decomposed in the following sequence of photon events as shown in Fig.4-7(A): first, the two counter-propagating pump beams induce a coherent electronic excitation, i.e., create virtual biexciton state. This macroscopic state oscillates at frequency 2ω with respect to the crystal ground state. The probe beam then induces the two-photon transition back to the crystal ground state, generating thereby a counter-propagating signal beam. The magnitude of the signal is proportional to the pump induced population of the k=0 state. Let us consider now the case of the BEC of biexcitons. In this case, the coherent macroscopic biexciton polarization with the frequency 2ω inherent in the BEC of biexctions can arise spontaneously. Therefore, one can expect the appearance of the PC signal even if the counter-propagating pump beams are absent as shown in Fig.4-7(B).

Within his proposal, several experiments had been done in the framework of the international cooperative project in the CNRS-JSPS Sientific Program. However, the appearence of the PC light without the counter-propagating pump beams has not been observed sofar.

There are two obstacles which interfere the direct observation of the PC light from the biexction condensate state. First difficulty is due to the features of the experiment. Usually, stray light of the

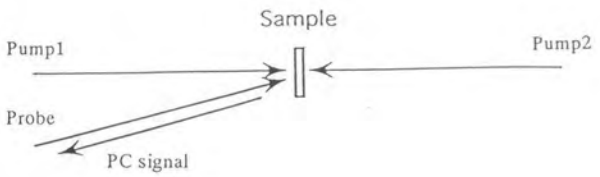

Fig.4-6 Generation of the phase-conjugation in usual case

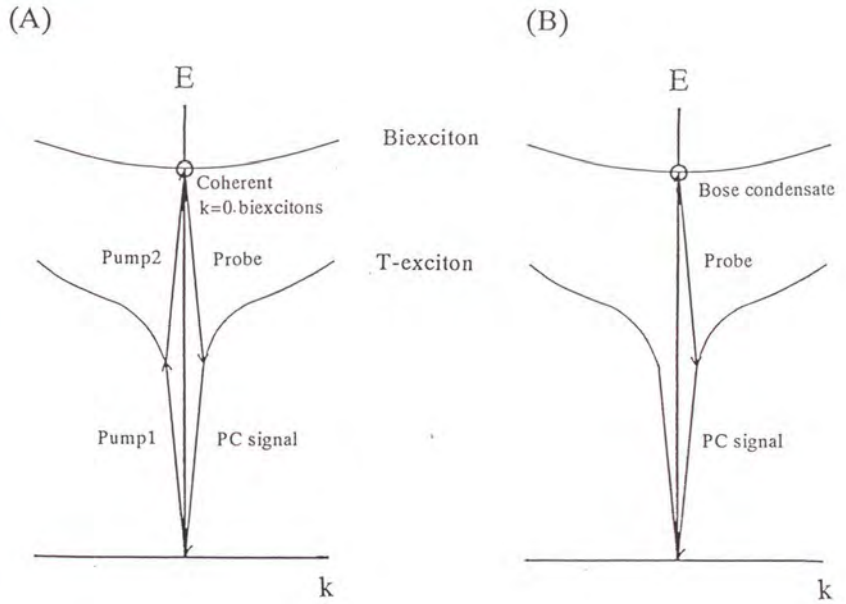

Fig.4-7 Schematic illustration of the photon events in the generation of the PC light in usual case (A) and in the case of the BEC of biexcitons (B)

laser light is too strong to find the PC signal and causes the large background photo-current of the detection. Therefore, the detecting position of the PC light should be removed far from the sample position in order to make this background as small as possible. However, it is not so easy to confirm in such a situation that the PC light enter the detector even if the PC light appears. The other difficulty is related to kinetics of the biexciton BEC. In the experiment, the pulse dye laser (The pulse width is about 10ns.) was used to generate the high density biexcitons. If the time for the BEC formation is longer than this pulse width, the phase transition to the BEC will not occur. Then the PC signal associated with the BEC will not appear. The time required for the formation of the BEC has been calculated by the several groups[42][43][44][45]. Recently, Y.Kagan et al. distinguish two regimes: the first formation of a quasi-condensate which are characterized by suppression of the density fluctuations, and the formation of a true condensate with suppressed phase fluctuations and long-range order. The second process is considerably slower than the first one[45].

To overcome these difficulties, N.Nagasawa suggested to observe the change of the PC signal generated by the two weak counter-propagating pump laser beams and the weak probe laser beam in the presence of the high density incoherent (thermal) biexcitons. In this case, the detection of the PC light and the reduction of the background noise signal become easy. Moereover, the stimulation of the transition to the BEC will be possible because the initial coherent k=0 biexcitons may act as a seed accelarating the phase transition into a true condensate[42].

Let us consider an experimental situation. Normally, the injection of the additional particles results in the destruction or deterioration of a prepared coherent biexciton state due to collision-induced fast dephasing processes. This leads to a decrease of the PC signal, because of collision-induced scattering of biexcitons out of the k=0 state. However, a new situation occurs if the intensity of the incoherent pump light is sufficient to create a biexciton density exceeding the critical density for the BEC. In this case, one expects the opposite behavior, i.e., an increase of the PC signal. If the density of the incoherent biexcitons will exceed the critical density at a given temperature, part of them will relax to the coherent macroscopic state at k=0 and will enhance the

PC signal.

Since the PC light has time-inversion symmetry with respect to the probe light, the signal beam has the same divergence as that of the probe beam. This means that it is possible to reduce the detection solid angle of the signal by appropriate spatial filtering and therefore to restrict the phase space of the observable decaying biexcitons to a few modes around k=0. This will be shown in section 4-4. "Analysis and discussion". From the number of radiating biexciton modes, it is possible to estimate the change of the occupation number per biexciton mode corresponding to the increase of the PC signal. This change can be interpreted as a contribution from the incoherent biexcitons relaxed to the condensate macroscopic state at k=0.

The experiments have been carried out following this scheme.

4-2. Probe of the k~0 biexciton state by PCS in the degenerate configuration[46][47]

4-2-1. Introduction

The PC signal at the two-photon resonance of the biexcitons was monitored alternately in the presence and in the absence of an intense light source that creates a high density of incoherent biexcitons. Hereafter, such a light source is referred as the incoherent pump light.

Firstly, we monitored the PC light in the degenerate configuration. In this case, the photon energies of the pump light and the probe light are same. We used this configuration due to the following reasons:

1) As shown in Appendix B, the phase matching condition is automatically satisfied in this configuration .
2) Only one dye laser system is necessary to generate the PC light.

4-2-2. Experiment

The experimental set-up is shown schematically in Fig.4-8. A Hansch type dye laser system excited by an excimer laser (Lambda Physik 53EMC) was used as a light source. Active medium of the dye laser was BBQ in p-dioxane. The laser light from this dye laser system was divided into three beams by a half mirror and a polarized beam splitter. These laser beams were used to generate the PC light. The spectral width and the pulse duration of this light were 26μeV and 10ns, respectively. The polarization of each laser beam was made circular by a polarizer and a quarter wave plate in order to excite the k=0 biexcitons predominantly. Details of the polarization selection rule are explained in Appendix B. After going through a pinhole with the diameter of 2mm, each laser beam was focused on the sample surface. The diameter of the beam spot on the sample surface was about 100μm. The external angle between the pump and the probe axis was 10 deg. This corresponds to the internal angle of 3.6 deg at the two-photon resonance energy of biexcitons. The sample thickness is usually about 10μm. Thus, the pump beams and the probe beam overlap completely each other in the sample. The PC light was extracted by an half mirror and detected by a photo-multiplier (Hamamatsu R654) at the distance of 3m apart from the sample. Photo-current from the photo-multplier was measured by a pico-ammeter and recorded by a chart recorder. It was verified that the PC light disappeared if any of the pump or the probe beams was blocked. It was also verified that the PC light had a circular polarization opposite to that of the probe beam.

Broad-band super-radiant emission from a dye cell pumped with the same excimer laser was used as an incoherent pump light. The intensity of the incoherent pump light could be continuously changed by a variable attenuator (Newport 935-5). This attenuator was driven by a pulse-motor up to the maximum intensity of 440kW/cm^2. The spectral bandwidth of the incoherent pump light was limited by a filtering monochromator to a width of 16meV. The corresponding photon energy is adjusted so as to cover the Z_3-exciton band as shown in Fig.4-9. Therefore, the intense incoherent pump light did not generate biexcitons directly. In this case, the biexcitons can be created

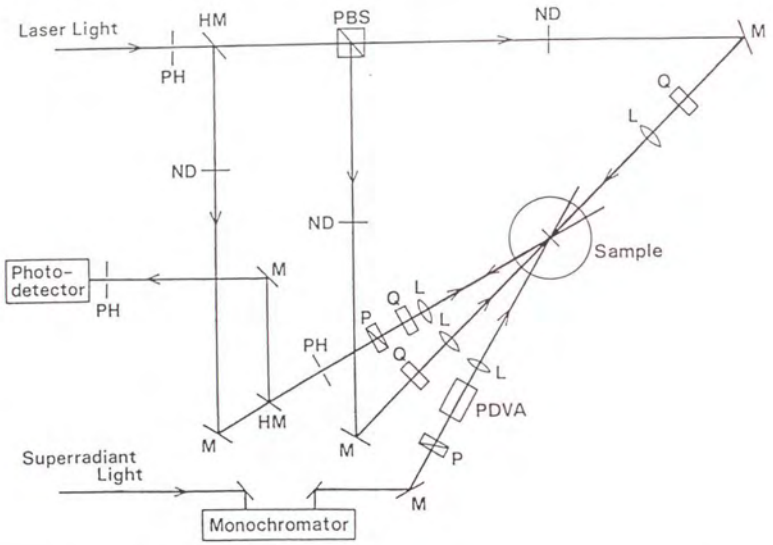

Fig.4-8 Schematic diagram of the experimental set-up in the degenerate configuration [46]
HM : half mirror, M : mirror, ND : neutral density filter, P : polarizer, Q : quarter wave plate, PH : pin hole, PBS : polarized beam splitter, L : lens, PDVA : variable intensity attenuator driven by a pulse-motor

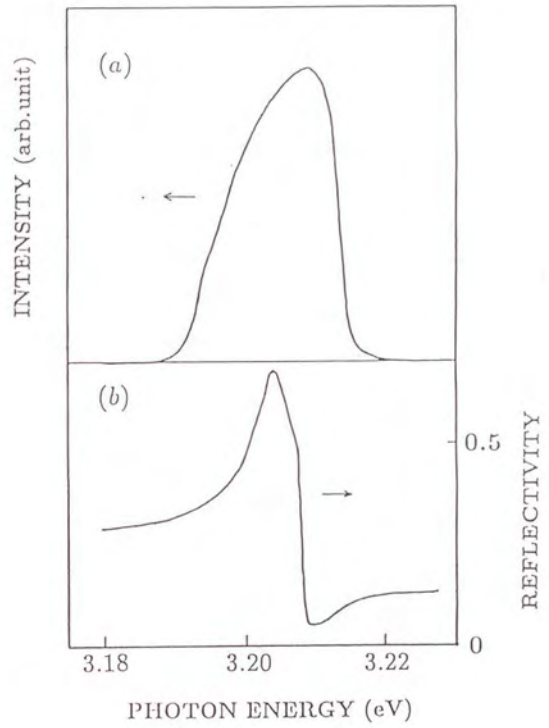

Fig.4-9 Spectrum of the incoherent pump light (a) and the reflection spectrum of CuCl at 2K (b) [46]

indirectly via bimolecular formation from an initially random population of free excitons. The incoherent pump light was focused on a sample surface with a diameter of the spot of about 200μm. This spot completely covered the spots of the laser beams that were used to generate the PC light. The pulse duration of the incoherent pump light was also about 10ns.

Samples were cooled in an immersion type cryostat at 2K.

In this experiment, four light beams should overlap each other not only spatially but also temporally. The procedure of the overlapping is as follows:

- Before setting the cryostat

1) Light pulse of each laser light was detected by a pin photo-diode at the sample position. The arrival time of each laser pulse to the photo-diode was measured by a boxcar integrator (PAR 163&162). This integrator was triggered by a laser light from the excimer laser detected by another pin photo-diode near the excimer laser. The arrival time of each light pulse was made identical by adjusting the length of the optical paths.

2) A white paper was set at the sample position. Four light spots on the paper were overlapped on the same position by adjusting the position of the lens. Because the two pump light beams should counter-propagate, the position of the spots is determined by the axis of the pump beams. The spots of the probe light and the incoherent pump light were checked to be overlapped with the spot of the pump light by eyes.

- After setting the cryostat

3) The spectrum of the incoherent pump light was set to cover the two-photon resonance energy of biexcitons. The photon energy of the laser light was also set around the two-photon resonance energy of biexcitons. Then, the nonlinear polarization rotation signal associated with the two-photon resonance of biexcitons was measured by the combination of the incoherent pump light and each laser light.

4) The nonlinear polarization rotation signal was made maximum by fine adjusting of the spot

position of each laser light beam. This is done by adjusting the position of the correponding lens. Usually, the PC light appears after this adjustment.

5) Because the spot size of the incoherent pump light is very large, one can not confirm that the spots of the pump beams and probe beam overlap completely each other. Therefore, the intensity of the PC light reached its maximum only after accurate adjusting the spot positions of the pump and probe light beams. Thus, the spots of the pump beams and probe beam overlapped completely each other.

6) In order to receive the maximum nonlinear polarization rotation signal by the combination of the incoherent pump light and each laser light, we tuned again the spot position of the incoherent pump light. Thus, the spots of the pump and probe beams overlapped each other at the center of the spot of the incoherent pump light.

The excitation spectra of the PC signal in two samples of different quality in the presence (a), and the absence (b), of the incoherent pump light of 400kW/cm^2 , and the corresponding differential signal (c)=(a)-(b) are shown in Fig.4-10. The intensities of the pump(forward) light, the pump(backward) light and the probe light were 50kW/cm^2, 50kW/cm^2 and 15kW/cm^2, respectively. Because the shape of each excitation spectrum has a simple smooth structure with a peak at the two-photon resonance of k=0 biexcitons, we attribute this PC signal to the 2ω coherence associated with the biexciton resonance rather than the effects of the population grating of excitons.

The spectra shown in Fig.4-10(A) were obtained in a sample of higher quality. The corresponding emission spectrum under the weak excitation by UV light is shown in Fig.4-11. Hereafter, this sample is called the sample A. The intensities and the shapes of the emission of the T-exciton polaritons and its 2LO-phonon side band emission are strong and sharp, respectively. On the other hand, the emissions due to the defects and impurities are rather weak. In particular, the I_2 emission whose photon energy overlaps the two-photon resonance energy of biexcitons did not appear. The thickness of the sample was determined from the interference fringes in the reflection spectrum of the sample to be 21μm. In this sample, the excitation spectrum of the PC signal was very narrow and the intensity of the PC signal was enhanced up to 30% under the presence of the incoherent pump light. The enhancement of the PC signal occurs only at the peak of the biexciton resonance over a very narrow spectral width of 25μeV. This width corresponds to the laser light linewidth.

On the other hand, the differential spectrum was negative in a sample of lower quality as shown in Fig.4-10(B). Hereafter, this sample is called the sample B. In this sample, a slightly broader spectrum was observed. The emission spectrum of this sample under the weak excitation by UV light is shown in Fig.4-12. The emission of the T-exciton polaritons and its 2LO-phonon side band

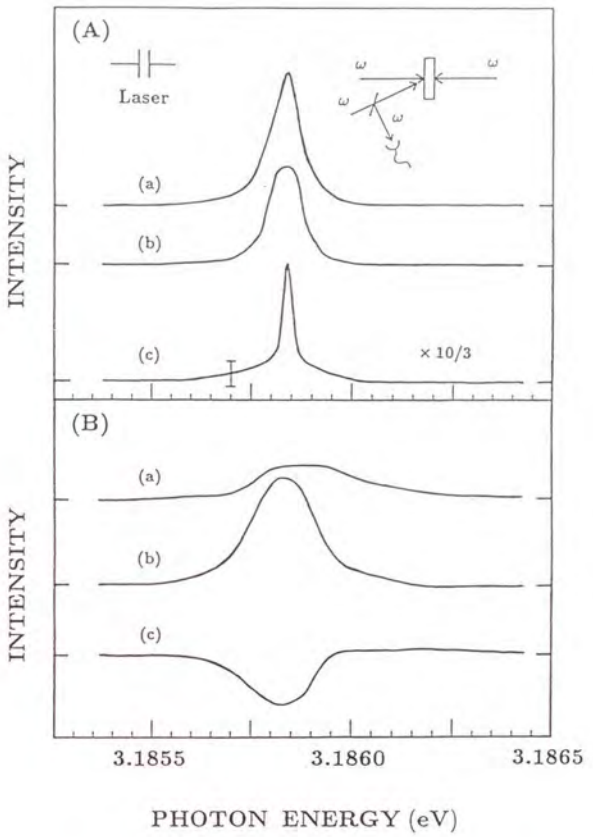

Fig.4-10 Excitation spectra of the PC light for two CuCl samples of different quality, (A) of higher quality and (B) of lower quality, shown successively (a) in the presence and (b) in the absence of the incoherent pump light. (c) is the differential signal, (a) - (b) [47]
The intensities of the pump(forward) light, the pump(backward) light, probe light and the incoherent pump light were 50kW/cm^2, 50kW/cm^2, 15kW/cm^2 and 400kW/cm^2, respectively.

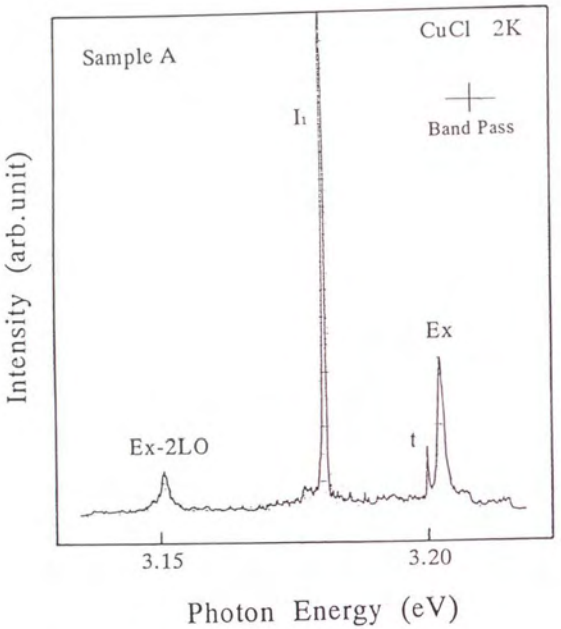

Fig.4-11 Emission spectrum of the sample A obtained with a weak excitation of UV light at 2K

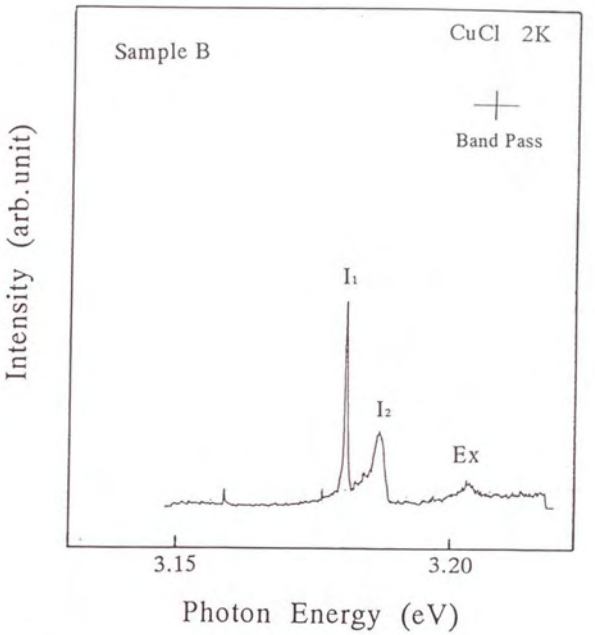

Fig.4-12 Emission spectrum of the sample B obtained with a weak excitation of UV light at 2K

emission did not appear clearly. On the other hand, I_2 emission was strong. The thickness of this sample was 7μm.

The intensity of the PC signal at the peak of the two-photon resonance of the k=0 biexcitons as a function of the intensity of the incoherent pump light is shown in Fig.4-13 for the sample A. Here, the intensity of the PC signal is normalized on the intensity of the PC signal in the absence of the incoherent pump light. The intensities of the pump(forward) light, the pump(backward) light and the probe light were 50kW/cm², 50kW/cm² and 15kW/cm², respectively. In this experiment, the intensity of the PC signal was enhanced by about 30% within the intensity region of the incoherent pump light. On the contrary, the monotonous decrease of the PC signal with the increase of the intensity of the incoherent pump light was observed in the sample B. The coherence of the k=0 biexciton state in the sample B is thought to be destroyed by collisions with the incoherent excitons or biexcitons created by the incoherent pump light.

The excitaiton spectra of the PC signal in the sample A at the several intensities of the pump and probe light are shown in Fig.4-14. The spectra in the absence and in the presence of the incoherent pump light are shown in the left side and the right side of the figure, respectively. When the intensities of the pump and probe light increase, the broadening of the spectrum is observed. This is usually observed in the high intensity excitation of biexctions. It was found that the enhancement of the PC signal strongly depended on the intensities of the pump and probe light. When the intensities were too weak (see Fig.4-14(a)) or too strong (see Fig.4-14(c)), the efficiency of the enhancement decreased. When the pump light was cut, the PC light did not appear even in the presence of the incoherent pump light. The presence of the coherent k=0 biexcitons created by the counter-propagating pump laser beams is thought to be crucial for this phenomenon.

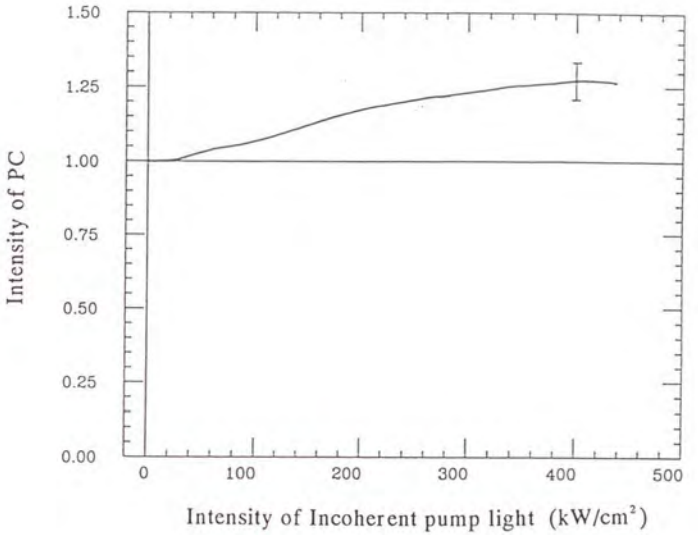

Fig.4-13 Change of the PC intensity as a function of the intensity of the incoherent pump light [46]
Intensities of the pump(forward) light, the pump(backward) light and the probe light were 50kW/cm², 50kW/cm² and 15kW/cm², respectively.

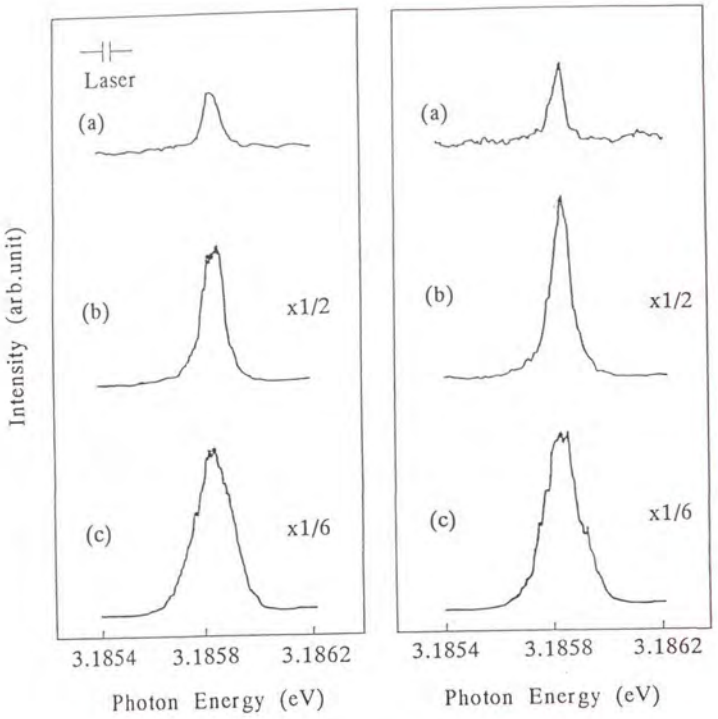

Fig.4-14 Excitation spectra of the PC signal at three defferent intensities of the laser light in the absence (left side) and in the presence (right side) of the incoherent pump light, 400kW/cm^2
Intensities of the pump(forward) light, the pump(backward) light and the probe light were (a) 25kW/cm^2, 25kW/cm^2 and 7.5kW/cm^2, (b) 50kW/cm^2, 50kW/cm^2 and 15kW/cm^2, (c) 100kW/cm^2, 100kW/cm^2 and 30kW/cm^2, respectively.

4-2-4. Sample fatigue

In Chapter 2, it was mentioned that samples suffer a damage by the humidity when they are exposed to air. Samples are also damaged gradually by the thermal cycle from a room temperature to a liquid helium temperature. In every experiment with the PC light, the sample quality was checked by measuring the reflection and emission spectra. These spectra are shown in Fig.4-15 and Fig.4-16, respectively. Here, the change of the quality of the sample A is shown.

In the first experiment, the visibility of the interference fringes observed in the reflection spectrum was good as shown in Fig.4-15(a). The sample surface is thought to be smooth and the scattering of polaritons is thought to be very small. The shapes of the emission of the T-exciton polaritons and its 2LO-phonon side band emission were very sharp as shown in Fig.4-16(a). In this case, the lifetime of the T-exciton polaritons is very long of the order of ns[30]. The sharp emission appeared at 3.189eV is thought to be due to impurities. However, the origin of this emission is not clear. The emission denoted by t in the figure is due to the t-exciton. Probably, a weak stress was present in the sample[3].

In the second experiment, the visibility of the interference fringes became worse than that observed in the first experiment as shown in Fig.4-15(b). Increase of the roughness of the sample surface or increase of the scattering of polaritons is supposed. The emission of the T-exciton polaritons and its 2LO-phonon side band emission were still sharp as shown in Fig.4-16(b). The lifetime of the T-exciton polaritons is thought to be still very long of the order of ns. On the other hand, the relative intensity of I_1 emission with respect to the emission of the T-exciton polaritons increased in comparison with the first experiment. The localization of I_1 emission at the sample surface was observed by T.Hatano et al. by using the spatially resolved spectroscopy[48]. Thus, I_1 emission is thought to reflect the surface condition of the sample. The surface of the sample is thought to be damaged between the first experiment and the second experiment. The emission at 3.189eV disappeared. The origin of this behavior is not clear up to now.

In the third experiment, the visibility becomes very bad as shown in Fig.4-15(c). The intensity of I_1 emission became so strong that it could be observed in the reflection spectrum. The shape of the 2LO-phonon side band emission was deformed very strongly as shown in Fig.4-16(c). It is supposed that the excitons are destroyed before they relaxed to the bottleneck region.

The further forth and fifth experiments followed this tendency. The intensity of I_1 emission increased monotonously while the 2LO-phonon side band emssion becomes too weak to be observed.

The enhancement of the PC signal mentioned in last subsection was observed in the second experiment. After the second experiment, the excitation spectrum of the PC signal showed a complicate structure as shown in Fig.4-17. The origin of this structure is not clear. Such a structure can not be explained by the third order nonlinear exciton-biexction polarization given by eqs.(B-6) and (B-7) in Appendix B. In this case, the enhancement of the PC signal was not observed. The intensity of the PC signal decreased monotonously with the increase of the intensity of the incoherent pump light.

Because the PC signal was not measured in the first experiment, the corresponding PC signal is unknown. However, one can expect that a similar or even more enhancement of the PC signal will be observed in comparison with the second experiment because the sample quality in the first experiment is better than that in the second one.

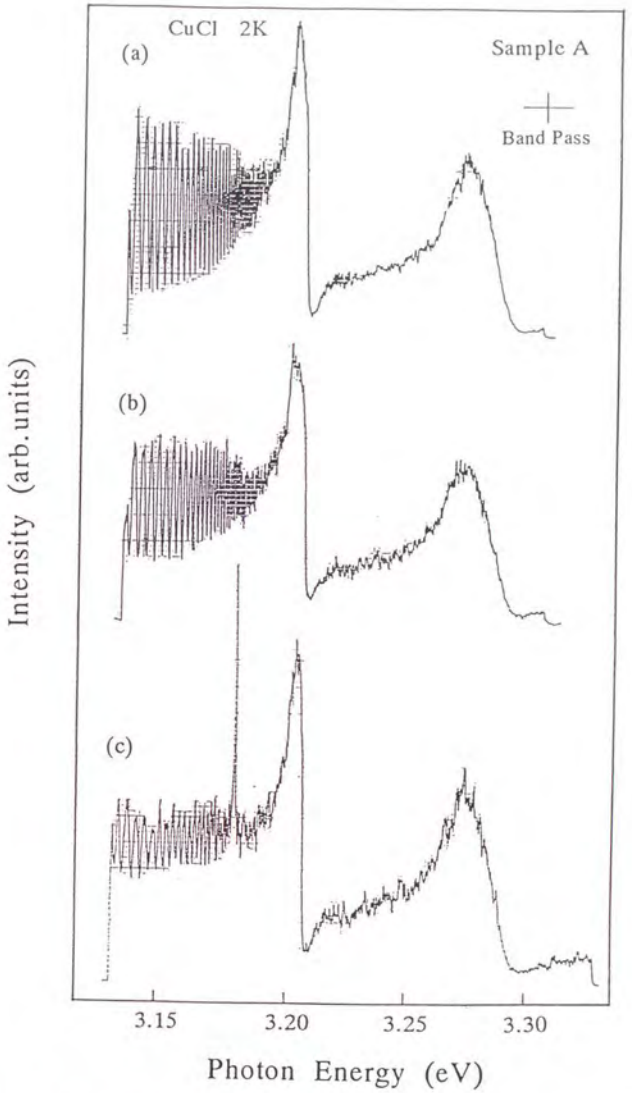

Fig.4-15 Reflection spectra of the sample A obtained in the first experiment (a), in the second experiment (b), and in the third experiment (c)

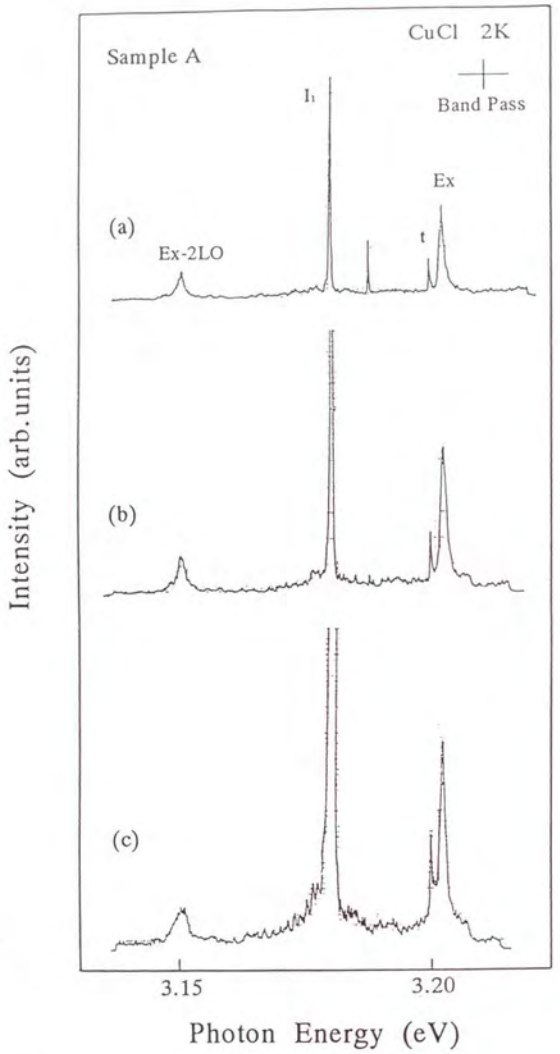

Fig.4-16 Emission spectra of the sample A obtained in the first experiment (a), in the second experiment (b), and in the third experiment (c)

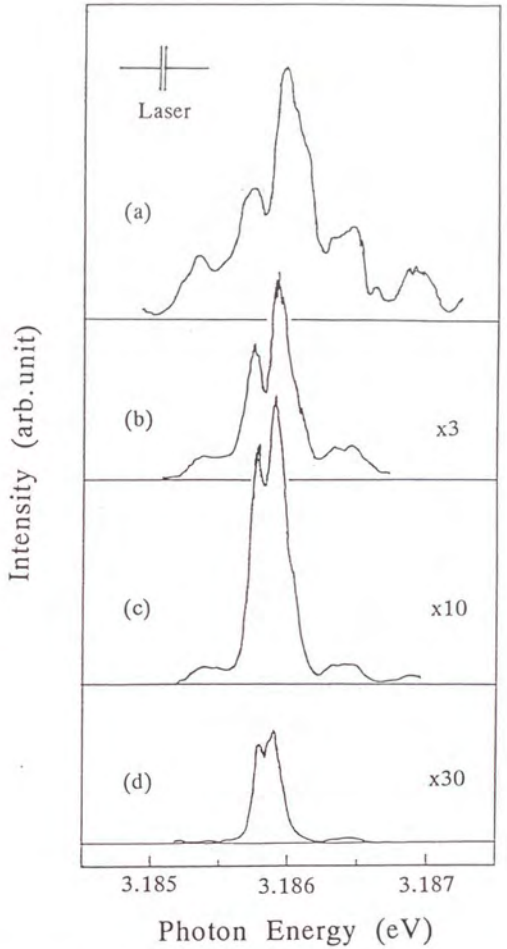

Fig.4-17 Excitation spectra of the PC light at the several excitation intensities of the laser light obtained in the third experiment
Intensities of the pump(forward) light, the pump(backward) light and the probe light were (a) 60kW/cm^2, 60kW/cm^2 and 20kW/cm^2, (b) 30kW/cm^2, 30kW/cm^2 and 10kW/cm^2, (c) 15kW/cm^2, 15kW/cm^2 and 5kW/cm^2, (d) 7.5kW/cm^2, 7.5kW/cm^2 and 2.5kW/cm^2, respectively.

4-2-5. Coclusion

We have demonstrated experimentally that it is possible to enhance the PC signal by the injection of incoherent pump light. This unusual effect can be attributed to the BEC of biexcitons if the density of biexcitons exceeds the critical value for the BEC.

It is found that the sample quality affects the change of the PC in the presence of the incoherent pump light. High quality samples are necessary to observe the enhancement of the PC signal.

The presence of the coherent biexcitons at k=0 generated by the counter-propagating pump beams seems to play a crucial role in the enhancement of the PC signal.

4-3. Probe of the k~0 biexciton state by PCS in the non-degenerate configuration[49]

4-3-1. Introduction

In the experiments in the degenerate configuration, the enhancement of the PC signal was observed in the presence of the high intensity of the incoherent pump light. The remarkable change of the excitation spectrum of the PC signal was also observed only at the vicinity of the two-photon resonance energy of the k=0 biexcitons. It was found that the coherent k=0 biexcitons created by the counter-propagating pump laser beams play a crucial role in the enhancement of the PC signal. However, in the observation of the excitation spectrum, the population of the coherent k=0 biexcitons created by the pump light beams changes when the photon energy of the pump light is tuned. Therefore, it is impossible to judge whether the change of the excitation spectrum of the PC signal is due to the change of the k=0 biexciton state directly or due to the change of the increase of the coherent k=0 biexcitons depending on the photon energy of the pump light. On the other hand, the energy region where the change of the excitation spectrum was observed was restricted by the spectral width of the laser light. A high resolution method is demanded to observe the real change of the spectrum.

To make these points clear, we monitored the PC signal in the non-degenate configuration. In this case, the photon energies of the pump light and the probe light are different.

4-3-2. Principle

In the experiment, spectrum of the PC light in the non-degenerate configuration is analyzed through a high resolution monochromator.

The principle of this method is as follows:

The spectrum of the PC light in this configuration is given as

$$I_{PC}(\omega) = \int_{\omega_p}\int_{\omega_f}\int_{\omega_b} F(\Delta k)\, G(\omega_f,\omega_b)\, f_f(\omega_f)\, f_b(\omega_b)\, f_r(\omega_r)\, \delta(\omega_f + \omega_b - \omega_p - \omega)\, d\omega_b\, d\omega_f\, d\omega_r \qquad (4\text{-}1),$$

where ω_f, ω_b and ω_p are the frequencies of the pump(forward), the pump(backward) and the probe lights, respectively. $f_i(\omega_i)$ is the spectral shape of each laser light. $G(\omega_f,\omega_b)$ is the spectral shape of the two-photon resonance of biexcitons reflecting the relevant $\chi^{(3)}$. This corresponds to $\beta(\omega)$ in Appendix B. Because we observe only the vicinity of the two-photon resonance of biexcitons, we assume that $G(\omega_f, \omega_b)$ have a Lorenzean shape as

$$G(\omega_f,\omega_b) = \frac{1}{\left(E_m - \hbar\omega_f - \hbar\omega_b\right)^2 + \left(\frac{\gamma_m}{2}\right)^2} \qquad (4\text{-}2),$$

where γ_m is the phenomenological damping constant of the k=0 biexciton state corresponding to the full width at half maximum of the resonance. E_m is the biexciton energy. $F(\Delta k)$ shows the phase matching condition mentioned in Appendix B and is given as

$$F(\Delta k) = \frac{\sin^2\frac{\Delta k d}{2}}{\left(\frac{\Delta k d}{2}\right)^2} \qquad (4\text{-}3),$$

where d is the sample thickness. Δk is the phase mismatch that is given as

$$\Delta k \equiv |k_f + k_b - k_p - k_s| \qquad (4\text{-}4).$$

Here, $k_{f,b,p,s}$ represents the respective wave vector of each laser and the signal light obtained from the dispersion curve of the T-exciton polariton around the two-photon resonance energy of biexcitons.

Figure 4-18 shows a schematic illustration of the PC spectrum reflecting one of the real experimental conditions mentioned later. The photon energy of the counter-propagating pump light beams is set at the two-photon resonance energy of the k=0 biexcitons, $E_m/2$, as shown by (a) in the figure. Let the spectral width of the pump light set much broader than the level width of the k=0 biexciton state. When the photon energy of the probe light is set at $\hbar\omega_p = E_m/2 + \delta$ as shown by (b) in the figure, the PC light appears at $E = E_m/2 - \delta$ reflecting the δ function in eq.(4-1) that represents the energy conservation law. The curve (d) shows $F(\Delta k)$. Here, d is adopted to be 15μm which is the thickness of the sample used in the experiment.

In the calculation to obtain the spectrum of the PC light, Gaussian and δ functional shapes were assumed for $f_f(\omega)=f_b(\omega)$ and $f_r(\omega)$, respectively. Unless the spectral shape of the PC light is deformed from the Lorentzian shape by the finite spectral width of the pump light and the phase matching condition, it reflects the spectral shape of $G(\omega_f, \omega_b)$ directly. The relation between the spectral width of the PC light, γ_{PC}, and γ_m obtained by a numerical calculation of eq.(4-1) is shown in Fig.4-19.

On the other hand, the spectral width of the excitation spectrum of the PC light in the degenarate configuration corresponds to $\gamma_m/2$ because the photon energies of all laser lights were scanned simultaneously.

Here, the advantages of this method summarized:

1) The two-photon resonance of the k=0 biexciton state can be measured keeping the photon energy of the pump light constant, i.e., keeping the number of the coherent k=0 biexcitons constant.
2) The spectral resolution of this method can be twice of that of the mothod in the degenerate configuration.

However, two dye laser systems are necessary to generate the PC light and a high resolution monochromator is necessary to measure the spectrum of the PC light in this method. Therefore, the

experiment set-up becomes very complicate.

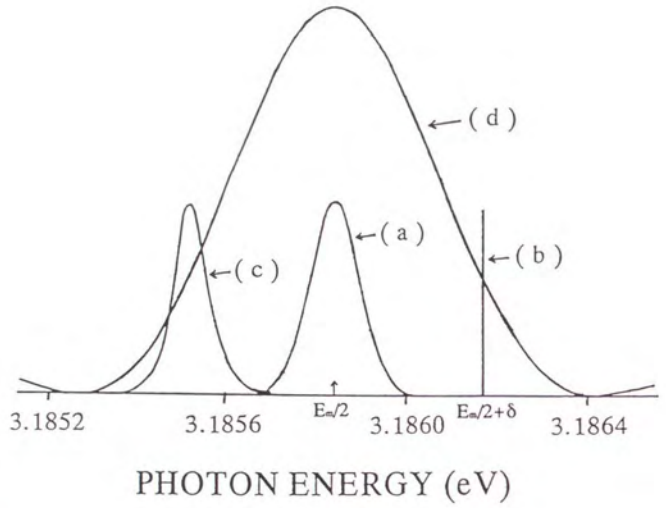

Fig.4-18 Schematic illustration of the non-degenerate PC spectrum
(a), (b) and (c) show the spectra of the pump light, the probe light and the PC light, respectively. (d) shows the phase matching condition.

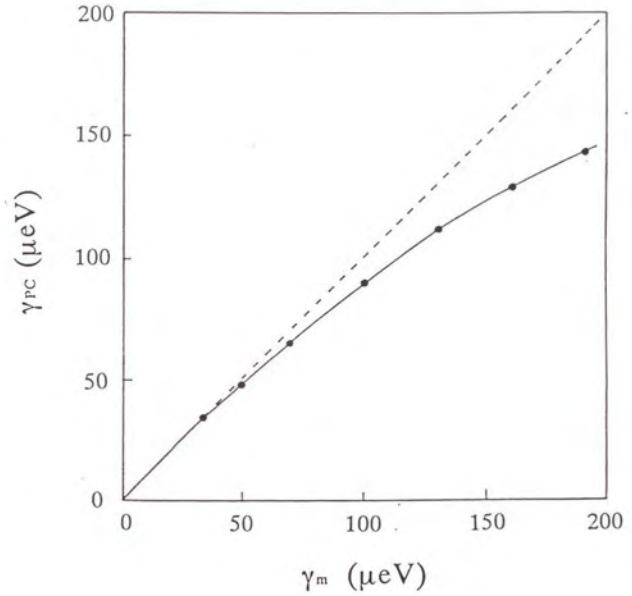

Fig.4-19 Relation between the spectral width of the PC light, γ_{PC}, and the spectral width of the biexciton resonance, γ_m, evaluated for the experimental condition
Dashed line shows $\gamma_{PC}=\gamma_m$.

4-3-3. Experiment

The schematic experimental set-up is shown in Fig.4-20.

An excimer laser (Lambda Phycik 53EMC) was used to pump dye lasers (BBQ in p-dioxane) providing the pump light (Dye laser A) and the probe light (Dys laser B), respectively. The pulse duration of each laser light was about 10ns. The polarization of the counter-propagating pump light was made circular so as to excite the k=0 biexcitons predominantly. Each pump beam was focused on sample surface to a spot of 100μm diameter. The photon energy of the pump light was set at $E_m/2$ with the linewidth of 138μeV. The circular polarized probe beam was focused on the area illuminated by the pump beams. The photon energy and the spectral width of the probe light were 3.1862eV and 37μeV, respectively. The external angle between the pump and the probe axis was 10 deg. The PC light was analyzed with a monochromator (Jobin Yvon THR1500, band pass= 16μeV).

Another laser light (Dye laser C) pumped by the same excimer laser was used as the incoherent pump light. The spectral width of the incoherent pump light was 1.36meV. The beam was focused on the sample surface to a spot of 200μm diameter to cover completely the area illuminated by the pump and probe beams. The intensity of the incoherent pump light was contineously adjusted with a variable attenuator (Newport 935-5). By adopting a laser light instead of the super radiant light, that was used in the experiment in the degenerate configuration, as the incoherent pump light, muximum intensity of the incoherent pump light could be increased up to 2.7MW/cm^2 and the photon energy of the incoherent pump light could be tuned easily. Therefore, it becomes possible to examine the change of the PC signal as a function of the photon energy of the incoherent pump light.

The sample was cooled in an immersion type cryostat at 2K. The thickness of the sample was 15μm. The emission spectrum of the sample under the weak excitation of UV light is shown in

Fig.4-21.

The procedure to overlap the light beams in this experiment was similar to that in the experiment in the degenerate configuration.

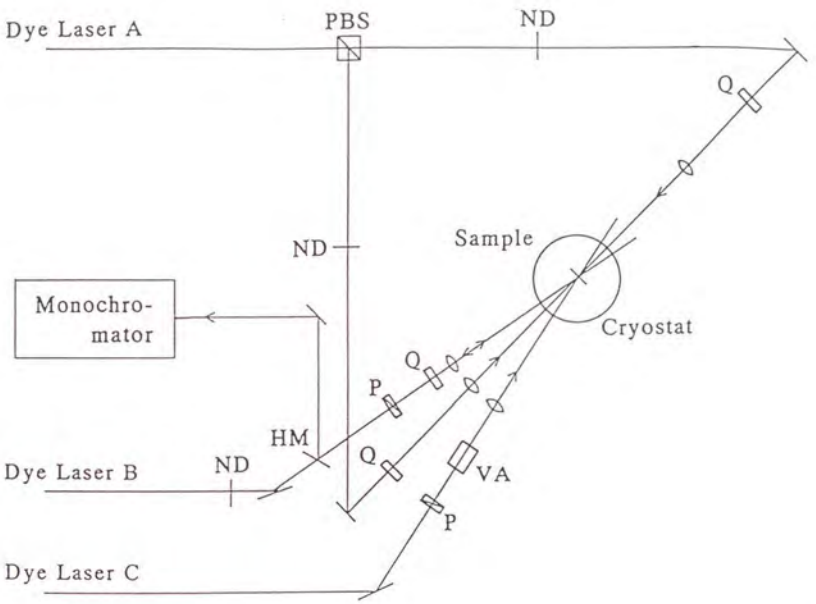

Fig.4-20 Schematic diagram of the experimental set-up in the non-degenerate configuration [49]
HM : half mirror, M : mirror, ND : neutral density filter, P : polarizer, Q : quarter wave plate, PBS : polarized beam splitter, PH : pin hole, PDVA : variable intensity attenuator driven by a pulse-motor

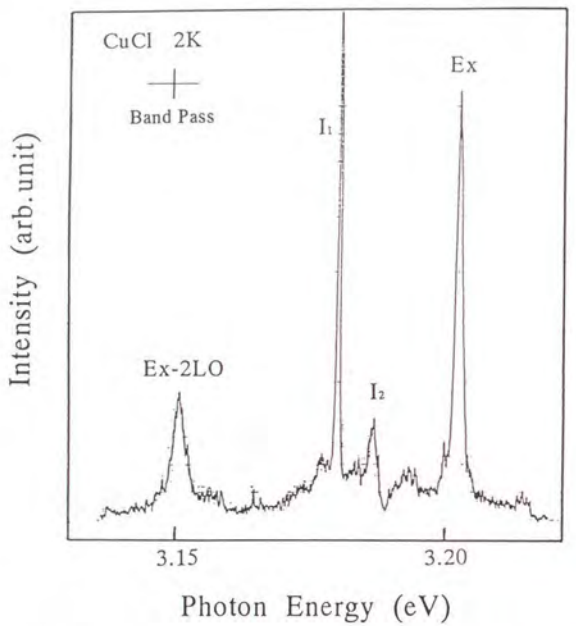

Fig.4-21 Emission spectrum of the sample obtained with a weak excitation of UV light at 2K

Figure 4-22 shows examples of the spectra of the PC light in the presence of various intensities of the incoherent pump light. The intensities of the pump(forward), the pump(backward) and the probe beams on the sample surface were 80kW/cm², 80kW/cm² and 10kW/cm², respectively. The enhancement of the intensity of the PC signal, the narrowing and the blue shift of the spectrum were observed when the intensities of the incoherent pump light were of the order of 100kW/cm². But these trends changed inversely when the intensity of the incoherent pump light was beyond 1MW/cm².

Figure 4-23 shows the peak intensity and the spectral width of the PC light as a function of the intensity of the incoherent pump light. The peak intensity and the spectral width are normalized on the values obtained in the absence of the incoherent pump light. It was found that the enhancement of the PC signal and the narrowing of the spectrum occured correlatively.

Figure 4-24 shows the shift of the resonant energy of the k=0 biexciton state as a function of the intensity of the incoherent pump light. This shift was about 20μeV at the intensity of the incoherent pump light of 400kW/cm². Such shift was not observed clearly in the experiment in the degenerate configuration. This shift is thought to be hindered in the spectral width of the laser light in that experiment because the corresponding shift is about 10μeV in the degenerate regime.

Figure 4-25 shows the fractional change of the intensity of the PC signal as a function of the photon energy of the incoherent pump light. Clearly, an increase of the intensity of the PC signal was only observed for high injected exciton densities, i.e., in the region of strong linear absorption of excitons, whereas the reversed trend was observed in 3.22eV corresponding to weaker absorption and lower particle density. Decrease of the PC signal was also observed at the two-photon resonance energy of biexcitons. This decrease is thought to be due to the two-photon absorption of biexcitons by the combination of the PC light and the intense incoherent pump light. However, if the condensation of biexcitons at $k=2k_l$ induced by the incoherent pump light, where

k_i is the wave vector of the incoherent pump light, occurs as observed by N Peyghambarian et al.[28], the population of k=0 biexcitons will decrease due to the attraction effect toward $k=2k_i$ state. This is another possibile explanation for the decrease of the PC signal when the photon energy of the incoherent pump light resonated the two-photon resonance energy of biexcitons.

In this experiment, the PC light did not also appear even in the presence of the incoherent pump light whose intensity was enough for the enhancement of the PC light when the pump light beams were cut. It was confirmed that the presence of the coherent k=0 biexcitons created by the counter-propagating pump beams was crucial for the enhancement of the PC signal.

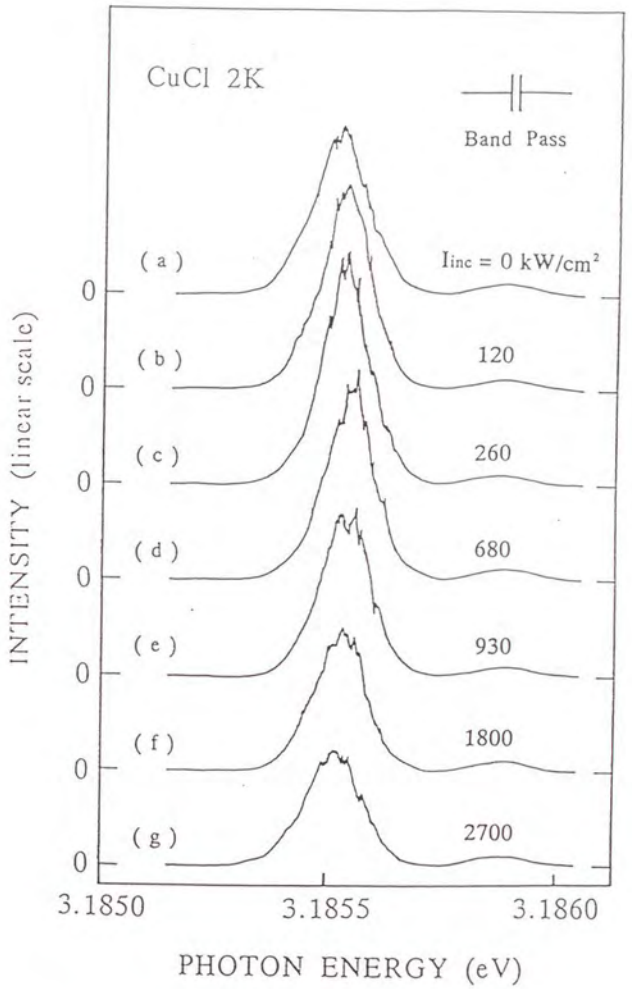

Fig.4-22 Spectra of the PC light at several intensities of the incoherent pump light, I_{inc} [45]
Intensities of the pump(forward) light, the pump(backward) light and the probe light was 80kW/cm², 80kW/cm² and 10kW/cm², respectively.

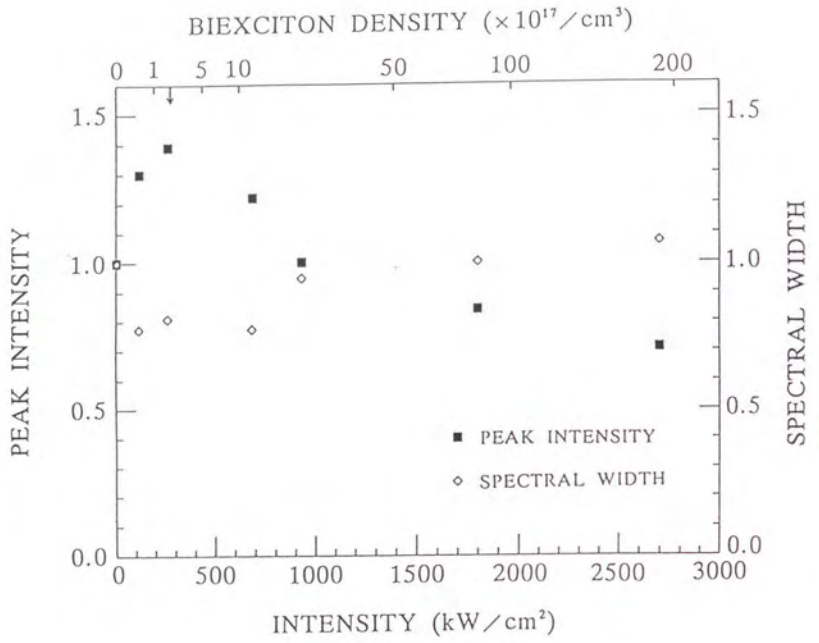

Fig.4-23 Peak intensity and the spectral width of the PC light as a function of the intensity of the incoherent pump light
The values of the peak intensity and the spectral width are normarized to those of the PC light in the absence of the incoherent pump light.
Biexciton density evaluated in the subsection 4-4-2 is shown in the top of the figure.

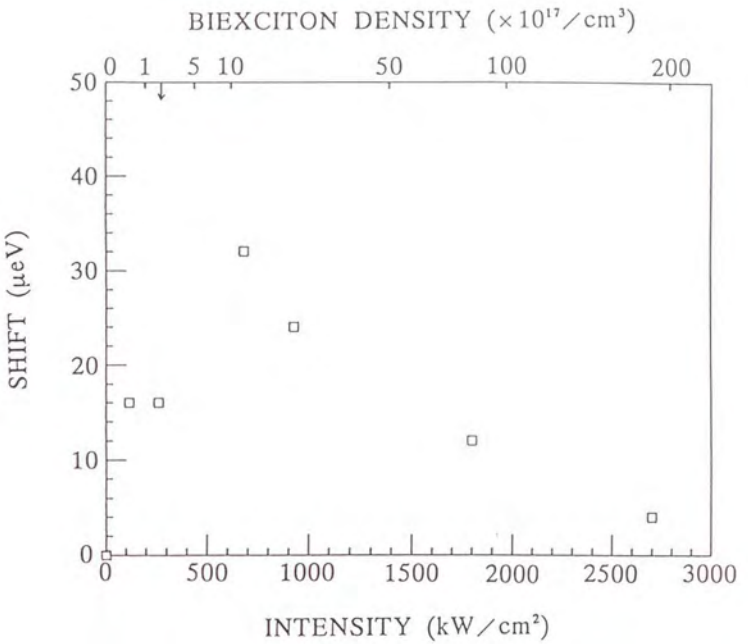

Fig.4-24 Energy shift of the PC light as a function of the intensity of the incoherent pump light
Biexciton density evaluated in the subsection 4-4-2 is shown in the top of the figure.

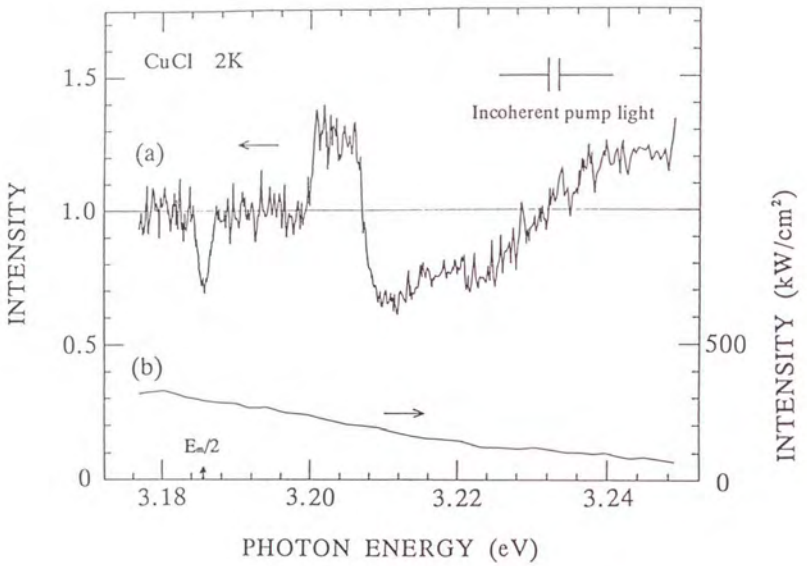

Fig.4-25 Variations of the intensity of the PC light (a) and the intensity of the incoherent pump light (b) with the photon energy of the incoherent pump light

4-3-5. Conclution

The enhancement of the PC signal in the presence of the incoherent pump light was reproduced in the experiment in the non-degenerate configuration.

The enhancement of the PC signal and the narrowing of the spectrum in the presence of the incoherent pump light were found to occur correlatively. The small blue shift of the resonant energy of the k=0 biexciton state was also observed in the presence of the incoherent pump light.

The enhancement of the PC signal was observed only for the excitaiton of the incoherent pump light in the region of strong linear absorption of excitons that corresponds to high injected exciton densities.

The presence of the coherent k=0 biexcitons generated by the counter-propagating pump beams was confirmed to be crucial for the enhancement of the PC signal.

4-4. Analysis and discussion

In this section, observed phenomena in the experiments are analized and their relations to the BEC of biexcitons are discussed.

4-4-1. Evaluation of the number of biexcitons collapsed into the k=0 state

Here, the number of the biexcitons increased at the k=0 state corresponding to the enhancement of the PC signal in the experiment is evaluated.

The number of the coherent k=0 biexcitons created by the counter-propagating pump laser beams, N_m^0, satisfies the following rate eqaution

$$\frac{dN_m^0}{dt} = \frac{I_{abs}\, S}{E_m} - \gamma_m N_m^0 \qquad (4\text{-}5),$$

where I_{abs} is the absorbed intensity of the pump light. S is the area of the laser spot on the sample surface. γ_m is the decay rate of biexcitons and is adopted here as the inversion of the radiative lifetime of biexcitons, 50ps[29]. E_m is the biexciton energy, 6.37164eV[37]. By solving the eq.(4-5) asumming the steady state condition, N_m^0 is obtained to be

$$N_m^0 = \frac{I_{abs}\, S}{\gamma_m E_m} = 4.0 \times 10^7 \qquad (4\text{-}6).$$

The enhancement of the PC signal in the presence of the incoherent pump light was about 30%. Therefore, corresponding increase of the number of the biexcitons at the k=0 state, N_{inc}^0, is

$$N_{inc}^0 = 0.3\, N_m^0 = 1.2 \times 10^7 \qquad (4\text{-}7).$$

In the discussion above, the PC signal is thought to be only due to the k=0 biexcitons. However, the signal due to the biexcitons having finite wave vectors in the vicinity of k=0 (exactly to say, this signal is not the PC light but the four wave mixing light) was detectable because a finite (but very small) solid angle of the detection was present in the experiment. Hereafter, we

estimate the number of biexciton modes observable in the experimental condition and the change of the occupation number per biexciton mode corresponding to the increase of the PC signal.

Figure 4-26 shows the schematic illustration of the detection. As can be seen in the figure, a four wave mixing light (denoted by B in the figure) is generated by inducing a biexciton that has a finite x-component of the wave vector by a probe light (denoted by A in the figure). In the experimental condition, the divergence of the probe light can be estimated from the diameter of the pin hole (2mm) and the focal length of the lens (300mm) to be 0.19 deg corresponding to the angle of 0.07 deg inside the sample. The detectable region of the wave number of biexcitons due to this divergence, $\Delta k_{x,y}$, is obtained to be

$$\Delta k_{x,y} \simeq 2 \times k_p \sin(0.07^\circ) = 1.1 \times 10^3\ \mathrm{cm}^{-1} \qquad (4\text{-}8),$$

where k_p is the wave number of the probe light.

On the other hand, the phase matching condition for the generation of the PC light, which is mentioned in Appendix B, limits the detectable region of the z-component of the wave vector of biexcitons. Using eq.(B-24), this region is obtained to be

$$\Delta k_z \simeq \frac{\pi}{d} = 1.5 \times 10^3\ \mathrm{cm}^{-1} \qquad (4\text{-}9),$$

where d=21μm is the the sample thickness.

If we assume that the biexcitons are confined in the excited volume by the laser light that is shown in Fig.4-27, one can easily calculate the biexciton modes. Here, the excited volume is assumed to be a retangular solid instead of a disk in order to simplify the calculation. The biexciton modes in the detectable region of the biexciton wave vector are shown in Fig.4-28. From this figure, the number of modes detectable in the experimental condition is obtained to be 22. Assuming that the PC signal observed in the experiment is equally distributed these modes, the occupation number of the lowest energy state corresponding to the enhancement of the PC signal is found to be at least $N_{inc}^0/22 = 5.5 \times 10^5$. This number is thought to be macroscopic.

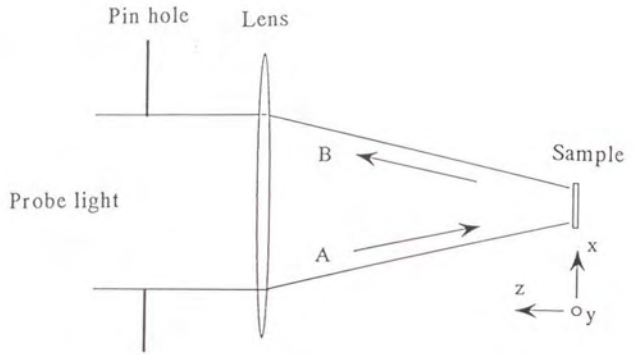

Fig.4-26 Schematic illustration of the relation between the divergence of the probe beam, A, and the detectable four wave mixing light, B

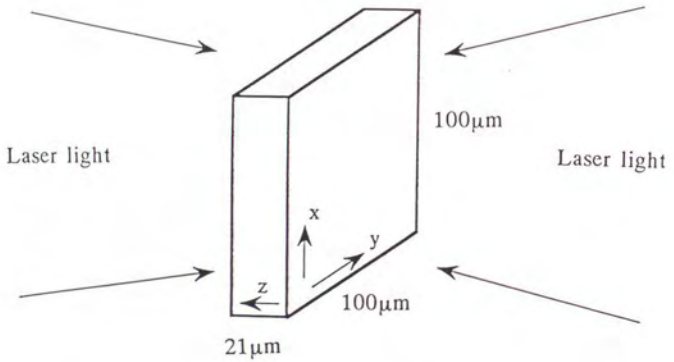

Fig.4-27 Area of the sample and the coordinates used for the calculation of the biexciton mode

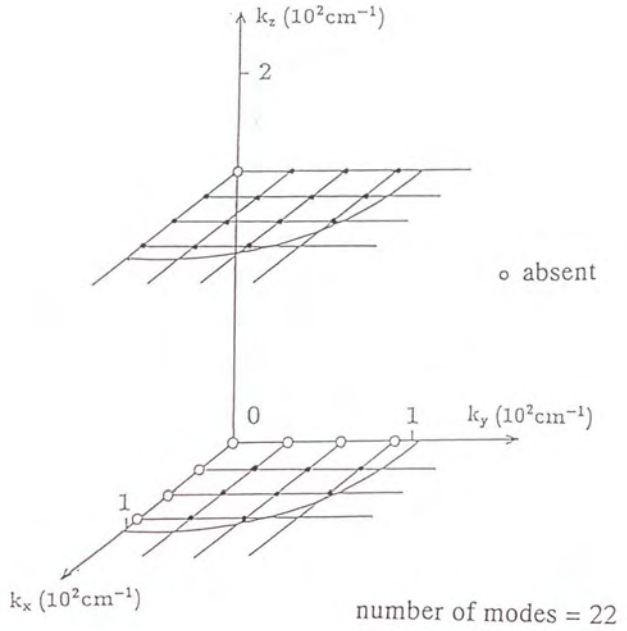

Fig.4-28 Biexction modes in phase space which are observable in the experimental condition

4-4-2. Evaluation of the biexciton density

In order to discuss these experimental results in the relation of the BEC, evaluation of the biexciton density is important.

From eq.(1-2), the critical density of biexcitons for the BEC, n_m^c, is obtained to be

$$n_m^c = 2 \times 10^{17}\ cm^{-3} \qquad (T = 2K) \qquad (4\text{-}10).$$

The density of the coherent biexcitons created by the pump beams, n_m^0, can be obtained from the number of the coherent biexcitons obtained in last subsection by dividing by the volume of the system, Sd, as

$$n_m^0 = \frac{N_m^0}{Sd} = 2.4 \times 10^{14}\ cm^{-3} \qquad (4\text{-}11).$$

This density is much smaller than n_m^c.

The density of the incoherent biexcitons created by the incoherent pump light can be evaluated by using the kinetics of exciton-biexciton system shown in Fig.4-29. The rate equations for excitons and biexcitons in this kinetics are given as

$$\begin{cases} \dfrac{dn_m}{dt} = \dfrac{\eta}{2} n_e^2 - \gamma_m n_m \\ \dfrac{dn_e}{dt} = -\eta n_e^2 + \gamma_m n_m - \gamma_e n_e + \dfrac{(1-R) I_{inc}}{L \times E_{inc}} \end{cases} \qquad (4\text{-}12),$$

where

n_m : Biexciton density
n_e : Exciton density
η : Biexciton formation rate ($6 \times 10^{-8}\ cm^3/s$)[50]
γ_m : Radiative decay rate of biexcitons ($1/(50ps)$)[29]
γ_e : Decay rate of excitons ($1/(5ns)$)[30]
I_{inc} : Intensity of the incoherent pump light
R : Reflectivity of the CuCl crystal at the photon energy of the incoherent pump light (0.5)
L : Excitation depth of the incoherent pump light
E_{inc} : Photon energy of the incoherent pump light (3.20286eV).

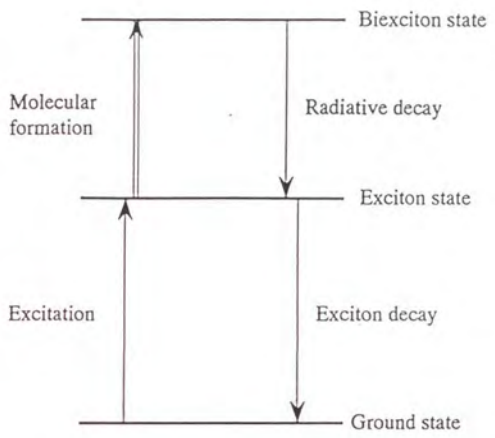

Fig.4-29 Kinetics of the biexciton and exciton system used for the evaluation of the density of incoherent biexcitons

Recent developments of pico-second pulse lasers and its detection systems make researches on the dynamics of the T-exciton polaritons possible. Fig.4-30 shows the group velocities of the T-exciton polariton in CuCl[30]. The group velocities obtained experimentally coincide well with the values calculated from the dispersion curve of the T-exciton polariton. Fig.4-31 shows the scattering rate of propagating polaritons in weak excitation regime in a high quality crystal[30]. From these results, it was found that the T-exciton polariton propagates ~10μm ballistically. Therefore, the excitation depth of the incoherent pump light was assumed here to be the ballistic propagation length of the incident polaritons that are converted from the incoherent pump light at the sample surface. For the case of the non-degenerate PC experiment, the excitation depth can be calculated by the following equation because the monochromatic laser light was used for the incoherent pump light.

$$L = \frac{v_g}{\gamma_{sc} + \eta n_e} \qquad (4\text{-}13),$$

where

v_g : Group velocity of the incident polariton (1.5×10^6 cm/s)[30]

γ_{sc} : Scattering rate of the incident polariton in weak excitation regime ($1\times10^9 s^{-1}$)[30].

Here, the collision rate of the incident polaritons due to the biexciton formation, ηn_e, that is expected to exist in high intensity excitation regime is considered.

After inserting eq.(4-13) into eq.(4-12), n_e and n_m are obtained assuming the steady state conditions as

$$n_e = \left\{\frac{(1-R)I_{inc}}{v_g E_{inc}} - \frac{\gamma_e}{\eta}\right\} + \left|\frac{(1-R)I_{inc}}{v_g E_{inc}} - \frac{\gamma_e}{\eta}\right| \left\{1 + \frac{2(1-R)\gamma_{sc} I_{inc}}{\left(\frac{(1-R)I_{inc}}{v_g E_{inc}} - \frac{\gamma_e}{\eta}\right)^2 \eta v_g E_{inc}}\right\} \qquad (4\text{-}14)$$

$$n_m = \frac{\eta}{2\gamma_m} n_e^2 \qquad (4\text{-}15).$$

n_e and n_m calculated by eqs.(4-14) and (4-15) are shown in Fig.4-32 as a function of I_{inc}. In Fig. 4-33, the number of biexcitons, $N_m = n_m SL$, calculated by eqs.(4-13), (4-14) and (4-15) and the

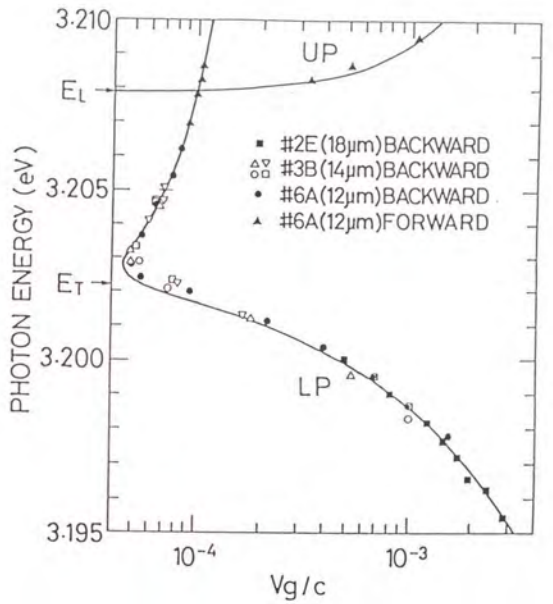

Fig.4-30 Group velocity of the T-exciton polaritons in CuCl at 2K [30]
Solid lines show theoretical curves calculated from the dispersion relation. LP and UP denote the lower-branch polariton and the upper-branch polariton, respectively.

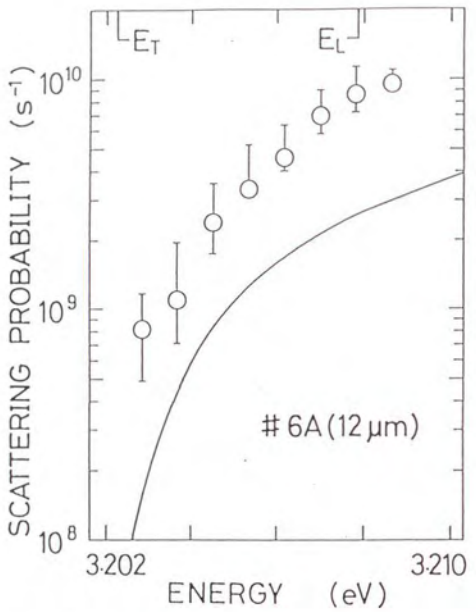

Fig.4-31 Scattering probability per unit time (momentum relaxation rate) of the lower-branch polariton obtained experimentally (open circles) [30]
Solid line represents the inelastic-scattering probability of the lower-branch polariton obtained theoretically for the one-LA-phonon emission at 2K.

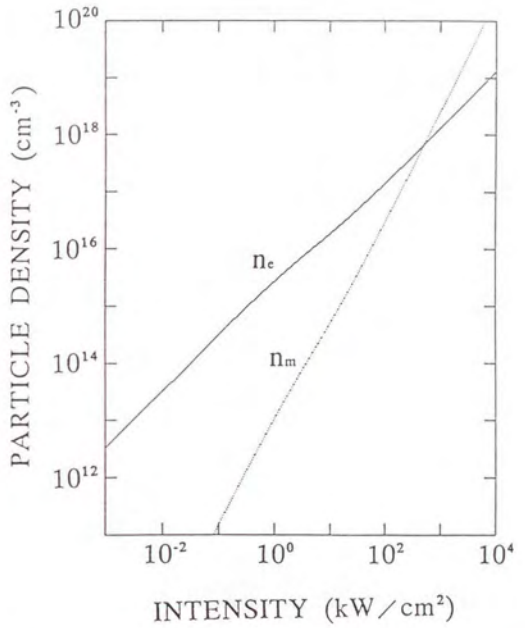

Fig.4-32 Densities of excitons, n_e, and biexcitons, n_m, as a function of the intensity of the incoherent pump light

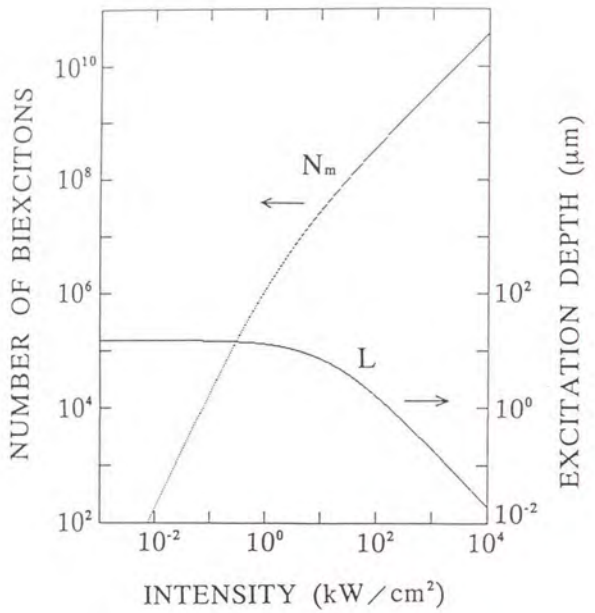

Fig.4-33 Number of biexcitons, N_m, and the excitation depth of the incoherent pump light, L, as a function of the intensity of the incoherent pump light

excitation depth calculated by eq.(4-13) and (4-14) are shown as a function of I_{inc}.

By using these results, the peak intensity and the spectral width of the PC light are plotted as a function of the biexciton density in Fig.4-34. It was found that the enhancement and the spectral narrowing of the PC light are observed around n_m^c. This result suggests that these phenomena are the results of the macroscopic increase of the occupation number and the enhancement of the coherence of the k=0 biexciton state due to the BEC of biexcitons.

On the other hand, the density at which the distance between biexcitons is same as the biexciton diameter is estimated as

$$n_m^{up} = \frac{1}{a_m^3} = 4.1 \times 10^{19}\ cm^{-3} \qquad (4\text{-}16),$$

where a_m is the diameter of a biexciton and adopted here as the sum of the distance between excitons which compose a biexciton[14] and the twice of Bohr radius of exciton, a_m~2.9nm. In the density region of n_m~$10^{19}cm^{-3}$, decrease of the the PC signal and broadening of the spectral width of the resonance were observed. These phenomena can be interpreted as an appearance of the instabiliy of the biexciton state.

On the other hand, it was found that the new nonlinear emission associated with the decay process of a biexciton due to the collision with an exciton appeared in the excitation intensity region where the decrease of the PC signal was observed. Details of this new nonlinear emission and corresponding collision process are explained in Appendix C. One can suppose that following things occurs where the such collision process is predominantly present.

1) Coherence of the biexciton state is easily broken.

2) Biexciton density does not increase with the increase of the intensity of the excitation light.

3) Nonelastic interaction between an exciton and a biexciton is dominant.

1) may cause the decrease of the PC signal and the broadening of the spectral width of the resonance. 2) and 3) may change the shift of the biexciton energy (Discussions about the shift of the biexciton energy are given in the next subsection.). In order to understand these phenomena

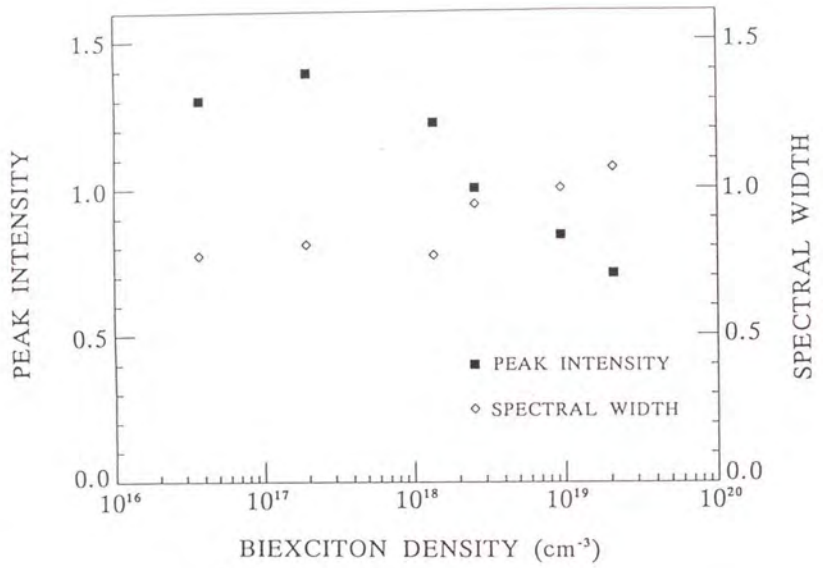

Fig.4-34 Peak intensity and the spectral width of the PC light as a function of the density of biexcitons.
The procedure of the estimation of the biexciton density is explained in the text. The values of the peak intensity and the spectral width are normarized to those of the PC light in the absence of the incoherent pump light.

qualitatively and consistently, kinetics of excitons and biexcitons in very high density regime should be examined. This is still an open problem.

On the other hand, the evaluation of the density of the incoherent biexcitons in the generate PC experiment is very difficult because the spectrum of the incoherent pump light was very broad to cover the Z_3-exciton band. In order to evaluate the density of the incoherent biexcitons in this case, the M-emission intensity obtained with the incoherent pump light was compared with that obtained with a single linear polarized laser beam tuned to the two-photon absorption peak of biexcitons. The biexciton density from the laser source can be estimated by measuring the two-photon absorbance of the transmitted laser beam and was obtained to be $4.7\times10^{14}cm^{-3}$ for a laser intensity of $100kW/cm^2$. The biexciton density from the incoherent pump light was estimated by multiplying this value by Cd/L where C=41 is the ratio of biexciton luminescence intensity due to the incoherent pump light ($400kW/cm^2$) and laser light ($100kW/cm^2$), L<1μm is the excitation depth of the incoherent pump light and d=21μm is the sample thickness. Finally, $n_{in}=4.0\times10^{17}cm^{-3}$ was obtained for the experimental condition. This value coincides the value obtained in the experiment in the non-degenerate configuration.

4-4-3. Shift of the biexciton energy

Figure 4-35 shows the shift of the resonant energy of the k=0 biexciton state as a function of the biexciton density estimated in last subsection in log-log scale.

M. Inoue et al. have calculated the biexciton energy by using the following Hamiltonean including the biexciton-biexciton and exciton-biexciton interactions as[51]

$$H = \sum_k (E_m(k) - \mu_m) C_k^+ C_k + \sum_k (E_e(k) - \mu_e) B_k^+ B_k$$
$$+ \frac{W}{2} \sum_{k,k',q} C_{k+q}^+ C_{k'-q}^+ C_{k'} C_k + V \sum_{k,k',q} C_{k+q}^+ B_{k'-q}^+ B_{k'} C_k$$

(B_k , B_k^+) : annihilation and creation operator of exciton

(C_k , C_k^+) : 〃 of biexciton

(4-17),

where E_m and E_e are the energies of a biexciton and a exciton, respectively. μ_m and μ_e are the chemical potential of a biexciton and a exciton, respectively.

As the results, they found that the biexciton energy shifts to high energy side and that this shift is proportional to the biexciton density. Quantitative estimation of this shift is not easy because the strength of the interaction between biexcitons is not known exactly. However, by assuming that the scattering length of biexcitons is the diameter of a biexciton, the shift, that corresponds to the change of the chemical potential of biexcitons, can be estimated along their procedure as,

$$n_m W = 4\pi \frac{\hbar^2 f_0}{m_m} n_m$$
$$= 5.25 \times 10^{-16} n_m \ (\mu eV) \ : \ n_m \ (cm^{-3}) \qquad (4\text{-}18)$$

where

f_0 : biexciton-biexciton scattering length $\approx$ 2.9 nm .

The result of the eq.(4-18) is shown by a solid line in Fig.4-35. Only in the lowest excitation case, the observed shift corresponded to that theoretically estimated. The origin of the deviation in

higher density region is not clear at present.

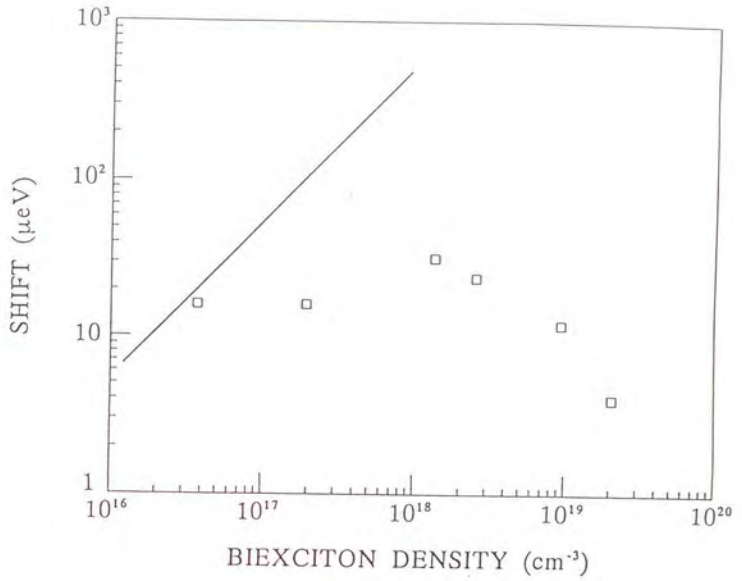

Fig.4-35 Energy shift of the PC light as a function of the density of biexcitons [49]
The procedure of the estimation of the biexciton density is explained in the preceding sub-section. Solid line shows the change of the chemical potential of biexcitons obtained theoretically.

4-5. Conclusions and future prospects

In this work, the k=0 biexciton state, which has been very difficult to be examined by the observation of the biexciton emission, was examined by the PCS.

As the results,

1) Enhancement of the PC signal by the injection of the incoherent pump light was observed both in the degenerate configuration and in the non-degenerate configuration.
2) Such enhancement of the PC signal was found to depend on the sample quality very much and to be observed only in samples of high quality.
3) Enhancement and the spectral narrowing of the PC light were found to occur correlatively, suggesting the increase of the occupation number and the enhancement of the coherence of the k =0 biexciton state.
4) Small blue shift of the resonant energy of the k=0 biexciton was observed, suggesting the change of the chemical potential of biexcitons.
5) Enhancement of the PC signal was observed only for the excitaiton of the incoherent pump light in the region of strong linear absorption of excitons.
6) Enhancement of the PC signal was found to appear under the injection of a high density of incoherent biexcitons corresponding to the critical density for the BEC.
7) Occupation number of the k=0 biexciton state corresponding to the enhancement of the PC signal was very large, i.e., 5.5×10^5 at least.

Then, it can be attributed to the results of the BEC of biexcitons.

In principle, one can expect that the appearance of the PC signal in the absence of the counter-propagating pump light where the biexciton density from the incoherent pump light alone exceeds the critical density if the time for the BEC formation is shorter than the pulse duration of the incoherent pump light. So far, we were unable to detect any PC signal under the such condition within the noise limit. Our results, which are thought to be sensitive to the phase coherence, seem

to indicate that a seed (provided by the counter-propagate coherent pump light) is necessary to achieve a true condensate within the pump duration.

In this work, the transient behavior of the phase transition as well as the cooling process of biexcitons could not be examined. In future, applications of this method to the time resolved spectroscopy will make clear these points. Recent developments of short pulse laser techniques will make us possible to detect the transient process of the phase transition. Such study is not so easy in other system like liquid ^{4}He.

On the other hand, the light source with a long pulse duration or a contineous wave (CW) to generate a high density of incoherent biexcitons will help us to study the spontaneous formation of the BEC. The developments of such light source are demanded for further progresses of this research.

The method developed in this work is applicable not only to the biexciton system in CuCl but also to any exciton and biexciton system that has the third order optical nonlinearity. Similar experiments on other systems will help us to understand the phenomena observed in this work and the BEC of the exciton and biexciton systems.

5. Conclution and future prospects of the thesis

The k~0 biexciton state which is very important not only for the study of the large optical nonlinearity associted with the two-photon resonance of biexcitons but also for the study of the Bose-Einstein condensation of biexcitons was examined by nonlinear spectroscopy methods.

By the high resolution nonlinear polarization spectroscopy that was carried out with developing a new laser system of very high resolution, following facts were found:

1) The spectral width of the two-photon resonance of the k~0 biexciton state under the weak excitation limit showed sample dependence and was obtained to be 24μeV for the sample #1 and 36μeV for the sample #2, respectively. These widths correspond to the phase relaxation times of 52ps and 36ps, respectively.
2) $|\chi^{(3)}|$ at the peak of the resonance of the k~0 biexcitons were obtained to be $(3.0\pm0.9)\times10^{-4}$esu for the sample #1 and $(1.7\pm0.6)\times10^{-4}$esu for the sample #2, respectively.
3) The saturation of $|\chi^{(3)}|$ and the broadening of the spectral width of the biexciton resonance were found to occur beyond the excitation intensity of 1kW/cm^2.
4) The validity of the effective mass approximation of biexcitons in the vicinity of k=0 was confirmed to be valid.

By the phase conjugation spectroscopy, following facts were found:

1) Enhancement of the PC signal by the injection of the incoherent pump light was observed both in the degenerate configuration and in the non-degenerate configuration.
2) Such enhancement of the PC signal was found to depend on the sample quality very much and to be observed only in samples of high quality.
3) Enhancement and the spectral narrowing of the PC light were found to occur correlatively,

suggesting the increase of the occupation number and the enhancement of the coherence of the k=0 biexciton state.

4) Small blue shift of the resonant energy of the k=0 biexciton was observed, suggesting the change of the chemical potential of biexcitons.
5) Enhancement of the PC signal was observed only for the excitaiton of the incoherent pump light in the region of strong linear absorption of excitons.
6) Enhancement of the PC signal was found to appear under the injection of a high density of incoherent biexcitons corresponding to the critical density for the BEC.
7) Occupation number of the k=0 biexciton state corresponding to the enhancement of the PC signal was very large, i.e., $5.5\text{x}10^5$ at least.

Therefore, these phonomena can be attributed to the result of the BEC of biexcitons.

8) Detection of the PC signal in the absence of the counter-propagating coherent pump light was not successful where the biexciton density from the incoherent pump light alone exceeds the critical density for the BEC. This result seems to indicate that a seed (the coherent k=0 biexcitons provided by the counter-propagate coherent pump light) is necessary to achieve a true condensate within the pump duration.

By overlooking these researches, one can imagine the a direction of the research on quantum optics using the biexciton system in CuCl. As mentioned in Chapter 1 and 3, the two-photon resonance of biexcitons is very efficient and suitable to generate the two-photon(polariton) pair from the decay of the k=0 biexciton. Generation of the PC light associated with the k=0 biexcitons does correspond to the generation of the degenerate two-photon(polariton) pair as mentioned in Chapter 4. On the other hand, the enhancement of the PC signal observed in this work can be interpreted as an amplification of the PC signal by using the quantum statistics of Bose particles. Therefore, it can be used for the amplification of the two-photon(polariton) pair creation. It seems interesting to consider the phenomena observed in this work in the relation with the development of the two-photon laser[52]. The

knowledge obtained in this work will contribute to new developments in such a research field.

Acknowledgements

The author would like to express his deep gratitude to Professor N.Nagasawa (Dept. of Physics. The Univ. of Tokyo) for his support and encouragement through the every stage of this work. Without his support, this work would have never been carried out by the author who was a stranger not only to the solid state physics but also to the nonlinear optics.

This work started as an international cooperative project between Japan and France in the framework of the CNRS-JSPS Scientific Cooperation Program including Profs. N.Nagasawa, A. Mysyrowicz (ENSTA, France), T.Itoh (Tohoku Univ.), E.Hanamura (The Univ.of Tokyo) and M. Gonokami (The Univ.of Tokyo). The author would like to thank all members of the project. Especially, he would like to thank Dr. A.Mysyrowicz for many useful suggestions and stimulating discussions not only during the project but also after the end of the project. He would like to thank Prof. T.Itoh for useful suggestions about the polariton and the t-exciton in CuCl with showing his unpublished data. He would like to thank Profs. E.Hanamura and M.Gonokami for fruitful suggestions about the phase conjugation.

He would like to thank Prof. M.Inoue (Tsukuba Univ.) for useful suggestions about the chemical potential of biexcitons. He would like to thank Dr. A.L.Ivanov (Geothe Univ. Germany) for fruitful discussions about the relation between the phase conjugation and the Bose-Einstein condensation of biexcitons.

He would like to thank Dr.T.Hatano for help and advice in the experiment. He would like to thank Messrs. Y.Obuchi, M.Morinaga, T.Ando and N.Kamiura for help in the experiment.

He would like to thank Mr. M.Nishino for the cooperation in developing the new laser system of a very narrow spectral width. He also would like to thank Drs. P.Grangier, P.Georges (Institut d' optique theorique appliquee, France) and Mr. K.Karitani (Marubun Co.) for advice in developing the new laser system.

He would like to thank Prof. E.Mohler (Frankfurt Univ. Germany) for supplying block crystals.

He would like to thank Mr. S.Otuka (Machine shop, The Univ. of Tokyo) for help and advice in making experimental tools. He also would like to thank Mr. R.Takahashi (Cryogenic Sub-Center, The Univ.of Tokyo) for supplying the liquid helium and the liquid nitrogen whenever he ordered.

He would like to thank Profs. T.Fujimoto and K.Ishii and Drs. H.Suemitsu and R.Okasaka (Kyoto Univ.) for teaching him the general techniques of spectroscopy.

Appendix A. Bose-Einstein condensation

It is well-known that the thermal distribution of ideal Bose particles at a temperature, T, obeys the Bose-Einstein distribution as

$$f(E_i) = \frac{1}{\exp\{(E_i - \mu)/k_BT\} - 1} \qquad \text{(A-1)},$$

because a single quantum state can be occupied by the plural number of Bose particles at a same time. Here, E_i is the kinetic energy of the particle. k_B is Boltzmann constant. μ is the chemical potential and is determined by the relation of

$$N = \sum_i \frac{1}{\exp\{(E_i - \mu)/k_BT\} - 1} \qquad \text{(A-2)},$$

where N is the total number of the particle.

As the temperature decreases, μ increases and finally becomes zero from a negaive value. Below a certain temperature, particles start collapsing into the $E_i=0$ state. This is the second order phase transition called the Bose-Einstein condensation. In this phase, the total number of the particles is given as

$$N = N(0) + V\left(\frac{2\pi m k_B T}{h^2}\right)^{3/2} \sum_{i=1}^{\alpha} \{\exp(\mu/k_BT)\}^i i^{-3/2} \qquad \text{(A-3)},$$

where V and m are the volume of the system and the mass of the particle, respectively. The first term, N(0), is written as

$$N(0) = \frac{1}{\exp(-\mu/k_BT) - 1} \qquad \text{(A-4)}.$$

This is the number of the particles that occupy the lowest energy state, i.e., the $E_i=0$ state. The second term in eq.(A-3) represents the number of the particles that occupy the excited state and is denoted here by N'. The temperature of this phase transition, T^c, which is called the critical

temperature, is determined by the condition of

$$N = N' \qquad \text{(A-5)}.$$

Then, T^c is explicitly given as

$$T^c = \frac{h^2}{2\pi m k_B T}\left(\frac{n}{2.612}\right)^{\frac{2}{3}} \qquad \text{(A-6)},$$

where n=N / V is the particle density.

On the other hand, if the density of the particles can be increased keeping the temperature constant, there is a certain density beyond that particles collapse into the $E_i=0$ state. This density, n^c, is called the critical density and given as

$$n^c = 2.612\left(\frac{2\pi m k_B T}{h^2}\right)^{\frac{3}{2}} \qquad \text{(A-7)}.$$

Appendix B. Optical phase-conjugation (PC) [33]

In Chapter 4, the PC signal at the GTA is adopted as the probe of the k~0 biexciton state. Here, the generation of the PC light and its character are explained.

B-1. Generation of the PC light and its polarization selection rule

Generally, when light enters into medium, the polarization, **P**, is generated in the medium as a response of the medium to the light field. Each component of the polarization, P_i, in Cartesian coordinate can be written by using each component of the electric fields of the incident light, E_i, as follows,

$$\begin{aligned} P_i = & \sum_j \chi^{(1)}_{ij} E_j(\mathbf{r},t) \\ & + \sum_{jk} \chi^{(2)}_{ijk} E_j(\mathbf{r},t) E_k(\mathbf{r},t) \\ & + \sum_{jkl} \chi^{(3)}_{ijkl} E_j(\mathbf{r},t) E_k(\mathbf{r},t) E_l(\mathbf{r},t) \\ & + \cdots \\ & + (\text{similar terms including time differentiation}) \end{aligned} \qquad \text{(B-1)}.$$

P has linear dependence on **E** in the first term. We call such polarization the linear polarization, $\mathbf{P}_L$. On the other hand, **P** has nonlinear dependence on **E** in terms below the second term. We call them the nonlinear polarizations, $\mathbf{P}_{NL}$. $\mathbf{P}_{NL}$ can be neglected when **E** is small. However, when **E** is large and resonates a certain level, it can not be neglected.

By carrying out the Fourier transformation of eq.(B-1), we obtain the expression of **P** by the terms which are functions of ω including the frequency dependent susceptibility, χ, as

$$P_i(\omega_1,\mathbf{r}) = \sum_j \chi^{(1)}_{ij}(-\omega_1,\omega_1) E_j(\omega_1,\mathbf{r})\, e^{i\mathbf{k}_1\cdot\mathbf{r}}$$

$$+\sum_{jk}\int_{\omega_2+\omega_3=\omega_1} d\omega_2 \chi^{(2)}_{ijk}(-\omega_1,\omega_2,\omega_3)E_j(\omega_2,\mathbf{r})E_k(\omega_3,\mathbf{r})\,e^{i(k_2+k_3)\cdot r}$$

$$+\sum_{jkl}\int_{\omega_2+\omega_3+\omega_4=\omega_1} d\omega_2 d\omega_3 \chi^{(3)}_{ijkl}(-\omega_1,\omega_2,\omega_3,\omega_4)E_j(\omega_2,\mathbf{r})E_k(\omega_3,\mathbf{r})E_l(\omega_4,\mathbf{r})\,e^{i(k_2+k_3+k_4)\cdot r}$$

$$+ \qquad\qquad (B\text{-}2),$$

where $E(\omega_i,\mathbf{r})\,e^{\mathbf{k}\cdot\mathbf{r}}$ is the ω_i component of the Fourier transformed $E(\mathbf{r},t)$.

Hereafter, we consider the case where the electric field is expressed by the sum of three plane waves as

$$\mathbf{E}(\mathbf{r},t)=\sum_{i=2}^{4}\mathbf{E}(\omega_i,\mathbf{r})\,e^{i(k_i\cdot r-\omega_i t)} \qquad (B\text{-}3).$$

In this case, the terms which are proportional to EEE as

$$P^{(3)}_i(\omega_2+\omega_3+\omega_4,\mathbf{r})=\sum_{jkl}6\chi^{(3)}_{ijkl}(-(\omega_2+\omega_3+\omega_4),\omega_2,\omega_3,\omega_4)E_j(\omega_2,\mathbf{r})E_k(\omega_3,\mathbf{r})E_l(\omega_4,\mathbf{r})\,e^{i(k_2+k_3+k_4)\cdot r} \qquad (B\text{-}4).$$

appear six times in the third term of eq.(B-2).

In eqs.(B-1)(B-2)(B-4), we express the amplitude of the electric field by E. However, E*, which is the complex conjugate of E, can appear in the equations instead of E. In this case, the signs of ω and $\mathbf{k}$ should be changed.

Here, we consider the case where three laser beams that have the same photon energy enter a nonlinear medium. The geometry of the three laser beams is shown in Fig.B-1. In this case, we can find a third order nonlinear polarization as

$$P^{(3)}_i(\omega,\mathbf{r})=\sum_{jkl}6\chi^{(3)}_{ijkl}(-\omega,\omega,\omega,-\omega)E_{f,j}(\omega,\mathbf{r})E_{b,k}(\omega,\mathbf{r})E^{*}_{p,l}(\omega,\mathbf{r})\,e^{i\{(k_f+k_b-k_p)\cdot r-\omega t\}} \qquad (B\text{-}5),$$

where $\mathbf{E}_f$, $\mathbf{E}_b$ and $\mathbf{E}_p$ are the electric fields of the pump(forward) light, the pump(backward) light and the probe light, respectively. $\mathbf{k}_f$, $\mathbf{k}_b$ and $\mathbf{k}_p$ are the respective wave vectors. Now, $\mathbf{k}_f+\mathbf{k}_b=0$,

then the wave vector of this polarization is $-\mathbf{k}_p$, which is completely opposite to the wave vector of the probe light. Therefore, the amplitude and spatial character of the mixed light wave induced by this nonlinear polarization is proportional to the phase conjugation of those of the probe light. This mixed light is called the phase conjugation light.

G.Mizutani calculated the third order nonlinear susceptibility, $\chi^{(3)}$, using the density matrix according to the four levels model of excitons and biexcitons in CuCl as shown in Fig.B-2[33]. He obtained the expression of the third order nonlinear polarization, $\mathbf{P}_{NL}^{(3)}$, as

$$\mathbf{P}^{(3)}_{NL}(\omega,\mathbf{r})=\alpha(\omega)\{(\mathbf{E}_f\cdot\mathbf{E}^{*}_p)\mathbf{E}_b+(\mathbf{E}_b\cdot\mathbf{E}^{*}_p)\mathbf{E}_f\}+\beta(\omega)(\mathbf{E}_f\cdot\mathbf{E}_b)\mathbf{E}^{*}_p \qquad (B\text{-}6)$$

$$\alpha(\omega)=\frac{3N|\mu_{Tg}|^4\gamma_{Tg\perp}}{\gamma_{Tg//}\{(E_T-\hbar\omega)-i\gamma_{Tg\perp}\}\{(E_T-\hbar\omega)^2+\gamma^2_{Tg\perp}\}}$$

$$\beta(\omega)=-\frac{2N|\mu_{Tg}|^2|\mu_{mT}|^2}{\{(E_m-2\hbar\omega)-i\gamma_{mg\perp}\}\{(E_T-\hbar\omega)-i\gamma_{Tg\perp}\}^2} \qquad (B\text{-}7),$$

where $\gamma_{Tg\perp}$ and $\gamma_{Tg\parallel}$ are the longitudinal and transverse damping constants between the T-exciton state and the ground state, respectively. $\gamma_{mg\perp}$ is the longitudinal damping constant between the biexciton state and the T-exciton state. μ_{Tg} and μ_{mT} are the dipole matrix elements between the T-exciton state and the ground state and between the biexciton state and the T-exciton state, respectively. E_T and E_m are the energies of the T-exciton and the biexciton, respectively. N is the electron density.

The first and second terms in eq.(B-6) represent the nonlinearity that resonate one photon transition of excitons (scattering by exciton population grating). Whereas, the third term represents the nonlinearity that resonates the biexciton state (scattering of the coherent k=0 biexcitons). Each term in eq.(B-6) can be selected experimentally by choosing the combination of the polarizations of the incident light as shown in Fig.B-3.

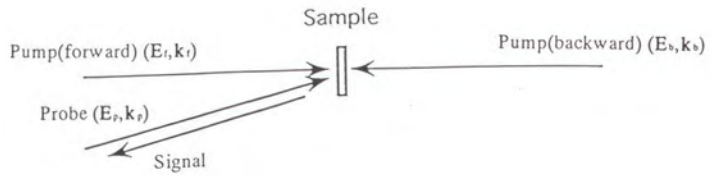

Fig. B-1 Geometry for the phase-conjugation

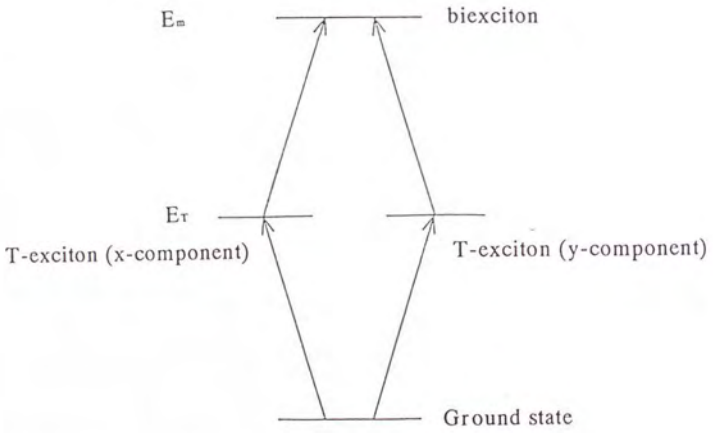

Fig. B-2 Four levels model used for the calculation of the third order nonlinear susceptibility associated with the exciton-biexciton system in CuCl (after ref. 52)

$$\vec{P}_{NL} = \alpha(\vec{E}_f \cdot \vec{E}_p^*)\vec{E}_b + \alpha(\vec{E}_b \cdot \vec{E}_p^*)\vec{E}_f + \beta(\vec{E}_f \cdot \vec{E}_b)\vec{E}_p^*$$

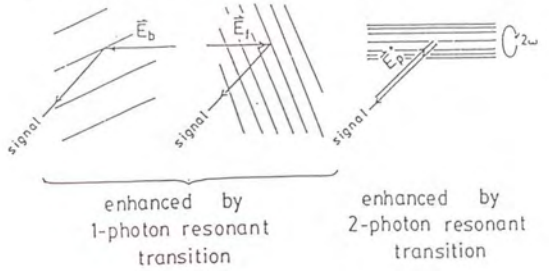

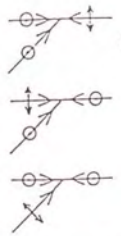

$\alpha(\vec{E}_f \cdot \vec{E}_p^*)\vec{E}_b$

$\alpha(\vec{E}_b \cdot \vec{E}_p^*)\vec{E}_f$

$\beta(\vec{E}_f \cdot \vec{E}_b)\vec{E}_p^*$

Combination of polarizations of incident light

Fig. B-3 Polarization selection rule for the PC [52]

B-2. Phase matching condition

In non-degenerate configuration where the frequency of the pump light, $\omega_f=\omega_b$, is different from that of the probe light, ω_p, the frequency of the PC light, ω_{PC}, is given as

$$\omega_{PC} = \omega_f+\omega_b-\omega_p \qquad \text{(B-8)}$$

due to the energy conservation law. In this case, $\mathbf{k}_{PC}(\omega_{PC})$ is different from the wave vector of the electric field induced by the nonlinear polarization, $\mathbf{k}_{NL}=\mathbf{k}_f+\mathbf{k}_b-\mathbf{k}_p=-\mathbf{k}_p$. Here, the spatial development of the PC light in the medium in such case is considered.

The nonlinear polarization, $\mathbf{P}_{NL}$, induces the electric flux density, $\mathbf{D}$, with the electric field, $\mathbf{E}$, as

$$\mathbf{D} = \mathbf{E}+4\pi\mathbf{P} = \mathbf{E}+4\pi(\mathbf{P}_L+\mathbf{P}_{NL}) \qquad \text{(B-9)}.$$

On the other hand, Maxwell equations for the system where no charge and no current are present are given as

$$\mathrm{rot}\mathbf{E} = -\frac{1}{c}\frac{\partial \mathbf{B}}{\partial t} \qquad \text{(B-10)}$$

$$\mathrm{rot}\mathbf{H} = \frac{1}{c}\frac{\partial \mathbf{D}}{\partial t} \qquad \text{(B-11)}$$

$$\mathrm{div}\mathbf{D} = 0 \qquad \text{(B-12)}$$

$$\mathrm{div}\mathbf{B} = 0 \qquad \text{(B-13)},$$

where c is the velocity of light.

Through eq.(B-11)(B-12), $\mathbf{P}_{NL}$ enters the Maxwell equations. Because $\mathbf{D}$ is determined from $\mathbf{E}$ through eq.(B-9) and $\mathbf{E}$ is determined from $\mathbf{D}$ through eqs.(B-10)~(B-13), eq.(B-9)~(B-13) should be solved self-consistently. However, it is difficult to solve it when eq.(B-9) is nonlinear on $\mathbf{E}$. Then usually, it is solved assuming that $\mathbf{P}_{NL}$ is small and can be treated as a perturbation.

By canceling $\mathbf{H}$ in eq.(B-10)(B-11) assuming $\mu=1$, the following equation is obtained

$$\mathrm{rot\ rot}\ \mathbf{E} = -\frac{1}{c^2}\frac{\partial^2 \mathbf{D}}{\partial t^2} \qquad \text{(B-14)}.$$

After inserting eq.(B-9) into this equation, Fourier transformation according to time is carried out. Then, we obtain the following equation

$$\mathrm{rot\ rot}\ \mathbf{E}(\omega,\mathbf{r}) - \frac{\varepsilon\omega^2}{c^2}\mathbf{E}(\omega,\mathbf{r}) = \frac{4\pi\omega^2}{c^2}\mathbf{P}_{NL}(\omega,\mathbf{r}) \qquad \text{(B-15)}.$$

Here ε is the the dielectric constant in the medium. ε is scalar when medium has cubic symmetry or full rotational symmetry. When $\mathbf{P}_{NL}$ is not negligible in eq.(B-15), $\mathbf{P}_{NL}$ induces the PC light, $\mathbf{E}_{MIX}$. The electric field in the medium, $\mathbf{E}_0+\mathbf{E}_{MIX}$, obeys eq.(B-15), where $\mathbf{E}_0$ is the electric field without perturbation. Then, we obtain the result as

$$\mathrm{rot\ rot}\ \mathbf{E}_{MIX}(\omega,\mathbf{r}) - \frac{\varepsilon\omega^2}{c^2}\mathbf{E}_{MIX}(\omega,\mathbf{r}) = \frac{4\pi\omega^2}{c^2}\mathbf{P}_{NL}(\omega,\mathbf{r}) \qquad \text{(B-16)}$$

because $\mathbf{E}_0$ satisfies the relation of

$$\mathrm{rot\ rot}\ \mathbf{E}_0 - \frac{\varepsilon\omega^2}{c^2}\mathbf{E}_0 = 0 \qquad \text{(B-17)}.$$

In order to solve eq.(B-16), $\mathbf{E}_{MIX}$ is assumed to be expressed by the product of $\mathbf{E}_{MIX0}(\mathbf{r})$, which varies slowly according to space, and $\exp(i\mathbf{k}_{PC}\mathbf{r}-\omega t)$ as

$$\mathbf{E}_{MIX}(\omega,\mathbf{r}) = \mathbf{E}_{MIX0}(\mathbf{r})\, e^{(i\mathbf{k}_{PC}\cdot\mathbf{r}-\omega t)} \qquad \text{(B-18)}.$$

Assuming that $\mathbf{E}_{MIX}$ is perpendicular to $\mathbf{k}_{PC}$ (transverse wave) and that the change of $\mathbf{E}_{MIX0}(\mathbf{r})$ is much slower than the change of $2\pi/\mathbf{k}_{PC}$, Eq.(1-16) can be approximated as

$$-2i(\mathbf{k}_{PC}\cdot\nabla)\mathbf{E}_{MIX0}(\mathbf{r})\, e^{i\mathbf{k}_{PC}\cdot\mathbf{r}} = \frac{4\pi\omega^2}{c^2}\mathbf{P}_{NL}(\omega,\mathbf{r}) \qquad \text{(B-19)}.$$

From this equation with the initial conditions for $\mathbf{P}_{NL}(\omega,\mathbf{r})$ and $\mathbf{E}_{MIX0}(\mathbf{r})$, the development of the mixed wave, $\mathbf{E}_{MIX0}(\mathbf{r})$, can be calculated.

When the nonlinear polarization is excited in the medium as

$$\mathbf{P}_{NL}(\omega,\mathbf{r}) = \mathbf{P}^0_{NL}\, e^{i\mathbf{k}_{NL}\cdot\mathbf{r}} \qquad \text{(B-20)},$$

the spatial evolution of the PC light is calculated by the equation of

$$\frac{d\mathbf{E}_{MIX0}}{dz} = i\frac{2\pi\omega^2}{k_{PC}c^2}\mathbf{P}^0_{NL}\, e^{i\Delta\mathbf{k}\cdot\mathbf{r}} \qquad \text{(B-21)},$$

where $\Delta \mathbf{k}$ is given as

$$\Delta k = k_{PC} - k_{NL} \qquad \text{(B-22).}$$

In order to make discussion simple, we assume here that the direction of $\mathbf{k}_{NL}$ is along z-axis and that the PC light develops obeying eq.(B-21) from $E_{MIX0}(z=0)=0$ in the sample. In this case, $E_{MIX0}(z=d)$, where d is the sample thickness, is obtained as

$$|E_{MIX0}|^2 = \left|\frac{2\pi\omega^2 d}{k_{PC}c^2} P_{NL}\right|^2 \left|\frac{\sin\left(\frac{\Delta k_z d}{2}\right)}{\frac{\Delta k_z d}{2}}\right|^2 \qquad \text{(B-23).}$$

Thus, $|E_{MIX0}|$ has the maximum at $\Delta\mathbf{k}=0$, i.e., $\mathbf{k}_{PC}=\mathbf{k}_{NL}$. This condition corresponds to the degenerate configuration, i.e., $\omega_{PC}=\omega_f=\omega_b=\omega_p$. However, if $\Delta\mathbf{k}$ is large and not satisfy the condition of

$$\Delta k_z \leq \frac{\pi}{d} \qquad \text{(B-24),}$$

$|E_{MIX0}|^2$ becomes small[54]. Eq.(B-24) is called the phase matching condition.

The phase matching condition can be thought to correspond to the uncertainty relation between the uncertainty of the momentum ($\Delta p_z=\hbar\Delta k_z$) and the uncertainty of the position ($\Delta z=d$) in the finite size of the medium, $\Delta p_z \Delta z \sim \pi\hbar = h/2$.

B-3. Observations of the PC in CuCl

The observations of the PC signal associated with the exciton and biexciton resonances in CuCl were done by G.Mizutani et al.[53] and L.L.Chase et al.[55]. L.L.Chase et al. noticed the PC signal at the two-photon resonance of biexcitons and evaluated the value of relevant $|\chi^{(3)}|$. On the other hand, G.Mizutani et al. noticed the polarization dependence of the PC generation associated with excitons and biexcitons.

Figure B-4 shows the excitation spectra of the PC light in the degenerate configuration obtained by G.Mizutani et al.[53]. The remarkable enhancement of the PC light around the two-photon resonant energy of biexcitons observed in Fig.B-4(d) is due to the 2ω coherence that is generate by the biexciton resonance. They thought that the sharp dip observed just at the two-photon resonant energy of biexcitons was caused by the two-photon absorption of biexcitons by the combination of the intense laser light and the generated PC light. On the other hand, the broad structure observed in higher energy region in Fig.B-4(b)(c) is thought to be due to the population grating of the T-exciton. One can see in these figures that the polarization selection rule mentioned in the section B-1 holds good.

In Fig.B-5, monochromized PC light in the non-degenerate configuration is shown[53]. It is clear that the PC light appears in the energy position opposite to the probe light against the pump light. Intensity spectra of the PC signal in the non-degenerate configuration as a function of the photon energy of the probe light are shown in Fig.B-6. It is clear that the efficiency for the generation of the PC signal in the non-degenerate configuration is determined by the phase matching condition mentioned in the section B-2.

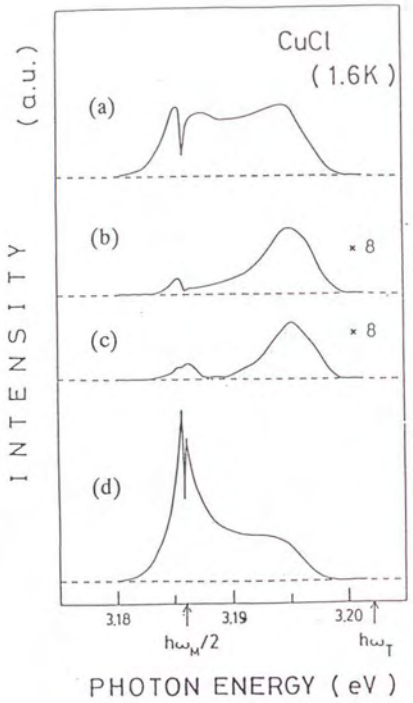

Fig. B-4 Excitation spectra of the degenerate PC light for different polarization configurations of the incident light beams [52]
(a) E_f // E_b // E_p, (b) E_f // E_p ⊥ E_b, (c) E_f ⊥ E_p // E_b,
(d) E_f // E_b ⊥ E_p.

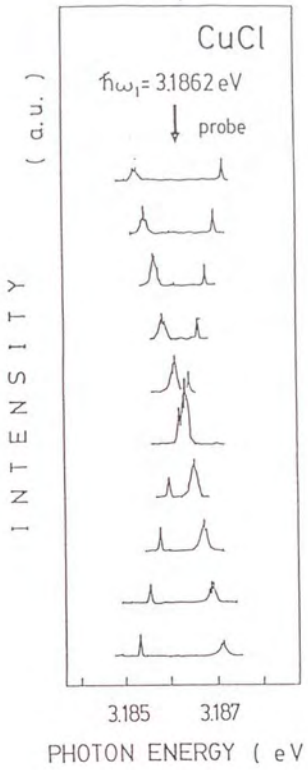

Fig. B-5 Spectra of the PC light in the non-degenerate configuration [52]
The photon energy of the pump beams was set at 3.1862eV and is indicated by an arrow. The phase-conjugate light and the scatter of the probe beam are seen as the broad peak and the narrow peak, respectively.

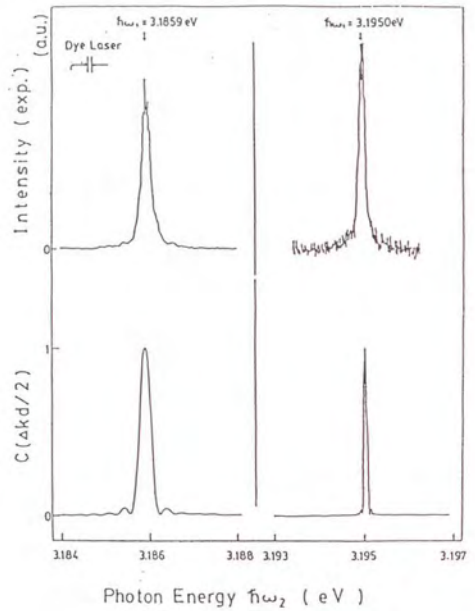

Fig.B-6 Intensity spectra of the PC light in the non-degenerate configuration[52] The top of the figure shows the experimental results. The bottom of the figure shows the results of the calculation of the phase matching condition.

Appendix C. New nonlinear emission associated with scattering between an exciton and a biexciton[56]

C-1. Introduction

The intensity of the PC signal started decreasing when the biexciton density was over a certain density. In the thesis, we supposed that this decrease was due to the appearance of the instability of the biexciton state because the estimated biexciton density where the decrease was observed is close to n_m^{sp}. Recently, we found that a new decay process of biexcitons from the observation of emission spectra of CuCl in such a high intensity excitation regime. One can think that such collision process will also make the biexciton state unstable. Here, we explain the details of this emission and the reason why this emission is thought to be related to the decay process of biexcitons.

Figure C-1 shows examples of the emission spectra in the M-emission region at several intensities of the excitation light. Laser light from a dye laser (BBQ in p-dioxane) excited by an excimer laser (Lambda Physik 53MSC) was used as the excitation light. The photon energy, the spectral width and the pulse duration of the excitation light were 3.2088eV, 50μeV and 10ns, respectively. The spot size of the excitation light on the sample surface was about 100μm. Emissions were observed at the right angle to the direction of the excitation light through a monochromator. Sample was a CuCl block crystal (4x5x10mm^3) supplied by Prof. E.Mohler and was cooled in an immersion type cryostat at 2K.

In a weak excitation intensity, the emissions thought to be M_L- and M_T-emissions were observed. The reason why the intensity of M_T-emission is weaker than that of M_L-emission is thought to be due to the reabsorption processes of M_T-emission, because the emissions pass a long distance about 50μm of the excitation region where a lot of T-excitons that absorb the M_T-emission are present. The sharp dip at 3.163eV is due to the two-photon absorption of biexcitons by the combination of the excitation laser light and an emitted photon.

As the intensity of the excitation light increased, the emission indicated by an arrow in the figure appeared in the M_T-emission region and increased remarkably. Fig.C-2 shows the integrated intensities of this new emission and M-emission as a function of the intensity of the excitation light. It was found that this new emission increased more than square of the intensity of the excitation light at the appearance. On the other hand, the intensity of M-emission saturated suddenly at the appearance of the new emission. Therefore, the new emission is thought to be associated with some decay processes of biexcitons.

Figure C-3 shows the emission spectra at several photon energies of the excitation light, E_L. The excitation intensity was 40MW/cm^2. With the increase of E_L, the intensity of M_L-emission increases

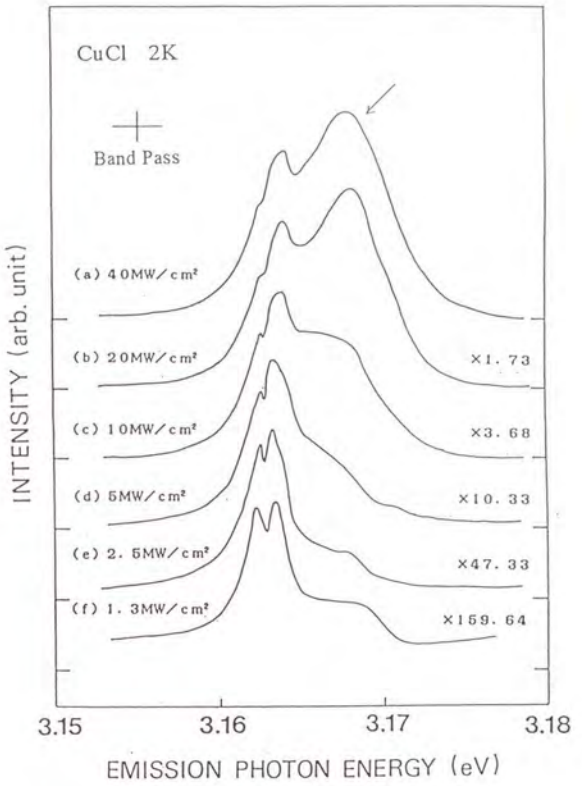

Fig.C-1 Emission spectra in the M-emission region of CuCl at 2K at several excitation intensities.
The photon energy of the excitation light is 3.2088eV. The intensities of the excitation light are shown in the figure.

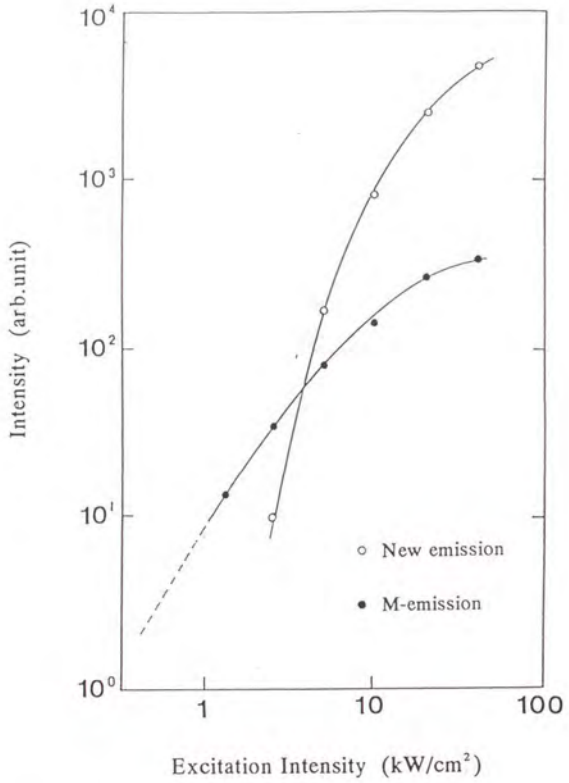

Fig.C-2 The integrated intensities of the M-emission and the new nonlinear emission as a function of the intensity of the excitation light
The photon energy of the excitation light was 3.2088eV.

until it reaches the energy region of the T-exciton. In this region, M_L-emission appears dominantly. This phenomenon is interpreted as the reabsorption processes of M_T-emission mentioned above. However, when $E_i > E_T(k_T=0)$, the energy of the T-exciton at zero wave vector, a new structure that is the new nonlinear emission mentioned above appears separately. This structure shifts toward the high energy side as E_i increases. When $E_i > E_L(k_L=0)$, the energy of the L-exciton at zero wave vector, the intensity of the new nonlinear emission decreases and M_L-emission becomes clear again.

Figure C-4 shows a contour map of the intensity of emissions as functions of E_i and the photon energy of the emission, E_s. Around the L-T gap region, the relation of E_i and E_s is expressed empirically as

$$E_i \approx E_s + E_m^b + \Delta_{LT} \qquad \text{(C-1)},$$

where E_m^b and Δ_{LT} are the binding energy of a biexciton and the L-T splitting of the Z_3-exciton at k= 0, respectively. From the definitions of E_m^b and Δ_{LT} as

$$\Delta_{LT} = E_L(k_L \approx 0) - E_T(k_T \approx 0) \qquad \text{(C-2)}$$

$$E_m(k_m \approx 0) = 2E_T(k_T \approx 0) - E_m^b \qquad \text{(C-3)},$$

eq.(A-1) is weritten as

$$E_i + E_m(k_m \approx 0) \approx E_s + E_L(k_L \approx 0) + E_T(k_T \approx 0) \qquad \text{(C-4)}.$$

As an interpretation of this equation, one can imagine a collision process between and incident polariton and a biexciton which results in the creation of an emitted photon, an L-exciton and a T-exciton as

incident exciton (polariton) + biexciton

-> emitted photon + L-exciton + T-exciton (polariton).

For more quantitative discussion, it is necessary to take the momentum conservation and the dispersions of the relevant excitons states into account as

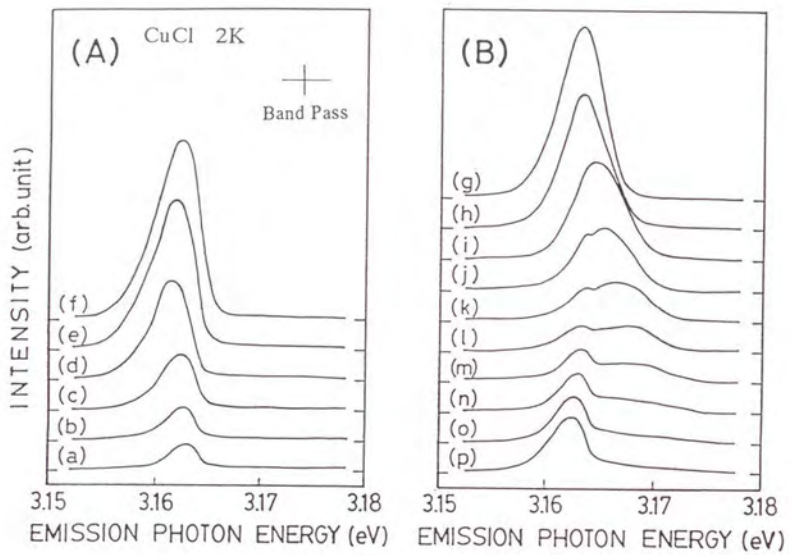

Fig. C-3 Emission spectra in the M-emission region of CuCl at 2K at several photon energies of the excitation light [55]
(a) 3.1891, (b) 3.1909, (c) 3.1927, (d) 3.1945, (e) 3.1962, (f) 3.1980, (g) 3.1998, (h) 3.2016, (i) 3.2034, (j) 3.2052, (k) 3.2070, (l) 3.2088, (m) 3.2106, (n) 3.2123, (o) 3.2142 and (p) 3.2159 eV. The intensity of the excitation light on the sample surface was 40MW/cm^2.

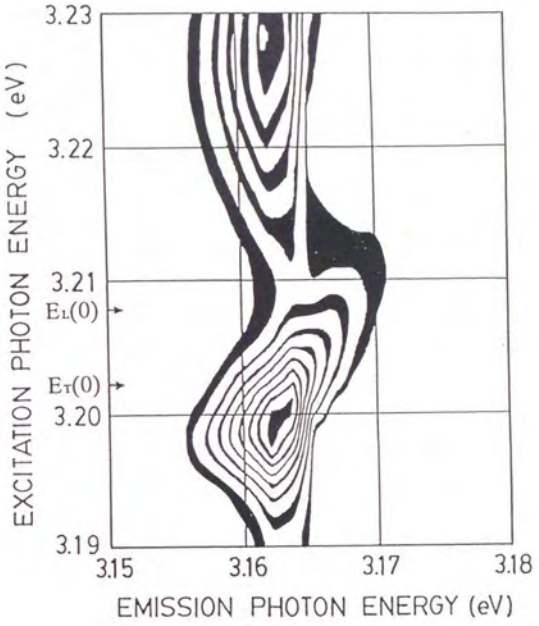

Fig. C-4 Contour map of the intensity of the emission as functions of the photon energies of the excitation light and the emitted light [55]
$E_L(0)$ and $E_T(0)$ are the energies of the L-exciton and the T-exciton of zero wave vector, respectively. The intensity of the excitation light on the sample surface was 40MW/cm^2.

$$E_i(k_i) + E_m(k_m) = E_s(k_s) + E_L(k_L) + E_T(k_T) \quad \text{(C-5)}$$

$$\mathbf{k}_i + \mathbf{k}_m = \mathbf{k}_s + \mathbf{k}_L + \mathbf{k}_T \quad \text{(C-6).}$$

To simplify the analysis, let the wave vector of biexcitons to be zero. The energy and momentum conservations are given by

$$E_i(k_i) + E_m(0) \simeq E_s + E_L(k_L) + E_T(k_T) \quad \text{(C-7)}$$

$$\mathbf{k}_i \simeq \mathbf{k}_L + \mathbf{k}_T \quad \text{(C-8),}$$

where the wave vector of the scattered photon is neglected.

The dispersions of the T- and L-exciton are given by the effective mass approximation neglecting the polariton effects of the T-exciton as

$$E_T(k_T) = E_T(0) + \frac{(\hbar k_T)^2}{2m_T} \quad \text{(C-9)}$$

$$E_L(k_L) = E_L(0) + \frac{(\hbar k_L)^2}{2m_L} \quad \text{(C-10),}$$

with $m_T=2.30m_0$ and $m_L=3.14m_0$, where m_0 is the electron rest mass.

Eq. (C-7) is then rewritten as

$$E_s \simeq E_m(0) - E_L(0) + \left(1-\left(\frac{k_T}{k_i}\right)^2 - \frac{m_T}{m_L}\left(\frac{k_L}{k_i}\right)^2\right)(E_i(k_i) - E_T(0)) \quad \text{(C-11),}$$

where we regarded the incident exciton as a T-exciton.

For a given E_i, E_s becomes maximum under the condition of

$$\mathbf{k}_T = \frac{m_L}{m_T+m_L}\mathbf{k}_i \quad \text{(C-12).}$$

Therefore, the spectrum of the new emission at E_i has to have an edge on the high energy side, E_s^e, at

$$E_s^e \simeq E_m(0) - E_L(0) + \frac{m_L}{m_T+m_L}(E_i(k_i) - E_T(0)) \quad \text{(C-13).}$$

Namely, E_s^e will shift linearly as a function of E_i with a gradient of

$$\frac{m_L}{m_T+m_L} = 0.58 \quad \text{(C-14).}$$

It seems difficult to identify the position of the edge in the relevant emission spectrum shown in Fig.C-3. However, we can see that the shape of the spectrum is asymmetrical and has a tail toward the low energy side. These facts might show the presence of the edge. The gradient of the peak shift of the new emission could be estimated instead of the edge to be 0.6, which corresponds to the value, 0.58, estimated by the simple model mentioned above.

For more quantitative analysis of the spectral shape of the new nonlinear emission, following things should be considered:

1) State density of the relevant excitation quantum

2) Distribution of the relevant excitation quantum in k-space

3) Polariton effects of the T-exciton

4) Momentum dependence of the efficiency of the collision.

But, it is impossible at present due to the lack of informations. However, 2) and 3) will contribute to extinguish the high energy edge of the spectrum. Such effects can be seen in the spectra qualitatively.

C-3. Conclusion

It was found that the new nonlinear emission appeared when the strong photo-excitation of the Z_3-exciton band of several MW/cm^2 was done. From the analysis of the dependence of this emission on the excitation intensity and on the excitation photon energy, it was found that this emission is associated with the collision process of

incident exciton (polariton) + biexciton

-> emitted photon + L-exciton + T-exciton (polariton).

In such excitation condition, biexcitons are destroyed by this collision process.

References

1. A.Goldmann : phys.stat.sol.(b) **81**, 9 (1977).
2. S.Nikitine : in Excition in High Density, Springer Tracts in Modern Physics, 73, Springer-Verlag (1975).
3. K.Cho : Phys.Rev.B **14**, 4463 (1976).
4. O.Akimoto and E.Hanamura : Solid State Commun. **10**, 253 (1972).
5. F.Bassani, J.J.Forney and A.Quattropani : phys.stat.sol.(b) **65**, 591 (1974).
6. E.Doni, R.Girlanda and G.P Parravicini : Solid State Commun. **17**, 189 (1975).
7. T.Mita, K.Sotome and M.Ueta : Solid State Commun. **33**, 1135 (1980), T.Mita : Doctor Thesis (Tohoku Univ., 1980).
8. A.Mysyrowicz, J.B.Grun, R.Levy, A.Bivas and S.Nikitine : Phys.Lett. **26A**, 615 (1968).
9. R.S.Knox, S.Nikitine and A.Mysyrowicz : Optics Commun. **1**, 19 (1969).
10. E.Hanamura : Solid State Commun. **12**, 951 (1973).
11. A.A.Gogolin : Fiz.Tverd.Tela **15**, 2746 (1973), Sov.Phys.Solid State **15**, 1824 (1974).
12. G.M.Gale and A.Mysyrowicz : Phys.Rev.Lett. **32**, 727 (1974).
13. N.Nagasawa, N.Nakata, Y.Doi and M.Ueta : J.Phys.Soc.Jpn. **38**, 593 (1975).
14. H.Akiyama : Doctor Thesis (Univ. of Tokyo, 1991).
15. M.Kuwata-Gonokami, R.Shimano, J.Iwamatsu, H.Akiyama, T.Kuga and M.Matsuoka : phys. stat.sol.(b) **159**, 347 (1990).
16. S.A.Moskalenko : Fiz.Tverd.Tela **4**, 276 (1962), Sov.Phys.Solid State **4**, 199 (1962).
17. J.M.Blatt, K.W.Boer and W.Brandt : Phys.Rev. **126**,1691 (1962).
18. A.Mysyrowicz, D.W.Snoke and J.P.Wolfe : phys.stat.sol.(b) **159**, 387 (1990).
19. E.Fortin, S.Fafard and A.Mysyrowicz : Phys.Rev.Lett. **70**, 3951 (1993).
20. J.L.Lin and J.P.Wolfe : Phys.Rev.Lett. **71**, 1222 (1993).
21. J.N.Plendl and L.C.Mansur : Appl. Opt. **11**, 1194 (1972).
22. R.C.Hanson, K.Helliwell and C.Schwab : Phys.Rev.B **9**, 2649 (1974).

23. T.Nanba, K.Hachisu and M.Ikezawa : J.Phys.Soc.Jpn. **50**, 1579 (1981).

24. P.Alonas, G.sherman, C.Wittig and P.C.Coleman : Appl. Opt. **8**, 2557 (1969).

25. K.Saito, M.Hasuo, T.Hatano and N.Nagasawa : Solid State Commun. **94**, 33 (1995).

26. T.Ando, M.Hasuo and N.Nagasawa : phys.stat.sol.(b) **179**, 453 (1993).

27. J.Ringeissen and S.Nikitine : J.Phys.(France) **28**, C3-48 (1967).

28. J.B.Anthony, A.D.Brothers and D.W.Lynch : Phys.Rev.B **5**, 3189 (1972).

29. H.Akiyama, T.Kuga, M.Matsuoka and M.Kuwata-Gonokami : Phys.Rev.B **42**, 5621 (1990).

30. T.Ikehara and T.Itoh : Phys.Rev.B **44**, 9283 (1991).

31. N.Nagasawa, M.Kuwata, E.Hanamura, T.Itoh and A.Mysyrowicz : Appl.Phys.Lett.**55**, 1999 (1989).

32. M.Kuwata, T.Itoh, E.Hanamura N.Nagasawa and A.Mysyrowicz : SPIE **1227**, 55 (1989).

33. R.Shimano and M.Kuwata-Gonokami : Phys.Rev.Lett. **72**, 530 (1994).

34. A.L.Ivanov and H.Haug : Proceedings of BEC'93, Trento (May 31-June 4, 1993), "Bose-Einstein condensation" ed. by A.Griffin, D.W.Snoke and S.Stringari, Cambridge Univ. Press, N.Y., (1995).

35. M.Kuwata : J.Phys.Soc.Jpn. **53**, 4456 (1984). M.Kuwata : Doctor Thesis (Univ. of Tokyo, 1985).

36. M.Hasuo N.Nagasawa and T.Itoh : Optics Commun. **85**, 219 (1991).

37. M.Hasuo, M.Nishino and N.Nagasawa : J.Lumin. **60&61**, 672 (1994).

38. C.S.Adams and A.I.Ferguson : Opt.Commun. **79**, 219 (1990).

39. N.Nagasawa, N.Nakata, Y.Doi and M.Ueta : J.Phys.Soc.Jpn. **39**, 987 (1975).

40. N.Peyghambarian, L.L.Chase and A.Mysyrowicz : Phys.Rev.B **27**, 2325 (1983).

41. R.C.Casella : J.Phys.Chem.Solids **24**, 19 (1963).

42. Y.Yakhot and E.Levich : Phys.Lett. **80A**, 301 (1980).

43. D.W.Snoke and J.P.Wolfe : Phys.Rev.B **39**, 4030 (1989).

44. H.T.C.Stoof : Phys.Rev.Lett. **66**, 3148 (1991).

45. Y.M.Kagan, B.V.Svistunov and G.V.Shlyapnikov : Sov.Phys.JETP **74**, 279 (1992); Sov. Phys.JETP **75**, 387(E) (1992).

46. M.Hasuo, N.Nagasawa and A.Mysyrowicz : phys.stat.sol.(b) **173**, 255 (1992).

47. M.Hasuo, N.Nagasawa T.Itoh and A.Mysyrowicz : Phys.Rev.Lett. **70**, 1303 (1993).

48. T.Hatano : Private communication.

49. M.Hasuo and N.Nagasawa : Proceedings of BEC'93, Trento (May 31-June 4, 1993), "Bose-Einstein condensation" ed. by A.Griffin, D.W.Snoke and S.Stringari, Cambridge Univ.Press, N.Y., (1995).

50. T.Hatano and N.Nagasawa : Optics commun. **97**, 16 (1993). T.Hatano : Doctor Thesis (Univ. of Tokyo, 1993).

51. M.Inoue and E.Hanamura : J.Phys.Soc.Jpn. **41**, 1273 (1976).

52. M.Brune, J.M.Raimond, P.Goy, L.Davidovich and S.Haroche : Phys.Rev.Lett. **59**, 1899 (1987).

53. G.Mizutani and N.Nagasawa : J.Phys.Soc.Jpn. **52**, 2251 (1983). G.Mizutani : Doctor Thesis (Univ. of Tokyo, 1986); Master Thesis (Univ. of Tokyo, 1983).

54. Y.Masumoto and S. Shionoya : J.Phys.Soc.Jpn. **49**, 2236 (1980).

55. L.L.Chase, M.L.Claude, D.Hulin and A.Mysyrowicz : Phys.Rev.A **28**, 3696 (1983).

56. M.Hasuo, T.Hatano and N.Nagasawa : phys.stat.sol.(b) **165**, K63 (1991).

1) "A New Nonlinear Emission Caused by High Density Excitation of Z_3-Excitons in CuCl"
H.Hasuo, T.Hatano and N.Nagasawa, phys.stat.sol.(b) **165**, K63 (1991).

2) "Measurement of the biexciton level width of CuCl at k~0 with a Ti-sapphire ring laser"
H.Hasuo, N.Nagasawa and T.Itoh, Optics Commun. **85**, 219 (1991).

3) "A New Approach to the Study of Bose Condensation of Biexcitons in CuCl"
M.Hasuo, N.Nagasawa and A.Mysyrowicz, XVIII Intern.Quantum Electronics Conf. June,1992 Vienna, Technical Digest.

4) "A New Approach to the Study of Bose-Einstein Condensation of Biexcitons"
M.Hasuo, N.Nagasawa and A.Mysyrowicz, phys.stat.sol.(b) **173**, 255 (1992).

5) "Progress of the Bose-Einstein Condensation of Biexcitons in CuCl"
M.Hasuo, N.Nagasawa, T.Itoh and A.Mysyrowicz, Phys.Rev.Lett. **70**, 1303 (1993).

6) "BEC of Biexcitons in CuCl"
M.Hasuo and N.Nagasawa, Proceedings of BEC'93, Trento Italy (1993). 'Bose-Einstein condensation', ed. by A.Griffin, D.W.Snoke and S.Stringari, Cambridge Univ. Press, N.Y., (1995).

7) "Evaluation of $|\chi^{(3)}|$ at the GTA of biexcitons in CuCl by high resolution polarization spectroscopy"
M.Hasuo, M.Nishino and N.Nagasawa, J.Lumin. **60&61**, 672 (1994).

8) "Bose-Einstein condensation of biexciton system in CuCl"
M.Hasuo, N.Nagasawa, T.Itoh and A.Mysyrowicz, J.Lumin. **60&61**, 758 (1994).